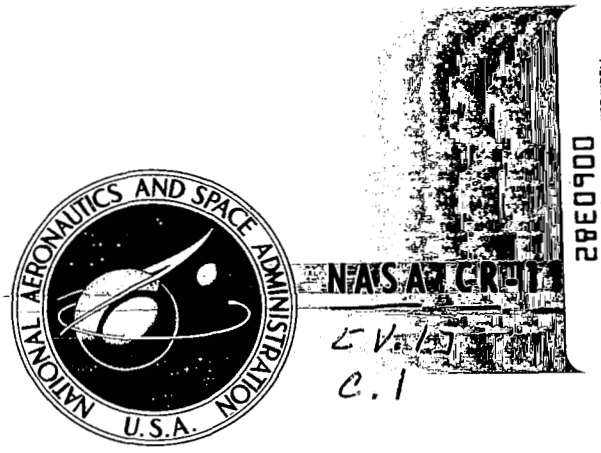

NASA CONTRACTOR REPORT

NASA CR-1116

INFLUENCE OF STRUCTURE AND MATERIAL RESEARCH ON ADVANCED LAUNCH SYSTEMS' WEIGHT, PERFORMANCE, AND COST

Phase III
Design Synthesis Of Recoverable Launch Vehicle Structures

by J. A. Boddy

Prepared by
NORTH AMERICAN ROCKWELL CORPORATION
Downey, Calif.
for NASA Headquarters

NATIONAL AERONAUTICS AND SPACE ADMINISTRATION • WASHINGTON, D. C. • JULY 1968

NASA CR-1116

INFLUENCE OF STRUCTURE AND MATERIAL RESEARCH ON ADVANCED LAUNCH SYSTEMS' WEIGHT, PERFORMANCE, AND COST, Phase III, Design Synthesis of Recoverable Launch Vehicle Structures

By J. A. Boddy

Issued by Originator as Report No. SD 67-1204-1

Prepared under Contract No. NAS 7-368 by
NORTH AMERICAN ROCKWELL CORPORATION
Downey, Calif.

for NASA Headquarters

NATIONAL AERONAUTICS AND SPACE ADMINISTRATION

For sale by the Clearinghouse for Federal Scientific and Technical Information
Springfield, Virginia 22151 – CFSTI price $3.00

FOREWORD

This report was prepared by North American Rockwell Corporation through its Space Division under NASA Contract NAS7-368 for the National Aeronautics and Space Administration. This report documents the Phase III study effort which included two separate tasks:

Design synthesis of recoverable first stage structures
Computer program turnover to NASA OART.

The structural design synthesis accounted for the thermal environment evaluation and protection system synthesis for the reentry mode of the recoverable first stages of a series of multistage launch vehicles. Relative benefits to be derived from structures/materials improvements when applied to these recoverable stages were considered in terms of their weight reductions, performance improvements, and cost reductions.

Phase III also included consolidation and documentation of the various synthesis subroutines developed for the Phase I study contract pertaining to expendable vehicle synthesis and structural design synthesis. These programs were made compatible with the NASA computer facility at the Electronic Research Center, Boston, Massachusetts. A detailed description of these programs is given in Volume II - Users Manual for Vehicle and Structural Design Synthesis Program.

This study was conducted for the National Aeronautics and Space Administration, Office of Advanced Research and Technology, Space Vehicle Structures Program. The study effort was accomplished at the Space Division, Downey, California, by the Structures and Dynamics Department, Research, Engineering, and Test Division, under the direction of Mr. H.S. Oder. All work was under the supervision of Mr. A.I. Bernstein, Project Manager, and J.A. Boddy, Project Engineer. Principal Investigators included J.C. Mitchell, W.L. Moss, and C.W. Martindale.

CONTENTS

	Page
SUMMARY	1
INTRODUCTION	4
APPROACH	6
VEHICLE DEFINITION AND ENVIRONMENT	9
Base-Point Vehicle Description	9
Aerodynamic Characteristics	15
Ascent Trajectory and Heating	30
Entry Trajectory and Heating	33
External Load Evaluation	55
Design Load Intensity	68
DESIGN SYNTHESIS	71
Thermal Evaluation	71
Thermal Stresses	83
Structural Synthesis	88
Assessment	110
COMPUTER PROGRAM TURNOVER	140
CONCLUSIONS AND RECOMMENDATIONS	147
Construction Concepts	147
Structural Costs	148
Manufacturing Development	149
Material Strength Improvement	149
REFERENCES	151

ILLUSTRATIONS

Figure		Page
1	Design Synthesis Logic	7
2	Typical Recoverable First-Stage Vehicle	10
3	Ascent Profile	11
4	Recoverable First-Stage Booster Concept	14
5	Vehicle Size Characteristics	16
6	Vehicle Weight and Performance Characteristics	17
7	Weight Distribution During First-Stage Boost - 1.3×10^6-Pound Vehicle	18
8	Weight Distribution During First-Stage Boost - 1.9×10^6-Pound Vehicle	19
9	Weight Distribution During First Stage Boost - 2.5×10^6-Pound Vehicle	20
10	Typical Dynamic Pressure and Velocity Variation With Initial Thrust-to-Weight Ratio and Typical Gravity-Turn Trajectory	22
11	Normal Force Distributions for 1.3×10^6-Pound Vehicle	23
12	Normal Force Distributions for 1.9×10^6-Pound Vehicle	24
13	Normal Force Distributions for 2.5×10^6-Pound Vehicle	25
14	Zero Lift-to-Drag Coefficient	26
15	Recoverable First-Stage Entry Aerodynamics - Configuration 1	27
16	Recoverable First-Stage Entry Aerodynamics - Configuration 2	28
17	Recoverable First-Stage Entry Aerodynamics - Configuration 3	29
18	Recoverable Vehicle Ascent Trajectory	31
19	Estimation of Thermal Environment	35
20	Recoverable First-Stage Entry Trajectory - Configuration 1	36
21	Recoverable First-Stage Entry Trajectory - Configuration 2	37
22	Recoverable First-Stage Entry Trajectory - Configuration 3	38
23	Body Point Locations for Heating Analysis	39
24	Recoverable First-Stage Entry Heating - Configuration 1 - Body Point 1	40

Figure		Page
25	Recoverable First-Stage Entry Heating - Configuration 1 - Body Point 2	41
26	Recoverable First-Stage Entry Heating - Configuration 1 - Body Point 3	42
27	Recoverable First-Stage Entry Heating - Configuration 1 - Body Point 4	43
28	Recoverable First-Stage Entry Heating - Configuration 1 - Body Point 5	44
29	Recoverable First-Stage Entry Heating - Configuration 2 - Body Point 1	45
30	Recoverable First-Stage Entry Heating - Configuration 2 - Body Point 2	46
31	Recoverable First-Stage Entry Heating - Configuration 2 - Body Point 3	47
32	Recoverable First-Stage Entry Heating - Configuration 2 - Body Point 4	48
33	Recoverable First-Stage Entry Heating - Configuration 2 - Body Point 5	49
34	Recoverable First-Stage Entry Heating - Configuration 3 - Body Point 1	50
35	Recoverable First-Stage Entry Heating - Configuration 3 - Body Point 2	51
36	Recoverable First-Stage Entry Heating - Configuration 3 - Body Point 3	52
37	Recoverable First-Stage Entry Heating - Configuration 3 - Body Point 4	53
38	Recoverable First-Stage Entry Heating - Configuration 3 - Body Point 5	54
39	Stationwise Weight Distribution for Base-Line Vehicles During Entry	57
40	Station Shear Load Due to Normal Inertia	58
41	Vehicle Bending Moments Due to Inertial Loading Only	59
42	Vehicle Shear Force Due to Aerodynamic Loading During Entry	60
43	Vehicle Bending Moments Due to Aerodynamic Forces Only	61
44	Vehicle Net Shear Force During Entry	63
45	Vehicle Maximum Bending Moments During Entry Trajectory	64
46	Bending Moments Experienced by 1.3×10^6-Pound Vehicle	65
47	Axial Load for 1.3×10^6-Pound Vehicle	66

Figure		Page
48	Effect of Initial Tank Temperatures on Surface Temperature History	76
49	Surface Temperature History for 1.3×10^6-Pound Vehicle	77
50	Effect of Vehicle Size on Surface Temperature History	78
51	Effect of Material on Surface Temperature	79
52	Maximum Surface Temperature During Entry	81
53	Thermal History Profile Through Microquartz Insulation	82
54	Thermal Stresses for Sandwich Design on Small Vehicle	86
55	Thermal Stresses for Sandwich Design on Large Vehicle	87
56	Material Properties Variation With Temperature - Aluminum	93
57	Material Properties Variation With Temperature - Titanium	94
58	Material Properties Variation With Temperature - Inconel	95
59	Material Properties Variation With Temperature - René 41	96
60	Effect of Temperature on Unit Weight of Pressurized Forward Tankwall	105
61	Effect of Temperature on Unit Weight of Unpressurized Crew Compartment	106
62	Material Efficiency With Temperature Restrictions on Crew Compartment	107
63	Unit Weight Reductions With Material Improvements	109
64	Exchange Ratios for Recoverable First Stage of 1.3×10^6-Pound Vehicle	119
65	Synthesis Program	142

TABLES

Table		Page
1	Stage Velocity Requirements for Recoverable-Expendable Vehicles	12
2	Propulsion and Propellant Characteristics	13
3	Vehicle Design Characteristics	15
4	Initial Conditions	32
5	Analytical Comparison for 1.3×10^6-Pound Vehicle	33
6	Recoverable First-Stage Entry Heating Loads	56
7	Base-Point Vehicle Design Pressure Matrix	67
8	Vehicle Design Load Intensities	70
9	Test Cases Synthesized for Fuselage Structural Shells	90
10	Structural Design Details	91
11	Minimum Skin Thicknesses for Temperature Control	98
12	Design Synthesis Printout - Minimum Weight Design	99
13	Unit Shell Weights for Insulated Aluminum Designs	101
14	Unit Shell Weights for René 41 Designs at Various Temperatures	102
15	Unit Shell Weights for Titanium Designs at Various Temperatures	103
16	Unit Shell Weights for Inconel Designs at Various Temperatures	104
17	Weight Complexity Factors	112
18	Base-Point Vehicle Payload Exchange Partials	118
19	Complexity Factors	122
20	Relative Cost Ratio Effectiveness	123
21	Computer Printouts for Component Merit Functions	124
22	Merit Functions for 1.3×10^6-Pound Vehicle - Aluminum Plus Insulation	126
23	Merit Functions for 1.3×10^6-Pound Vehicle - René 41	127
24	Merit Functions for 1.3×10^6-Pound Vehicle - Titanium	128
25	Merit Functions for 1.3×10^6-Pound Vehicle - Inconel	129
26	Merit Functions for 1.9×10^6-Pound Vehicle - Aluminum Plus Insulation	130
27	Merit Functions for 1.9×10^6-Pound Vehicle - René	131
28	Merit Functions for 1.9×10^6-Pound Vehicle - Titanium	132
29	Merit Functions for 1.9×10^6-Pound Vehicle - Inconel	133

Table		Page
30	Merit Functions for 2.5 x 10^6-Pound Vehicle - Aluminum Plus Insulation	134
31	Merit Functions for 2.5 x 10^6-Pound Vehicle - René 41	135
32	Merit Functions for 2.5 x 10^6-Pound Vehicle - Titanium	136
33	Merit Functions for 2.5 x 10^6-Pound Vehicle - Inconel	137
34	Options on Program Routing	146

INFLUENCE OF STRUCTURE AND MATERIAL RESEARCH ON ADVANCED LAUNCH SYSTEMS' WEIGHT, PERFORMANCE, AND COST

Phase III

Design Synthesis of Recoverable Launch Vehicle Structures

By J.A. Boddy
Space Division
North American Rockwell Corporation

SUMMARY

The third phase of this contract was concerned with the design synthesis of recoverable first stages to assess the relative benefits to be derived from advancements in structures and materials, and with the documentation and turnover to NASA of the synthesis programs used during Phase I of this study.

The parametric vehicle synthesis approaches initiated in Phase I for a wide spectrum of expendable vehicle systems were extended in Phase II to encompass vehicle systems with recoverable first stages. Recovery was considered to be accomplished with winged body stages possessing flyback propulsion systems and horizontal landing capability. Base-point recoverable vehicles were derived in Phase II for predicted improvements in propulsion systems and propellant characteristics considering advances through two time periods: near term - 1970 to 1980, and future - post 1980. For each of these periods, three vehicle systems were defined and classified into the following sizes:

1.3×10^6-pound launch weight - small payload
1.9×10^6-pound launch weight - medium payload
2.5×10^6-pound launch weight - large payload

These launch weights were associated with vehicle systems that, in a fully recoverable flight mode for both first- and second-stage, would deliver in orbit useful payloads of 20, 000, 40, 000 and 60, 000 pounds respectively.

During this Phase (III), structural synthesis was conducted for the major structural shell components of the recoverable first stages. Conventional constructions (skin stringer, waffle, and honeycomb sandwich) were considered for the pressurized and unpressurized shells. These shells were synthesized as "hot structures" using titanium, Rene´41, and Inconel alloys and as insulated aluminum concepts with microquartz insulation and a Rene 41 heat shield.

The method of evaluation involved a component-by-component substitution in the base-point vehicle systems. Estimated manufacturing complexity factors, material costs with year, and man-hour requirements were included in the cost assessment. Cost assessment was accomplished by isolating each structural component and performing a comparative evaluation of the new component to the base-point component, which was considered to be aluminum integral skin-stringer construction. Final assessment is made in terms of component weight reduction, equivalent payload gained from this reduction, and cost ratio for the new component, which is identified as additional dollars cost per pound of payload gained. The three merit functions are then organized in arrays to order their importance.

The family of recoverable first stages that were investigated did not experience a severe thermal profile during the entry trajectory. The vehicle systems were staged at 6300 ft/sec and 150, 000-ft altitude, which will produce an optimal proportioned two-stage vehicle system. With these burnout conditions and the ensuing small heat load, the unprotected "hot structure" should not experience temperatures greater than 1300°R. The insulated concepts required only a nominal protection system to adequately protect the aluminum load-carrying structure.

With the reusable structures, it was found that the minimum weight design for an acceptable arrangement was the most beneficial. This is due to the high payload exchange ratios and the repeated missions over which the original construction cost can be amortized. Therefore, the predominant parameter in the cost makeup will be the relative cost of refurbishing the structural concepts. These costs will be different for the "hot structures" and the fully insulated concepts.

For the weight penalties assigned to the external thermal protection system, it appears that the insulated aluminum designs for this series of vehicles would produce the most efficient structure from the weight and cost standpoint. With the load-carrying structure designed for the ascent portion of the trajectory, there was sufficient skin thickness to act as a heat sink and keep the maximum temperature experienced by the "hot structures" within acceptable bounds. Of the three materials used for the "hot structures,"

it was found that titanium produces the lightest weight design. When restrictions are imposed on the operating temperature (1000 to 1100°R) of the load-carrying structures, severe weight penalties result for the "hot structures" concept.

Although the lightest construction concept is honeycomb sandwich, when it is designed for the hot structural concept the thin outer facing sheet does not act as a large heat sink. The honeycomb core will act as a thermal barrier between the facing sheets and will cause a substantial thermal gradient and, hence, thermal stresses. Therefore, with the honeycomb design, the high-working temperatures of René 41 and Inconel cannot be effectively used because of increased skin thicknesses required to handle the high thermal stresses.

Although waffle pattern and integral skin stringer designs are the lightest construction concepts, they have an adverse cost ratio. This is because of the material cost of the parent stock before fabrication. This was not so noticeable for aluminum; but when the other materials were considered, materials costs outweighed fabrication costs.

Generally, research would be more beneficial when devoted to manufacturing and design development for new and advanced structural concepts and for developing materials with markedly improved mechanical and physical properties rather than by forcing improvement of current material ultimate strength properties.

The computer programs for vehicle synthesis and structural design synthesis were consolidated with a master executive control program, and the total program was demonstrated on the NASA computer facility at the Electronic Research Center, Boston, Massachusetts. A detailed description of these programs is given in Volume II of this report.

INTRODUCTION

For investigation of the effects and benefits from material and structural research as applied to vehicle systems, a realistic series of base-point vehicle systems is required. This requirement is more applicable when structural improvements are assessed against a vehicle system that possesses a recoverable stage. For such a system, the ratio of payload weight to vehicle lift-off weight can be about 3 to 4 percent, and any weight reductions will have a noticeable effect on payload improvement.

To size a realistic vehicle, one has to consider the development period in order to include not only predicted advancements in material and structures, but also those advancements that would probably occur in the other disciplines that primarily influence the vehicle design. For example, the vehicle propulsion system must be representative of the period considered: items such as changes in thrust, specific impulse, propellant density, and the basic engine accessories must be unique to that particular period. The complicated interplay of these parameters is difficult to measure manually and, therefore, requires this automated procedure to make these interactions fully understood.

From a structural standpoint, the size, design loading, and thermal environment of a structural component have considerable influence upon the choice of materials, types of constructions, and fabrication method employed. For a realistic determination of what these advanced launch vehicles and their structural design environments might represent, it is necessary to begin with a mission definition and to establish payload, vehicle size, and performance characteristics. Vehicle system parameters strongly interact, and the vehicle structural system is greatly influenced by each of them. With its strong dependency on other subsystems, structural sciences research cannot be evolved in a vacuum. It must reflect the basic mission requirement and its interaction with the structural system and the other functional systems. Economic measurements must be included to determine the worth of conducting research in a particular structural area.

During the Phase II study a series of base-point vehicles with recoverable first stages were defined by the parametric vehicle synthesis programs. The vehicles considered were vertical-launched, tandem-staged, bipropellant systems. Major elements of the study were the evaluation of comparative

configurations and their performance for several orbital transport systems having recoverable first stages with a typical range of payload capability (20 000 to 60 000 pounds).

Identical system design philosophy was maintained, where possible, in order to enhance the comparison with expendable vehicle systems. Consequently, both systems utilized the same tandem stage and tankage arrangement, vertical takeoff mode, boost trajectory profile, and design and load criteria. Sensitivity to some of these parameters was monitored during the study to investigate their effects on the complete base-point vehicles.

This series of base-point vehicles were further analyzed for better definition of the design and thermal loading environment and to conduct detail structural analysis and tradeoff studies. The preliminary design synthesis program defines the major structural components of the fuselage of the recoverable first stage. Each component is designed for a variety of design load conditions encountered during various regions of the vehicle mission trajectory. The major structural shell components were synthesized for investigation of the relative benefits arising from structure and material advances applied to their design. The types of materials considered included superalloys and conventional material thermally protected with conventional insulation.

APPROACH

The design synthesis techniques developed for expendable vehicles during Phase II were extended to provide specific design synthesis subroutines for the structural design evaluation of recoverable first stages. The family of vehicle systems (both near term and projected future concepts) developed in the previous phase of the contract was used as the base-point vehicles for the design synthesis exercise to investigate the effects of structures and material advancements.

The design synthesis consists of three steps: environment definition, design synthesis, and tradeoff studies.

The interconnection for these three steps is indicated in figure 1. The starting inputs for the preliminary design synthesis are specific base-point vehicle configurations defined by the parametric synthesis programs in Phase II. The vehicle definition consists of stage size, performance, major component weight breakdown, and an empirical relationship for the design environment. This environment has been defined more explicitly for the parametric base-point vehicles to allow realistic design loads, temperature, etc., to be used for the structural design tradeoff studies. Since the main emphasis is on the structural design and its interaction with new concepts and materials, a comprehensive integrated automatic analysis of the vehicle's trajectory, aerothermal environment, and loading is outside the scope of this study. Instead, existing Space Division programs were used to evaluate the required environmental data for the preliminary design. These programs are outside the main framework of the automatic design synthesis programs and were used only to substantiate the parametric environment data.

Additional synthesis routines were developed to describe the effects of the entry thermal profile on the first-stage fuselage. These routines were used to investigate the temperature-time histories of the base-point vehicles for a variety of construction designs and materials. The structural concepts of a hot structure (superalloys) or a conventional insulated concept were considered in order to determine the effect the back face thermal temperature had on the load-carrying capability of the primary structure and the associated weight penalties incurred.

The preliminary design synthesis program defines the major structural components of the recoverable first stage. Each component is designed for

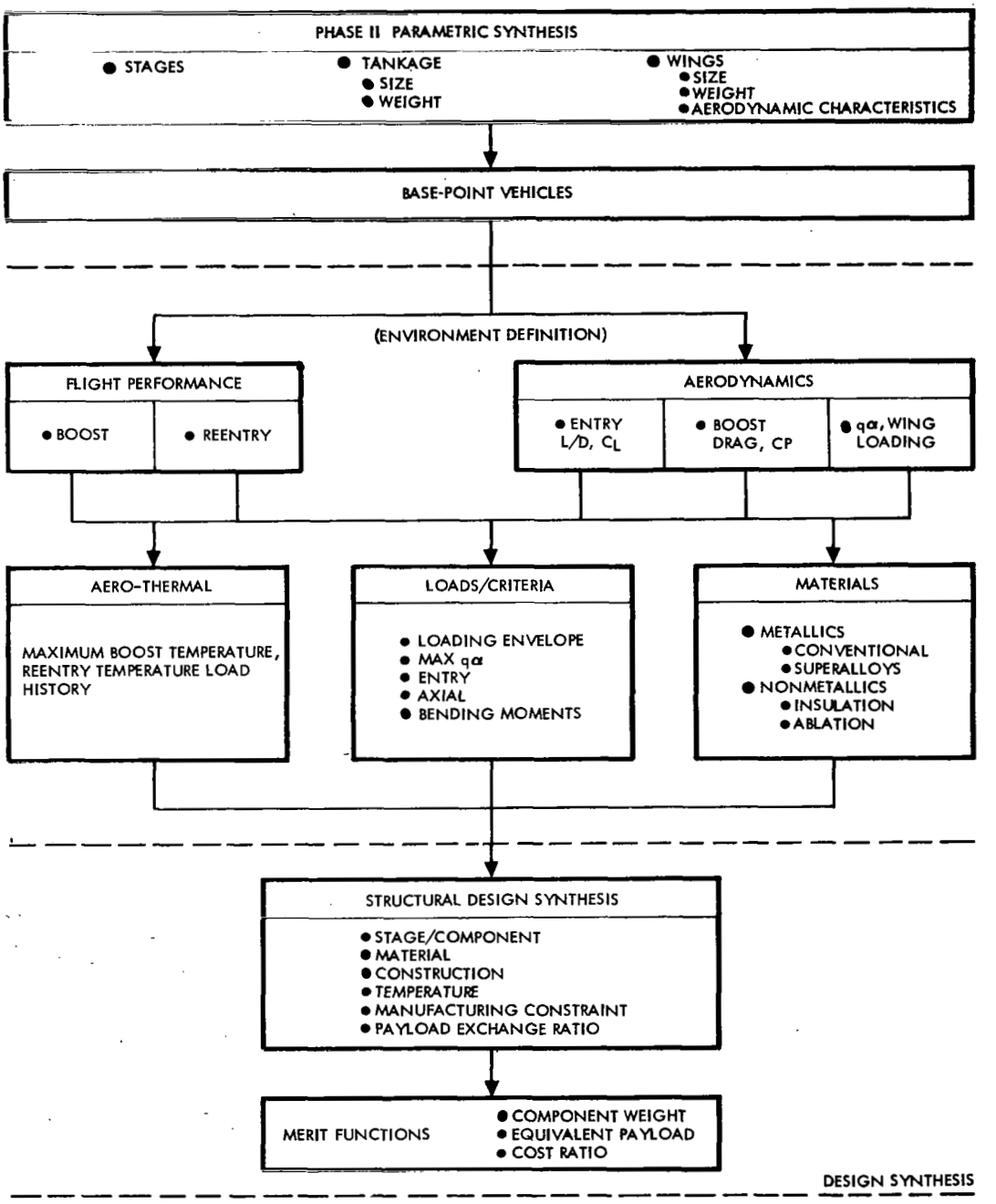

Figure 1. - Design Synthesis Logic

a variety of design load conditions encountered during various regions of the vehicle mission trajectory. The major components (shells and tanks) were synthesized to investigate the relative benefits arising from their design improvements. The remaining subsystems of the recoverable stage were still only considered in a parametric weight estimation in order to develop the overall mass fraction of the stage. Initial data cases were involved with defining the individual structural element weights for the base-point vehicle, using a nominal baseline material and construction. Additional synthesis test cases were generated and compared with the baseline material and construction by the assessment subroutine.

VEHICLE DEFINITION AND ENVIRONMENT

Base-Point Vehicle Description

The area of interest for the fully recoverable vehicle system was defined in Phase II to be for vehicle systems with capability of placing in Earth orbit payloads ranging from 20 000 to 60 000 pounds. To achieve these payloads with a practical size and cost-effective system, it was decided to use uprated propulsion and propellant systems; that is, post-1975 system characteristics. Three typical launch weights (1.3, 1.9 and 2.5 million pounds) were found to correspond approximately to fully recoverable vehicles with 20 000; 40 000; and 60 000-pound payloads, respectively. Therefore, these three launch weights were used to assist in the parametric design of vehicle systems where only the first stage was recoverable.

Phase II of the study was limited to the parametric synthesis of vertical-launched, tandem-staged, bipropellant vehicles, with the first stage having a fully recoverable capability and with an expendable upper stage (fig. 2). The recovery mode for the first-stage vehicle was to perform various flight maneuvers to reduce apogee and entry heating and loading and to provide subsonic cruise capability for a specified range and a final horizontal landing.

For a family of mission requirements and typical velocities, a series of design ground rules emerge for the recoverable vehicle systems synthesized for this study and are given as follows:

1. Vertical launched, horizontal recovery

2. Two-stage (first stage recoverable, second stage expendable), tandem-staging arrangement.

3. Designed with near-term (1970 to 1980) and future (post-1980) system characteristics

4. Payload spectrum associated with 20 000 to 60 000 pounds for a fully recoverable system

5. Eastward launch from Atlantic Mission Range (AMR) and mission orbit attitude of 262 nautical miles

6. Maximum boost acceleration: 4 g's

7. Boost phase terminates with circular injection at 50 nautical miles

8. Propellant: LO_2 - RP1 first stage
   LO_2 - LH_2 second stage

9. Thrust-to-weight ratios of 1.25 first stage and 1.0 second stage

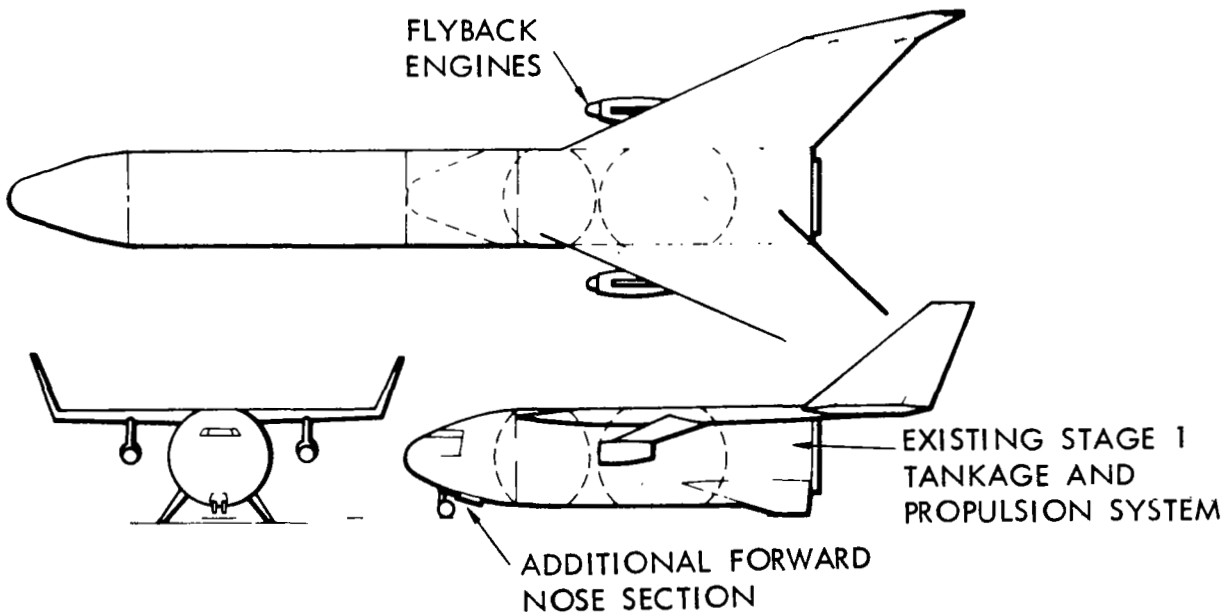

Figure 2. - Typical Recoverable First-Stage Vehicle

The total mission profile and its associated velocity requirements were considered for a two-stage vehicle system. Preliminary parametric sizing of the vehicle indicated that with regard to minimization of launch weight for the design conditions considered, an efficient staging velocity would be around 6500 fps. Therefore, the total mission profile, particularly the ascent phase, was similar to that of the vertically launched Reusable Orbital Transport (ref. 1). A schematic of the ascent profile is shown in figure 3 with first-stage boost to 6500 fps at an altitude of 175 000 feet and a flight

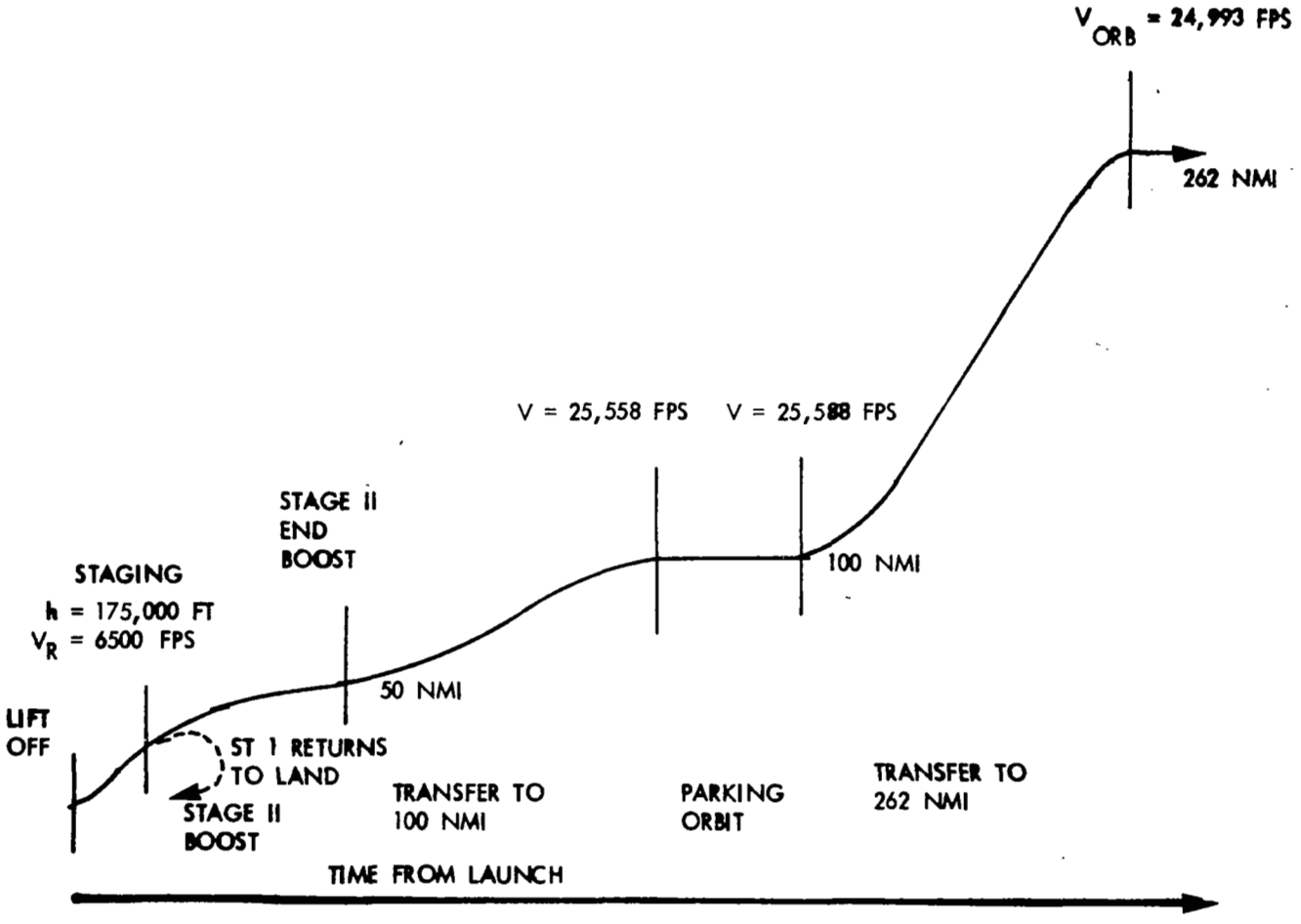

Figure 3. - Ascent Profile

path angle of 20 degrees. At this point, stage separation is commanded, and the second stage proceeds to a parking orbit and thence, via Hohmann transfer, to its rendezvous orbit. The velocity requirement associated with the ascent, rendezvous, and deorbit are defined in Table 1.

TABLE 1. - STAGE VELOCITY REQUIREMENTS FOR RECOVERABLE-EXPENDABLE VEHICLES

Velocity Factor	Requirement (fps)
Circular velocity at 50 n. mi.	25 740
Less Earth rotation	1 246
Net velocity to be gained	24 494
Total velocity requirement for first stage (includes velocity losses)	10 060
Second-stage boost requirements	17 694
Hohmann transfer at 50 to 100 n. mi.	91
Launch window	100
Hohmann transfer to 100-n. mi. apogee V	91
Hohmann transfer to 262-n. mi.	529
1.5% reserve for deviation from normal operating procedure	300
Second-stage velocity losses	1 010
Total velocity requirement for second stage	19 815

The recoverable launch stages involve two primary propulsion systems: one for the launch phase and one for the powered flyback phase of recovery. During Phase 1 of this study (ref. 2) liquid-propellant rocket engines were investigated on the basis of past developments, scheduled future developments, and projected capabilities during the 1975 to 1985 period. Advanced propulsion systems investigated during Phase 1 of the study were taken to be applicable for the recoverable vehicle systems. For consistency between the phases of this study, identical characteristics were used, as follows:

Near-term: Post-1975

First stage	LO_2/RP_1 system	308 seconds average
Second stage	LO_2/LH_2 system	460 seconds

Fixture: Post-1985

First stage	LO_2/RP_1 system	340 seconds average
Second stage	LO_2/LH_2 system	500 seconds

The remaining propulsion and propellant characteristics used for the vehicle sizing are shown in table 2.

TABLE 2. - PROPULSION AND PROPELLANT CHARACTERISTICS

Characteristic	Value	
	Stage 1	Stage 2
Engine system propellants	LO_2/RP_1	LO_2/LH_2
Thrust-to-weight at liftoff	1.25	1.0
Number of engines	5	1
Number of movable engines	4	
Chamber pressure, psi	1000	632
Engine expansion ratio	25	35
Gimbal range at max q	4.0°	
Mixture ratio oxid/fuel	2.25	5.0
Oxidizer density, lb/in^3	0.0413	0.0413
Fuel density, lb/in^3	0.0292	0.00256
Ullage factor, percent	10	15
Ullage pressure, lb/in^2	39.0	36.0

The flyback propulsion and range requirements were assumed to be for a typical subsonic turbofan engine, these engines being assumed to be adequately protected against high temperature during entry. The system design parameters for the flyback system are shown below.

Flyback range	300 n. mi.
Flyback (L/D) maximum	5.0
Flyback cruise Mach number	0.6
Specific fuel consumption	0.7 lb/hp/hr
Thrust to installed engine weight ratio	3.0

The basic vehicle design characteristics for the tanks, bulkheads, wing planform, etc., are given in table 3; a pictorial representation of the structural arrangement for the recoverable stage is shown in figure 4.

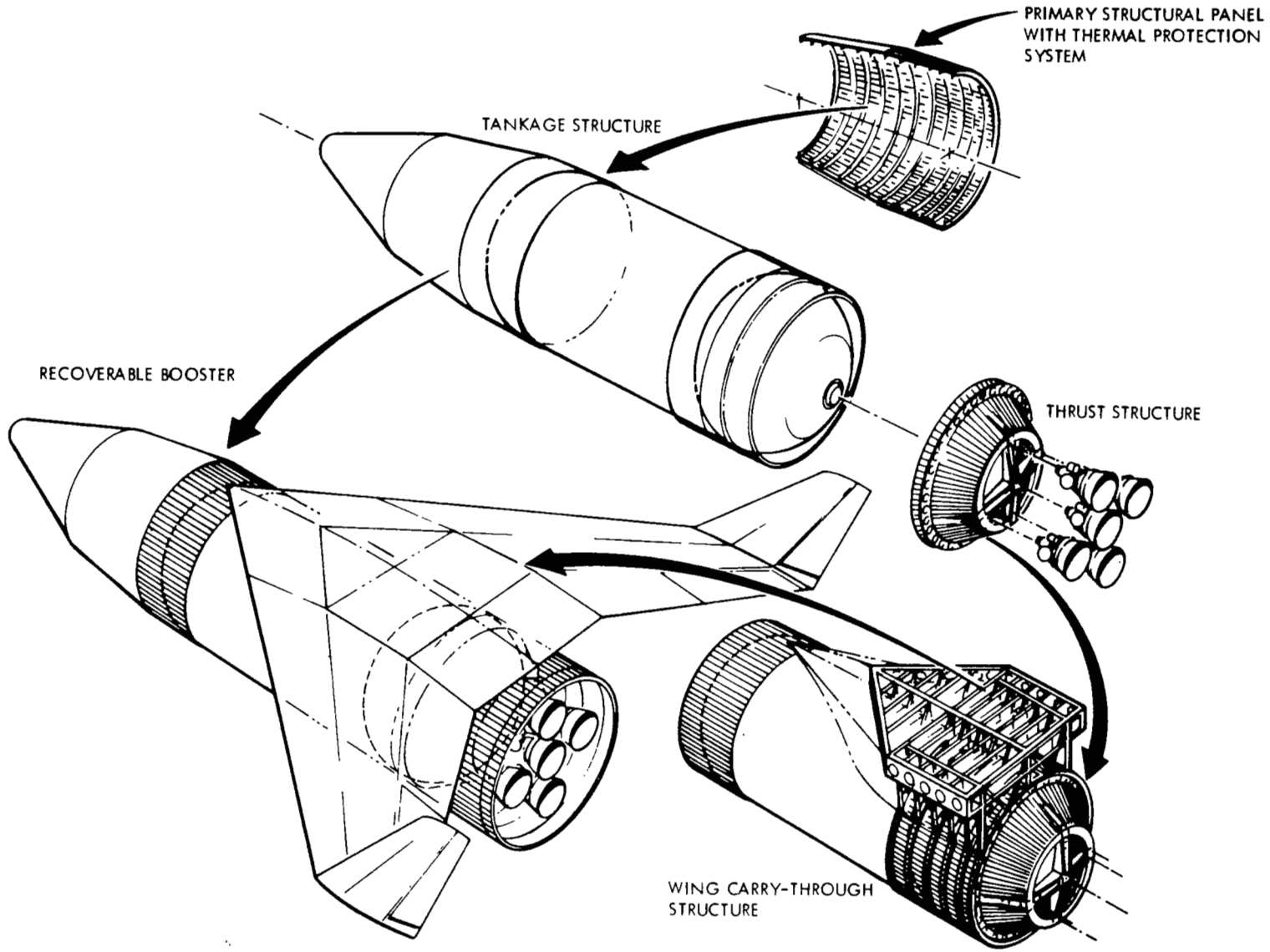

Figure 4. - Recoverable First-Stage Booster Concept

TABLE 3. - VEHICLE DESIGN CHARACTERISTICS

Characteristic	Value
Bulkhead aspect ratio	
Stage 1	$\sqrt{2}$
Stage 2	$\sqrt{2}$
Separate bulkheads Stage 1	
Common bulkheads Stage 2	
Payload fineness ratio for cylinder	0.5
Payload cone half-angle	35°
Crew equipment weight	3000 lb
Wing aspect ratio, minimum	2.25
Wing aspect ratio, maximum	2.5
Wing taper ratio	0.45
Maximum allowable leading edge sweep	60°
Thickness-to-chord ratio, percent	8
Fin area to wing area, percent	8
Hypersonic wing loading during entry	50 lb/ft^2

The parametrically derived vehicle systems were subsequently subjected to detailed analysis to see if the basic assumed empirical relationships and aerodynamic coefficients were consistent with the final sized vehicle systems. The subsequent sections of this report dealing with the redefinition of the environment, performance, and design characteristics indicate that the parametric assessment was quite realistic and the differences sufficiently small that the original base-point vehicles were not resized, but their design thermal environment was updated. The appropriate sizes and dimensions for the six base-point vehicles are given in figure 5, the performance and major weight breakdown in figure 6, and the system weight distribution for prelaunch, maximum dynamic pressure, and end boost are given in figures 7, 8, and 9.

Aerodynamic Characteristics

The prime objective of this analysis was to determine the aerodynamic characteristic of the vehicle system to assure satisfactory flight performance

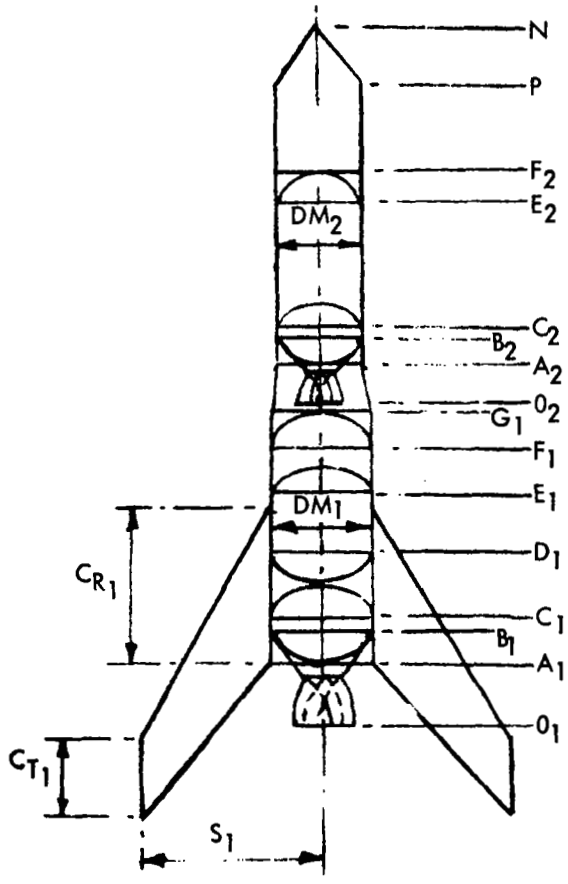

Dimensions in inches

	Station	VEHICLE LAUNCH WEIGHT					
		1.3×10^6 lb		1.9×10^6 lb		2.5×10^6 lb	
		Near	Future	Near	Future	Near	Future
STAGE ONE	N	—	—	—	—	—	—
	P	—	—	—	—	—	—
	C_T	216.0	213.0	258.0	255.0	295.0	292.0
	C_R	479.0	473.0	573.0	567.0	655.0	648.0
	S	521.0	516.0	617.0	612.0	694.0	689.0
	DM	260.0	260.0	300.0	300.0	320.0	320.0
	G	915.8	889.5	1001.7	972.9	1118.7	1085.4
	F	785.8	759.5	851.7	822.9	958.7	925.4
	E	693.9	667.6	780.5	751.7	895.0	861.7
	D	524.8	515.1	602.7	592.2	676.7	664.4
	C	325.3	315.6	372.6	362.0	431.2	418.9
	B	264.5	265.3	313.3	314.2	350.0	350.9
	A	172.6	173.4	207.2	208.1	236.8	237.8
	0	0	0	0	0	0	0
STAGE TWO	N	2025.9	2075.8	2232.7	2283.4	2429.0	2475.1
	P	1868.8	1918.7	2047.1	2097.7	2214.8	2260.8
	C_T	—	—	—	—	—	—
	C_R	—	—	—	—	—	—
	S	—	—	—	—	—	—
	DM	220.0	220.0	260.0	260.0	300.0	300.0
	G	—	—	—	—	—	—
	F	1758.8	1808.7	1917.1	1967.7	2064.8	2110.8
	E	1681.0	1730.9	1825.1	1875.8	1958.7	2004.7
	D	—	—	—	—	—	—
	C	1254.7	1175.3	1293.3	1383.2	1428.3	1422.8
	B	1124.3	1106.8	1250.9	1232.6	1405.3	1383.7
	A	1046.5	1029.0	1159.0	1140.6	1299.2	1277.7
	0	1026.5	1007.6	1134.9	1114.8	1271.6	1248.1

Figure 5. - Vehicle Size Characteristics

LAUNCH WEIGHT	PROPULSION SYSTEM	NEAR TERM I_{SP}		FUTURE I_{SP}	
1.3×10^6 POUNDS	STAGE	1	2	1	2
	WEIGHT (LB)				
	PAYLOAD	339212.	58528.	389469.	80351.
	BURN-OUT	133664.	30492.	130778.	33403.
	STRUCTURE/SUBSYSTEMS	111764.	23296.	108878.	25417.
	ENGINES	21900.	7196.	21900.	7986.
	PROPELLANT	831124.	250192.	783754.	275715.
	STAGE	964788.	280684.	914531.	309117.
	RATIOS				
	PERFORMANCE	0.63736	0.73757	0.60104	0.70793
	MASS FRACTION	0.86146	0.89137	0.85700	0.89194
	DELTA VELOCITY (FPS)	10060.	19815.	10060.	19815.
	SPECIFIC IMPULSE (SEC)	308.	460.	340.	500.
1.9×10^6 POUNDS	PAYLOAD	499852.	88023.	572358.	120232.
	BURN-OUT	189155.	43153.	185669.	46939.
	STRUCTURE/SUBSYSTEMS	157746.	33514.	154260.	36263.
	ENGINES	31409.	9639.	31409.	10676.
	PROPELLANT	1210993.	368675.	1141972.	405187.
	STAGE	1400148.	411829.	1327642.	452126.
	RATIOS				
	PERFORMANCE	0.63736	0.73757	0.60104	0.70793
	MASS FRACTION	0.86490	0.89522	0.86015	0.89618
	DELTA VELOCITY (FPS)	10060.	19815.	10060.	19815.
	SPECIFIC IMPULSE (SEC)	308.	460.	340.	500.
2.5×10^6 POUNDS	PAYLOAD	663651.	117696.	758655.	160220.
	BURN-OUT	242936.	56467.	238750.	61364.
	STRUCTURE/SUBSYSTEMS	202083.	44530.	197896.	48161.
	ENGINES	40854.	11936.	40854.	13203.
	PROPELLANT	1593412.	489489.	1502595.	537071.
	STAGE	1836349.	545955.	1741345.	598435.
	RATIOS				
	PERFORMANCE	0.63736	0.73757	0.60104	0.70793
	MASS FRACTION	0.86771	0.89657	0.86289	0.89746
	DELTA VELOCITY (FPS)	10060.	19815.	10060.	19815.
	SPECIFIC IMPULSE (SEC)	308.	460.	340.	500.

Figure 6. - Vehicle Weight and Performance Characteristics

NEAR-TERM I_{SP}

		PRELAUNCH		MAX Q ALPHA		END BOOST	
STATION	DIA	WEIGHT	STATION	WEIGHT	STATION	WEIGHT	STATION
173.	260.	24669.	121.	24669.	121.	24669.	121.
265.	260.	138021.	219.	138021.	219.	13415.	219.
325.	260.	91270.	295.	50071.	295.	8871.	295.
525.	260.	305759.	425.	170582.	425.	35405.	425.
694.	260.	245436.	609.	130857.	609.	16278.	609.
786.	260.	133457.	740.	8851.	740.	8851.	740.
916.	260.	15516.	851.	15516.	851.	15516.	851.
1046.	220.	19776.	994.	19776.	994.	19776.	994.
1124.	220.	29800.	1085.	29800.	1085.	29800.	1085.
1177.	220.	20148.	1151.	20148.	1151.	20148.	1151.
1255.	220.	29800.	1216.	29800.	1216.	29800.	1216.
1681.	220.	163307.	1468.	163307.	1468.	163307.	1468.
1759.	220.	29800.	1720.	29800.	1720.	29800.	1720.
1759.	220.	0.	1720.	0.	1720.	0.	1720.
2026.	220.	58528.	1861.	58528.	1861.	58528.	1861.
TOTAL WEIGHT		1305285.		911623.		496062.	
CENTER OF GRAVITY		739.		805.		1142.	

FUTURE I_{SP}

		PRELAUNCH		MAX Q ALPHA		END BOOST	
STATION	DIA	WEIGHT	STATION	WEIGHT	STATION	WEIGHT	STATION
173.	260.	24668.	121.	24668.	121.	24668.	121.
265.	260.	136242.	219.	136242.	219.	13313.	219.
316.	260.	74614.	290.	40952.	290.	7291.	290.
515.	260.	302035.	415.	168677.	415.	35318.	415.
668.	260.	218464.	591.	116536.	591.	14609.	591.
760.	260.	131739.	714.	8809.	714.	8809.	714.
890.	260.	15457.	825.	15457.	825.	15457.	825.
1029.	220.	21351.	973.	21351.	973.	21351.	973.
1107.	220.	29979.	1068.	29979.	1068.	29979.	1068.
1175.	220.	26411.	1141.	26411.	1141.	26411.	1141.
1253.	220.	29979.	1214.	29979.	1214.	29979.	1214.
1731.	220.	184105.	1492.	184105.	1492.	184105.	1492.
1809.	220.	29979.	1770.	29979.	1770.	29979.	1770.
1809.	220.	0.	1770.	0.	1770.	0.	1770.
2076.	220.	80351.	1911.	80351	1911.	80351.	1911.
TOTAL WEIGHT		1305372.		935395.		543519.	
CENTER OF GRAVITY		780.		861.		1202.	

Figure 7. - Weight Distribution During First-Stage Boost - 1.3×10^6-Pound Vehicle

NEAR-TERM I_{SP}

STATION	DIA	PRELAUNCH WEIGHT	PRELAUNCH STATION	MAX Q ALPHA WEIGHT	MAX Q ALPHA STATION	END BOOST WEIGHT	END BOOST STATION
207.	300.	35711.	145.	35711.	145.	35711.	145.
313.	300.	208778.	260.	208778.	260.	19677.	260.
373.	300.	116621.	343.	63806.	343.	10992.	343.
603.	300.	463774.	488.	258631.	488.	53487.	488.
780.	300.	339018.	692.	180580.	692.	22142.	692.
887.	300.	202314.	834.	13213.	834.	13213.	834.
1002.	300.	17336.	944.	17336.	944.	17336.	944.
1159.	260.	29232.	1096.	29232.	1096.	29232.	1096.
1251.	260.	48651.	1205.	48651.	1205.	48651.	1205.
1293.	260.	22412.	1272.	22412.	1272.	22412.	1272.
1385.	260.	48651.	1339.	48651.	1339.	48651.	1339.
1825.	260.	232794.	1605.	232794.	1605.	232794.	1605.
1917.	260.	48651.	1871.	48651.	1871.	48651.	1871.
1917.	260.	0.	1871.	0.	1871.	0.	1871.
2233.	260.	88023.	2038.	88023.	2038.	88023.	2038.
TOTAL WEIGHT		1901965.		1327877.		722380.	
CENTER OF GRAVITY		829.		898.		1267.	

FUTURE I_{SP}

STATION	DIA	PRELAUNCH WEIGHT	PRELAUNCH STATION	MAX Q ALPHA WEIGHT	MAX Q ALPHA STATION	END BOOST WEIGHT	END BOOST STATION
208.	300.	35724.	146.	35724.	146.	35724.	146.
314.	300.	206041.	261.	206041.	261.	19589.	261.
362.	300.	92887.	338.	50859.	338.	8831.	338.
592.	300.	458033.	477.	255763.	477.	53493.	477.
752.	300.	300327.	672.	160091.	672.	19855.	672.
858.	300.	199651.	805.	13199.	805.	13199.	805.
973.	300.	17320.	915.	17320.	915.	17320.	915.
1141.	260.	31542.	1074.	31542.	1074.	31542.	1074.
1233.	260.	48949.	1187.	48949.	1187.	48949.	1187.
1291.	260.	31241.	1262.	31241.	1262.	31241.	1262.
1383.	260.	48949.	1337.	48949.	1337.	48949.	1337.
1876.	260.	262265.	1629.	262265.	1629.	262265.	1629.
1968.	260.	48949.	1922.	48949.	1922.	48949.	1922.
1968.	260.	0.	1922.	0.	1922.	0.	1922.
2283.	260.	120232.	2088.	120232.	2088.	120232.	2088.
TOTAL WEIGHT		1902112.		1362534.		791548.	
CENTER OF GRAVITY		873.		958.		1329.	

Figure 8. - Weight Distribution During First-Stage Boost - 1.9×10^6-Pound Vehicle

NEAR-TERM I_{SP}

STATION	DIA	PRELAUNCH WEIGHT	PRELAUNCH STATION	MAX Q ALPHA WEIGHT	MAX Q ALPHA STATION	END BOOST WEIGHT	END BOOST STATION
237.	320.	46461.	166.	46461.	166.	46461.	166.
350.	320.	257871.	293.	257871.	293.	24107.	293.
431.	320.	185088.	391.	101196.	391.	17303.	391.
677.	320.	574751.	554.	321155.	554.	67559.	554.
895.	320.	481913.	786.	256459.	786.	31005.	786.
1008.	320.	249838.	952.	16074.	952.	16074.	952.
1119.	320.	18704.	1063.	18704.	1063.	18704.	1063.
1299.	300.	37577.	1227.	37577.	1227.	37577.	1227.
1405.	300.	73778.	1352.	73778.	1352.	73778.	1352.
1428.	300.	16034.	1417.	16034.	1417.	16034.	1417.
1534.	300.	73778.	1481.	73778.	1481.	73778.	1481.
1959.	300.	295102.	1747.	295102.	1747.	295102.	1747.
2065.	300.	73778.	2012.	73778.	2012.	73778.	2012.
2065.	300.	0.	2012.	0.	2012.	0.	2012.
2429.	300.	117696.	2204.	117696.	2204.	117696.	2204.
TOTAL WEIGHT		2502370.		1746517.		949811.	
CENTER OF GRAVITY		926.		999.		1395.	

FUTURE I_{SP}

STATION	DIA	PRELAUNCH WEIGHT	PRELAUNCH STATION	MAX Q ALPHA WEIGHT	MAX Q ALPHA STATION	END BOOST WEIGHT	END BOOST STATION
238.	320.	46492.	166.	46492.	166.	46492.	166.
351.	320.	254729.	294.	254729.	294.	24044.	294.
419.	320.	153070.	385.	83759.	385.	14448.	385.
664.	320.	568242.	542.	317986.	542.	67730.	542.
862.	320.	430151.	763.	229105.	763.	28059.	763.
975.	320.	246783.	918.	16098.	918.	16098.	918.
1085.	320.	18727.	1030.	18727.	1030.	18727.	1030.
1278.	300.	40558.	1201.	40558.	1201.	40558.	1201.
1384.	300.	74305.	1331.	74305.	1331.	74305.	1331.
1423.	300.	27341.	1403.	27341.	1403.	27341.	1403.
1529.	300.	74305.	1476.	74305.	1476.	74305.	1476.
2005.	300.	333325.	1767.	333325.	1767.	333325.	1767.
2111.	300.	74305.	2058.	74305.	2058.	74305.	2058.
2111.	300.	0.	2058.	0.	2058.	0.	2058.
2475.	300.	160220.	2250.	160220.	2250.	160220.	2250.
TOTAL WEIGHT		2502554.		1792110.		1040813.	
CENTER OF GRAVITY		970.		1060.		1457.	

Figure 9. - Weight Distribution During First-Stage Boost - 2.5×10^6-Pound Vehicle

during the entire flight regime—from liftoff through boost, separation, reentry and landing. Wing size and shape for the recoverable first stage was based upon the required aerodynamic characteristics associated with the entry stage touchdown, subsonic longitudinal stability, and hypersonic wing loading. Because of heating of the empty stage during entry, the wing was restrained to a loading 50 lb/ft^2 during the vertical entry phase. The subsonic maximum lift was assessed to determine its adequacy during the touchdown maneuver. The wing so derived was located to provide neutral stability for the landing condition. The ascent boost during maximum dynamic pressure will produce a high wing loading and will provide the design criteria for several of the major structural components of the first stage. Figure 10 shows that for a typical vertical launched trajectory, the vehicle velocity is supersonic at q_{max}.

Estimated normal force, C_{N_α}, distributions are presented in figures 11 through 13 - for three launch vehicle sizes with recoverable first stages. These loadings are for the maximum q condition at $\alpha = 4°$. The loadings for the body include the interference loading on the body due to the wing panels. Loading distributions for the body alone were based on Saturn V data of reference 3 (fig. 13). This part comprises only five percent or less of the total load. Interference effects were taken from reference 4 which is based on DATCOM.

These values were assumed to hold for angles of attack of approximately 4 degrees, which correspond to the minimum load trajectory and wind gust condition. Figure 14 shows the zero lift-to-drag coefficients as a function of Mach number, which were used for the ascent trajectory evaluation. These drag coefficients were held constant for the entire family of launch vehicles.

To determine the thermal histories of the entry configurations, it was necessary to define the hypersonic aerodynamic characteristic of the first stage by itself. The entry configuration consists of the cylindrical first-stage tankage with fixed-wing panels attached in the yaw plane of the cylinder. The dimensions of the cylinder and wing panels are given in figure 5. The wings are sized for the subsonic landing flare maneuver, and their large area results in a substantial contribution to the aerodynamic forces acting on the vehicle during hypersonic flight. The vehicle nose was assumed to be a hemisphere, tangent to the cylinder at the separation plane of the first and second stages (Station F_1). A blunt nose with a shape other than hemispherical should not greatly affect the hypersonic aerodynamic force characteristics at the angles of attack at which the vehicle is trimmed. The hypersonic lift and drag characteristics for the three entry configurations, based on Newtonian theory, are presented in figures 15, 16, and 17. The maximum lift

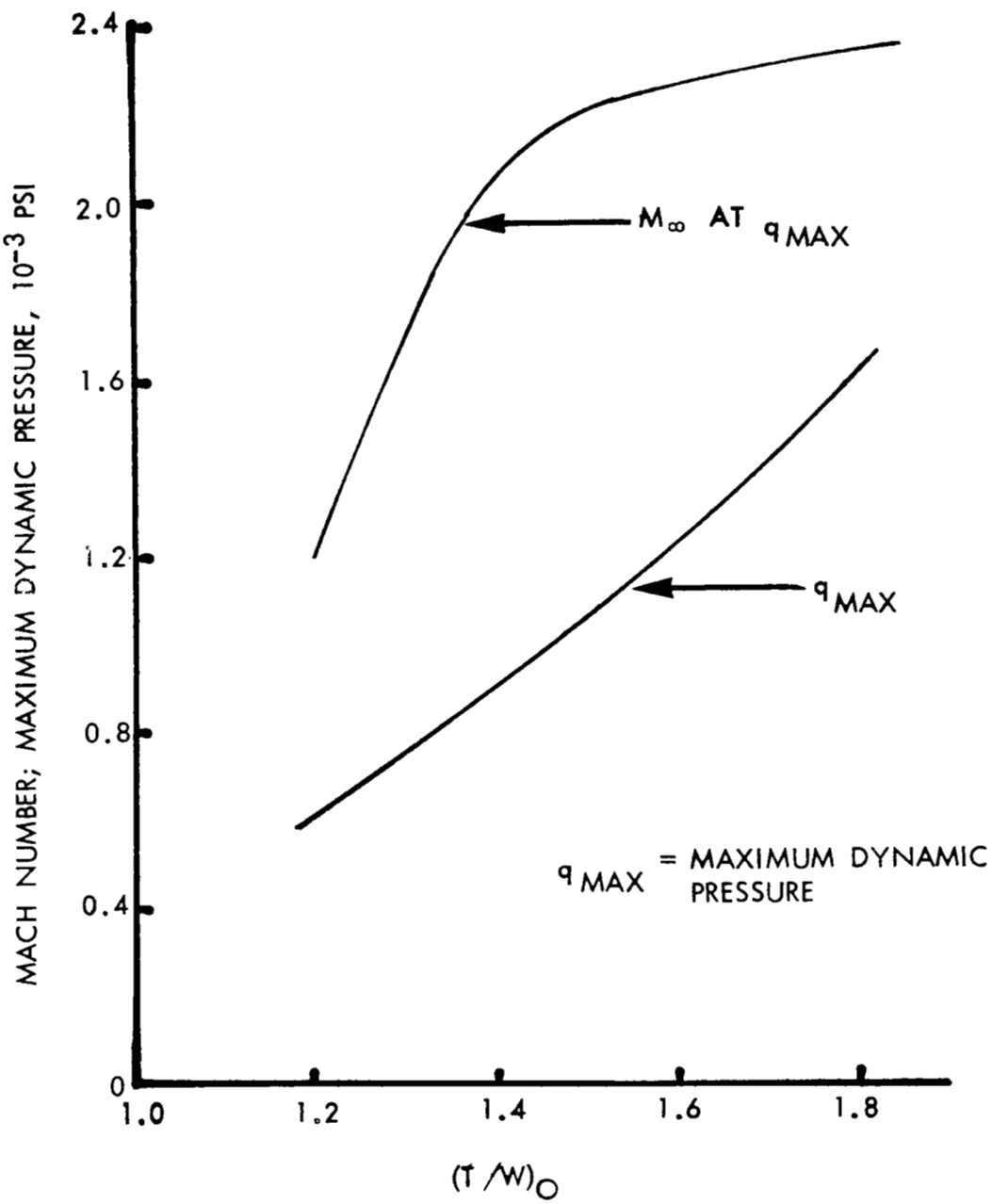

Figure 10. - Typical Dynamic Pressure and Velocity Variation With Initial Thrust-to-Weight Ratio and Typical Gravity-Turn Trajectory

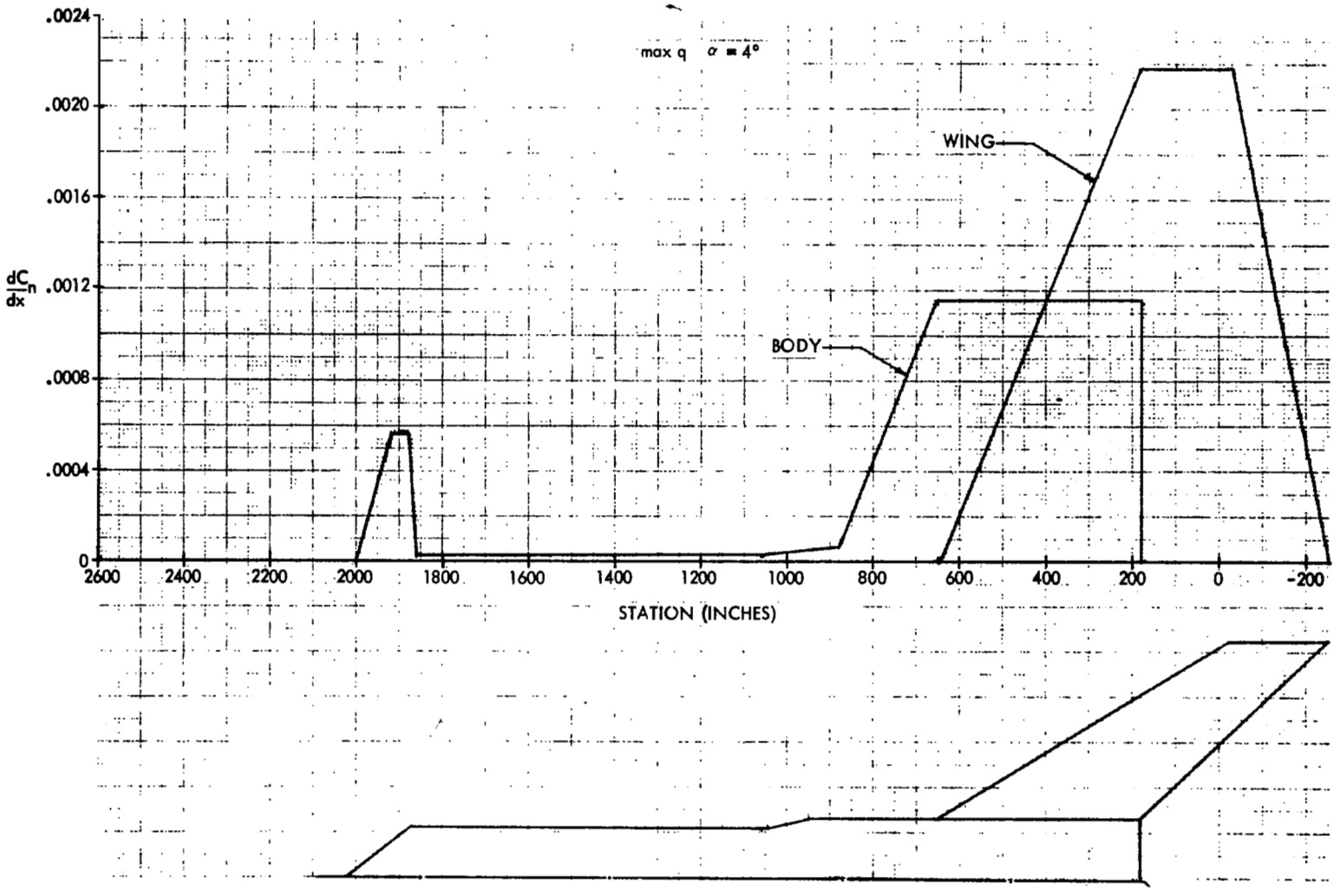

Figure 11. — Normal Force Distributions for 1.3×10^6 - Pound Vehicle

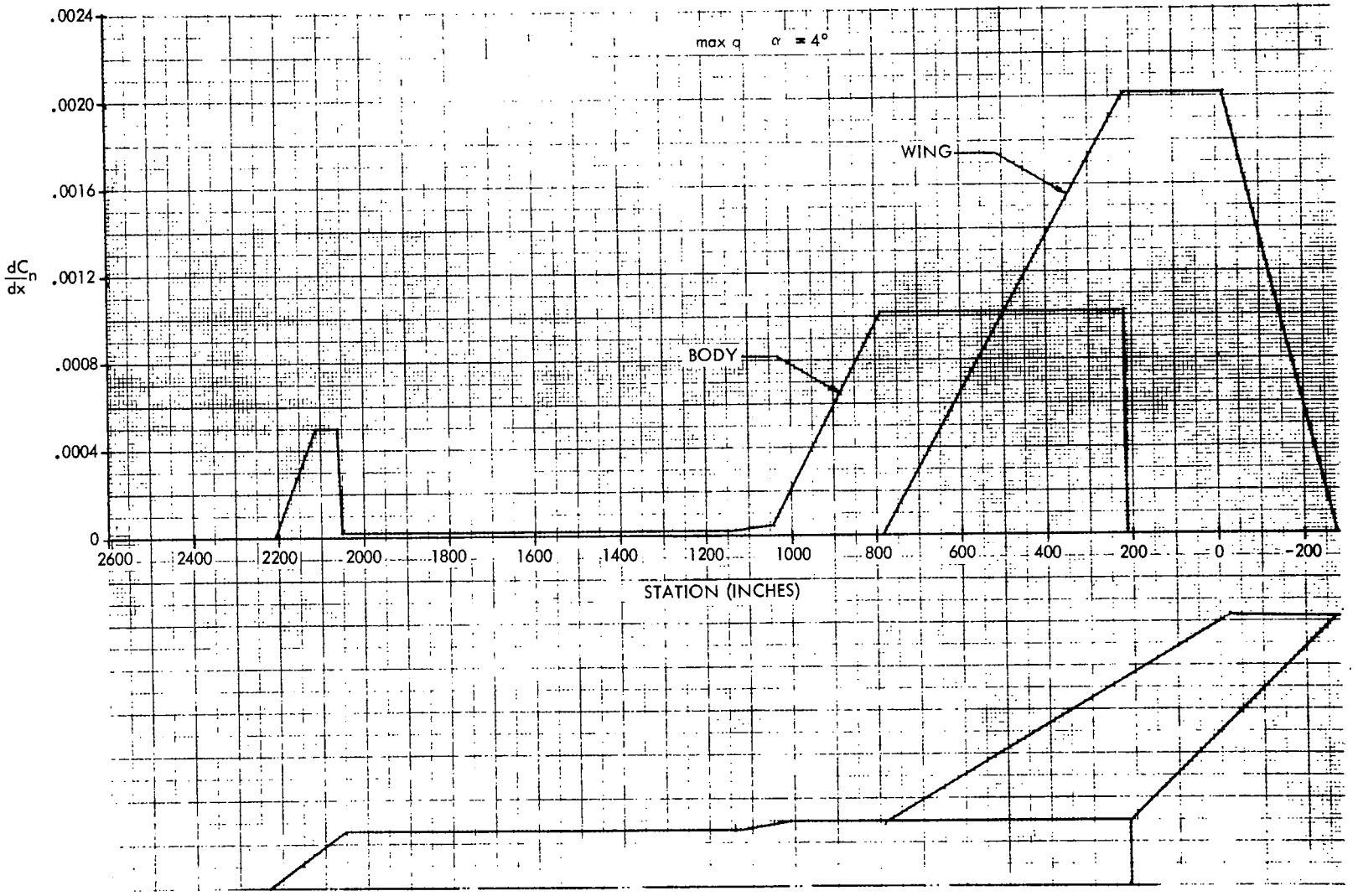

Figure 12. — Normal Force Distributions for 1.9×10^6 - Pound Vehicle

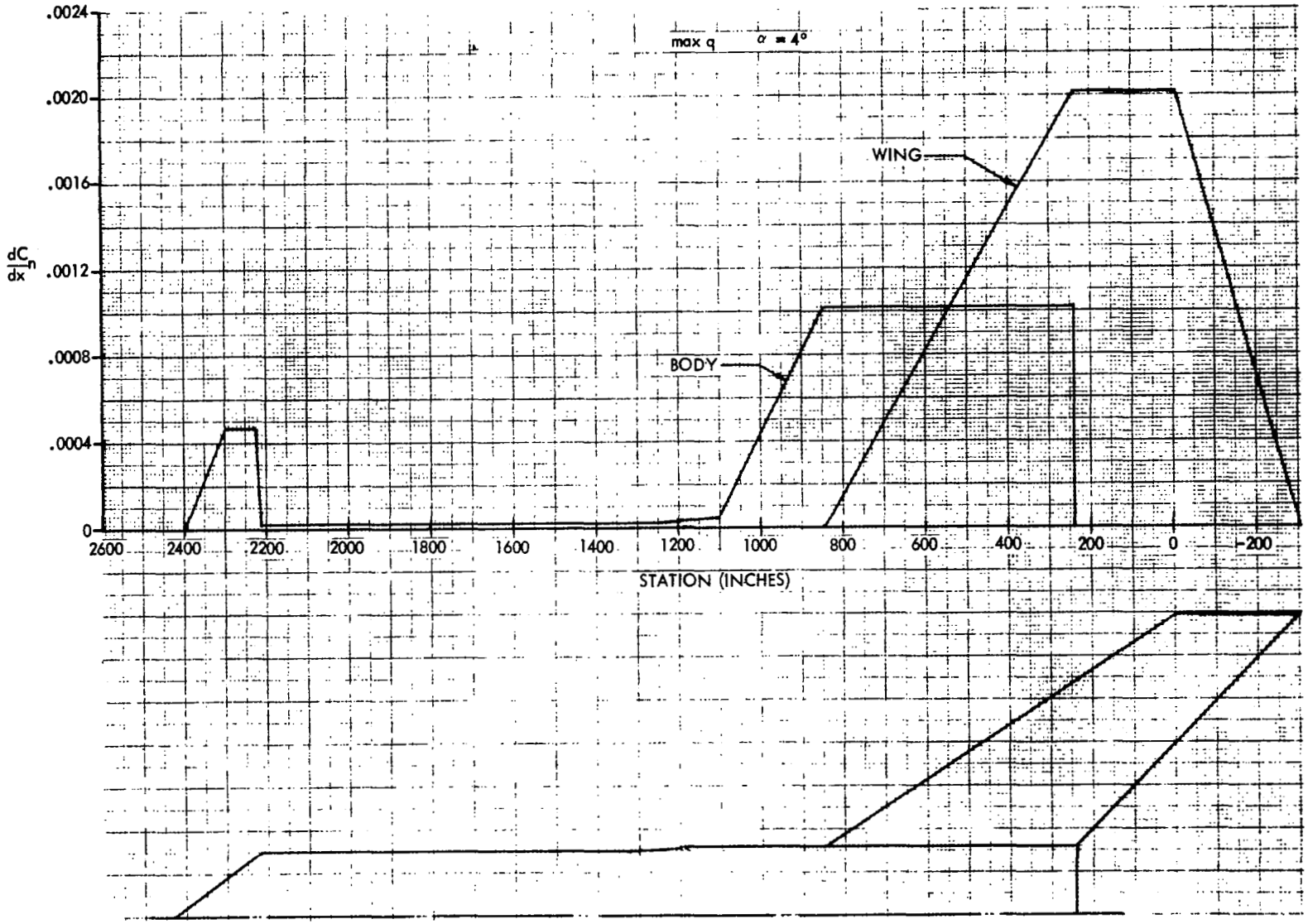

Figure 13. — Normal Force Distributions for 2.5×10^6 - Pound Vehicle

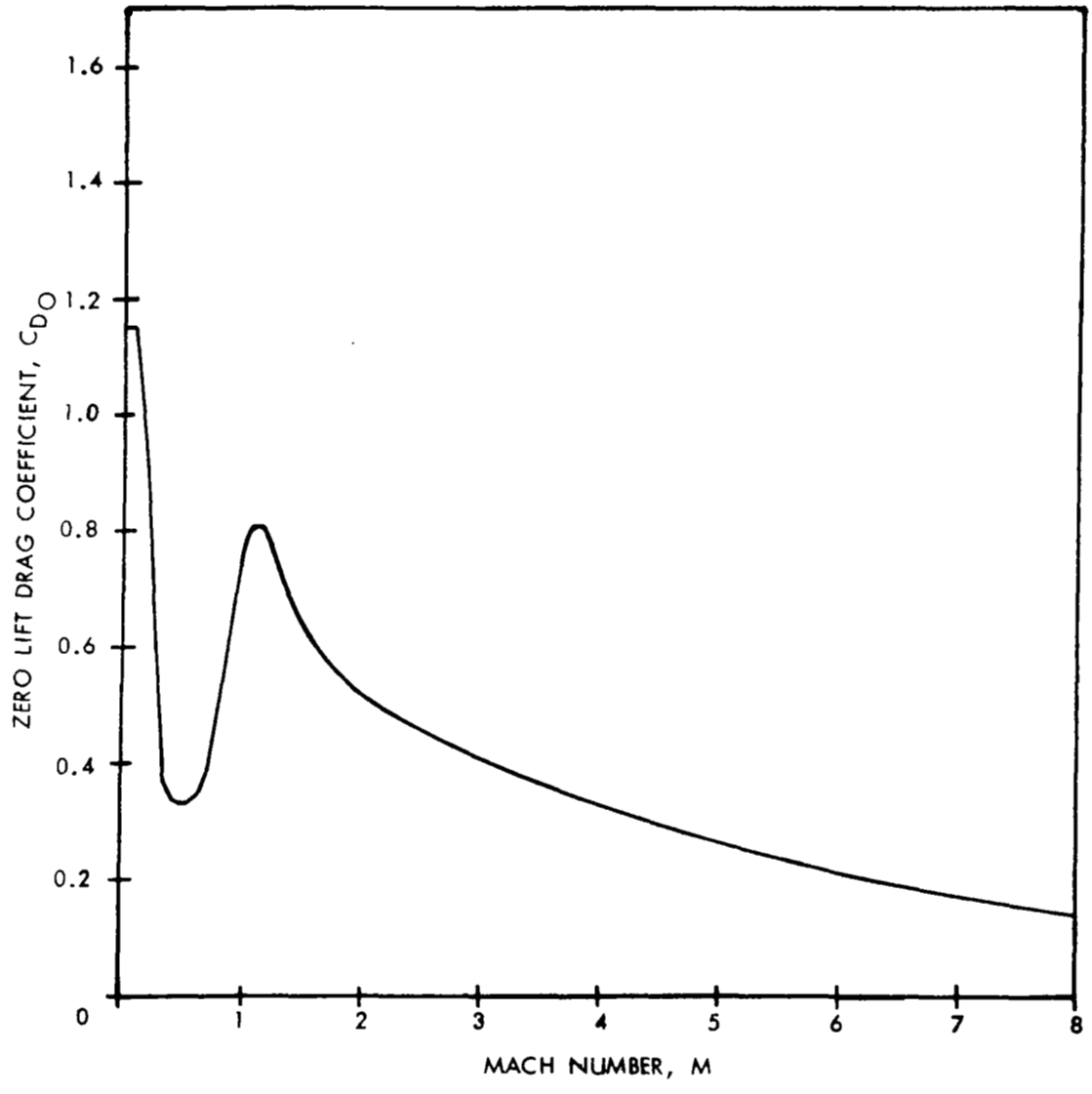

Figure 14. - Zero Lift-to-Drag Coefficient

$W_{GROSS} = 1.3 \times 10^6$ LB $\quad S_{REF} = \frac{\pi D^2}{4}$

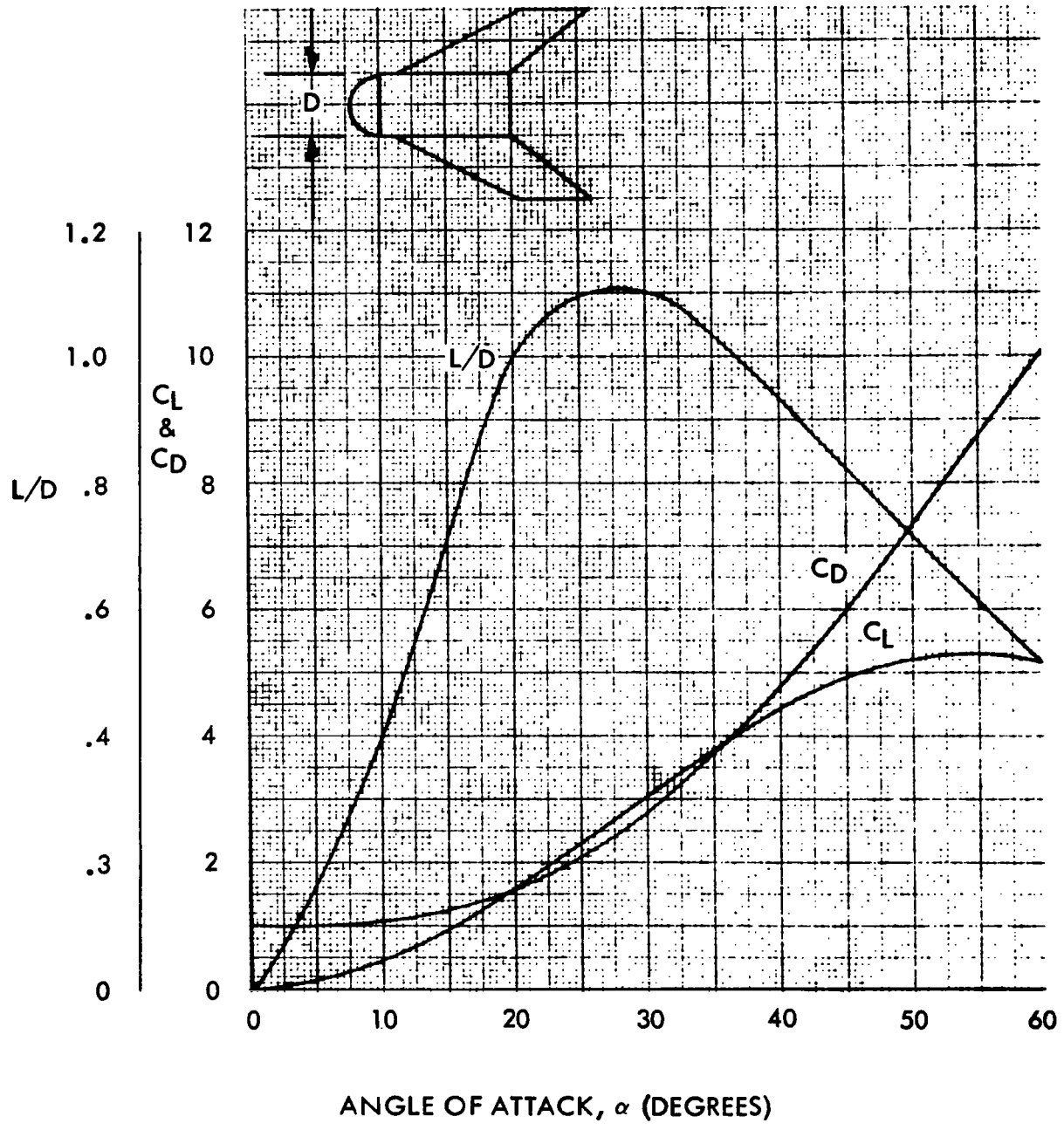

Figure 15.- Recoverable First-Stage Entry Aerodynamics - Configuration 1

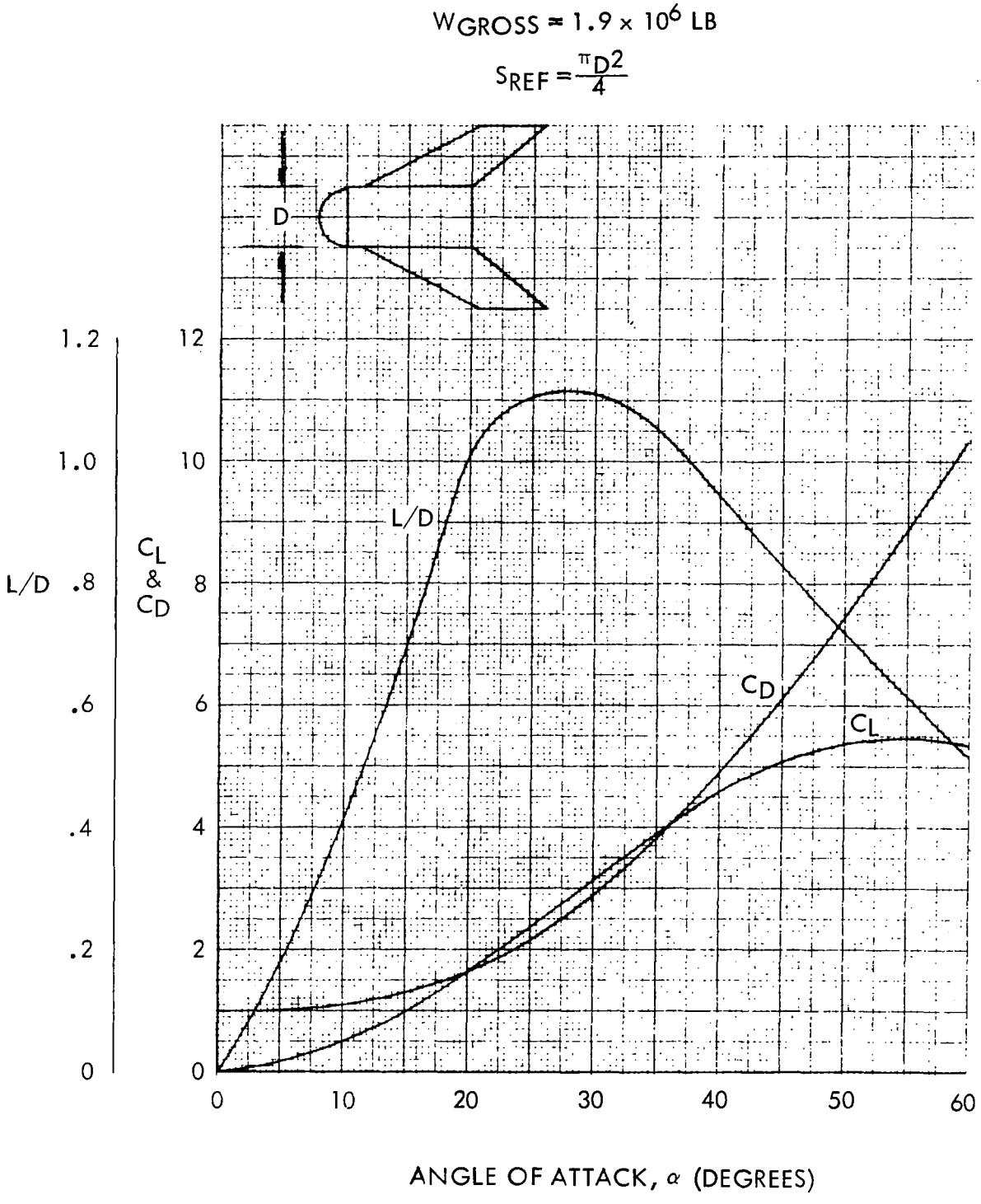

Figure 16. - Recoverable First-Stage Entry Aerodynamics - Configuration 2

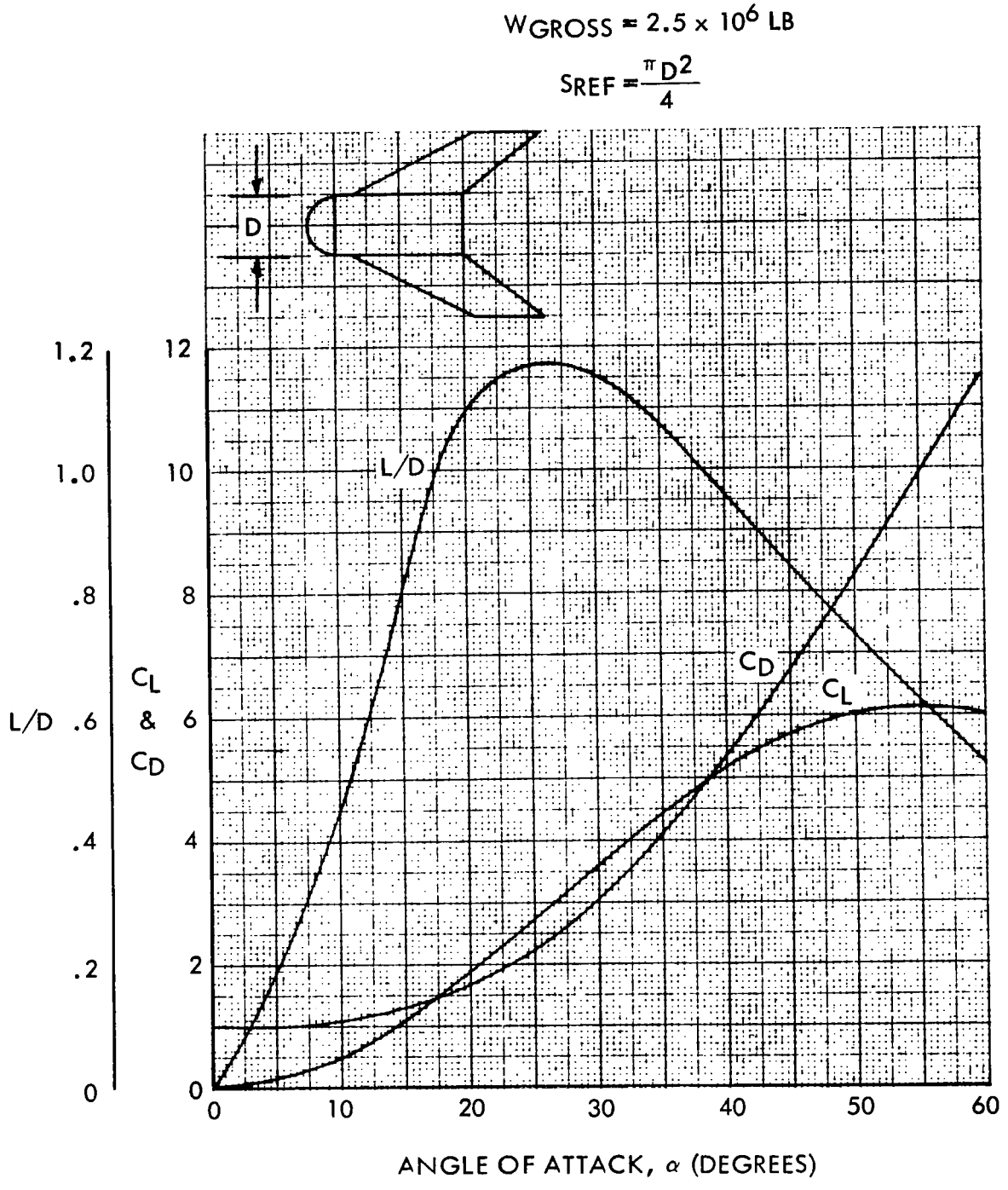

Figure 17.- Recoverable First-Stage Entry Aerodynamics - Configuration 3

condition occurs at an angle of attack of 55 degrees, with a corresponding L/D of approximately 0.6. The major contribution to the lift force is provided by the large wing.

These results were used in redefinition of the entry temperature profile and were evaluated using optimized aerodynamic heating-entry trajectory computer programs developed at the Space Division. The entry trajectories and thermal environment are discussed in detail later in this report.

Using the updated aerodynamic characteristics, a complete trajectory with heating analysis was run for the boost and descent phases, giving the performance characteristics of the recoverable first stage. Optimization trajectory computer programs developed at SD with aerodynamic heating indicators were run for the ascent and descent trajectories to provide transverse variation of the major flight parameters.

Ascent Trajectory and Heating

The initial boost trajectory through the denser atmosphere was considered to be a minimum-lift flight path to help alleviate severe loading through the maximum dynamic pressure regime.

Design load environments during the maximum dynamic pressure were considered as the result of the vehicle system encountering a sharp edge gust. The vehicle was assumed to be programmed for a minimum-load flight profile to alleviate severe wing loading prior to encountering a gust. This requirement supposes that the vehicle control system will respond to the gradual build-up of the winds and is only required to be designed for the additional wind gust of 9 meters/second, maximum. The gust velocities, vehicle velocity of $M \approx 1.2$ at 35 000 feet altitude, and the relative attitude of the flight profile to the local wind stream are considered to introduce a relative angle of attack of about 3 degrees. If a control delay lag of 1 degree is assumed, the total angle of attack was taken as 4 degrees. The maximum dynamic pressure is dependent upon the flight profile and the rocket performance.

After the maximum dynamic pressure region, the first-stage burn was considered to be a zero-gravity turn until separation. The second stage will follow a pitch control optimized path to achieve desired orbit with the maximum performance. These flight profiles were investigated using Space Division computer programs to determine an efficient trajectory with the proposed baseline vehicles. The three near-term baseline vehicles 1.3, 1.9, and 2.5 million pounds launch weight were evaluated by the programs to compare the analytical performance with the performance assessed with the parametric synthesis subroutines. The flight parameters' variations with burn time for the smallest vehicle are shown in figure 18 and indicate good

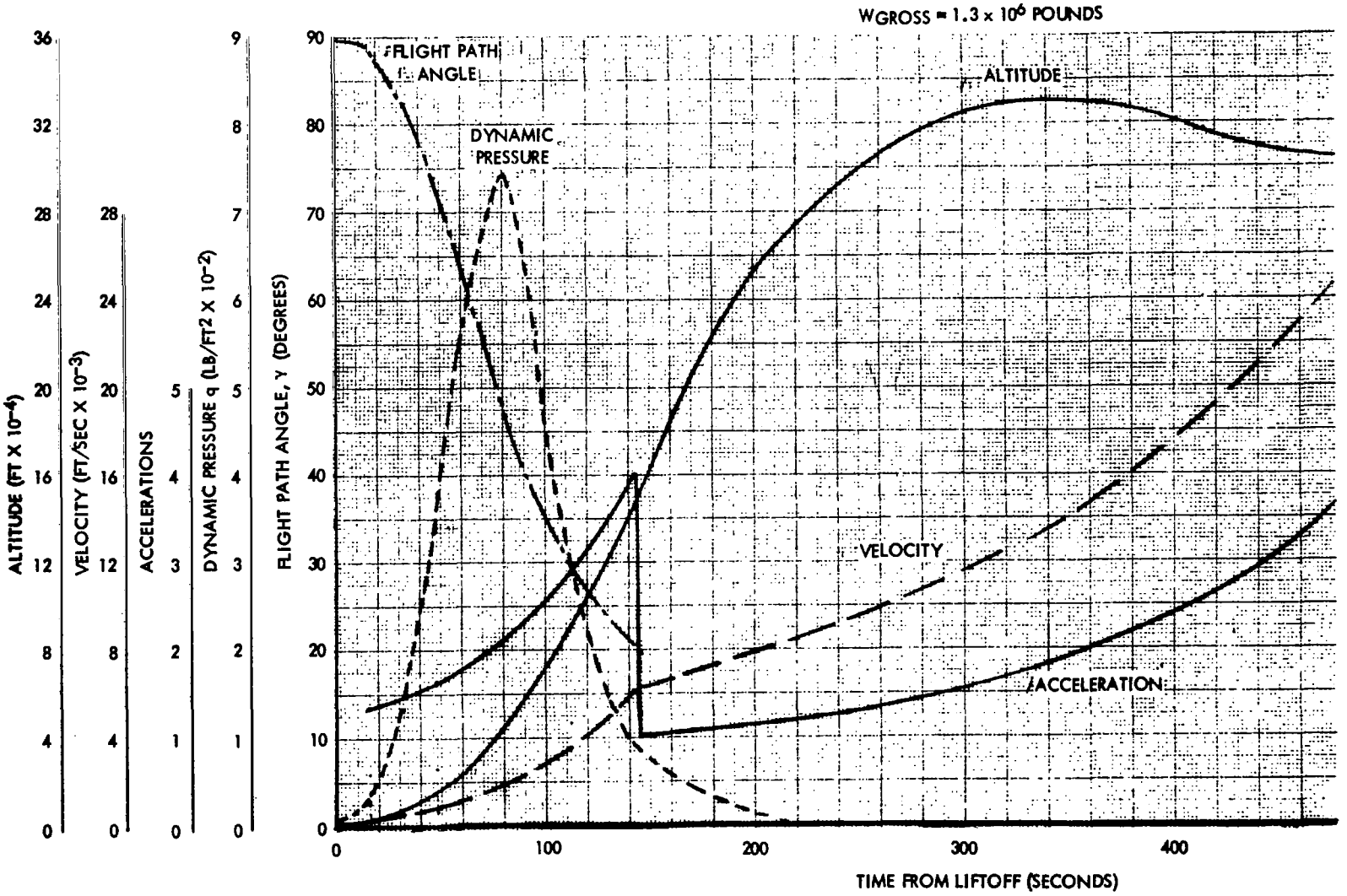

Figure 18. - Recoverable Vehicle Ascent Trajectory

agreement with the previously developed data. The burnout conditions of the first stage provide the initial conditions for the ballistic coast and entry trajectory calculations. These initial conditions are given in table 4 for the three launch vehicles.

TABLE 4. - INITIAL CONDITIONS

Configuration	D_{ref} (in.)	Gross Weight (lb)	Burnout Weight	h (ft)	V (fps)	γ (°)
1	260	1.3×10^6	133, 664	145, 900	6296	19.53
2	300	1.9×10^6	189, 155	151, 500	6289	21.16
3	320	2.5×10^6	242, 936	154, 700	6321	21.81

It is interesting that these staging conditions are at 6300 fps, which is 200 fps lower than indicated by the synthesis program. This difference is due to the underestimation of the velocity losses associated with the first-stage burn, and, if required, this effective variation can be included in the synthesis empirical evaluation of losses, thus updating the parametric program. The staging altitude is now only 150, 000 feet, which will affect the thermal profile during entry, as was determined by the subsequent thermal analysis programs.

The maximum dynamic pressure attained during boost (fig. 18) was 735 lb/ft^2, which was within limits of the estimate of 720 lb/ft^2, used for Phase II studies. Also the relative angle of attack for the zero lift (minimum load) was less than one degree. Therefore the external loads defined during Phase II of the study realistically represent the environment during the boost ascent phase of the trajectory.

With this load minimum flight path, etc., the attainable payloads into Earth orbit are within acceptable limits. Table 5 compares the two sets of values from the computer analysis and the parametric synthesis. The analytical results do not include the velocity allowances for Hohmann transfers and launch window. These extra velocity requirements account for an additional 811 feet per second (table 1), which, with the engine system proposed, will result in an additional performance mass ratio of 1.054. If the burnout weight quoted in table 5 is factored by this additional ratio, a

true burnout weight is obtained of 87 600 pounds which is approximately 1400 pounds less than the original parametric estimate, an error of about 1-1/2 percent.

TABLE 5. - ANALYTICAL COMPARISON FOR 1.3×10^6 POUND VEHICLE

	Computer Analysis	Parametric Values
Velocity gained, stage 1	6 296	6 500
Velocity losses, gravity, stage 1	3 424	3 565
Velocity losses, steering, stage 1	344	
Characteristic velocity, stage 1	10 063	10 065
Velocity gained, total	24 426	24 426
Velocity losses, gravity	4 126	4 575
Velocity losses, steering	836	
Characteristic velocity	29 364	*29 880
Weight at burnout	92 068	

*Characteristic velocity includes requirement for Hohmann transfer, etc.

Entry Trajectory and Heating

Using the updated aerodynamic characteristics, a complete trajectory with heating analysis was run on optimization trajectory computer programs developed at the Space Division. These programs, with aerodynamic heating indicators, were run for the descent trajectory analysis and provided data to determine the temperatures on the wing leading edge, upper surfaces, lower surface, and body stagnation point. From the above analysis, the thermal protection requirements were assessed.

The Space Division thermodynamic performance digital computer program combines the features required to accomplish an integrated study of vehicle flight and heat transfer characteristics. Combined into a single program are the trajectory, aerodynamic heating, ablation, and wing temperature distribution computations.

The trajectory subroutines predict the vehicle performance characteristics for a variety of hypersonic flight applications. The aerodynamic heating portion of the program analyzes the heating environment experienced

by a vehicle in the supersonic to the hypersonic flight spectrum and is applicable to circular and parabolic entry conditions. Nonblowing convective and radiant heating environments are considered at the vehicle's nose and leading edge stagnation regions and at locations along the fuselage or wing wetted surface. The structural temperature prediction evaluated one-dimensional heat transfer problems for spherical or cylindrical surfaces subjected to convective and radiative heating. A finite difference technique is utilized to compute the structural temperatures. A simplified schematic of the thermal evaluation approach is shown in figure 19.

The trajectory profile of the recoverable stage consists of a ballistic coast from first-stage burnout to apogee, followed by a reorientation to the maximum lift attitude and entry into the denser layers of the atmosphere at this high angle of attack. A load factor limit of 4 g's was established as an entry constraint, with angle of attack modulation utilized to keep the peak deceleration below this value. However, due to the low m/C_LS of the vehicle, it was not found necessary to modulate the angle of attack, and the entire descent was flown at the maximum lift attitude.

The entry trajectory characteristics are shown in figures 20 through 22 as a function of time from first-stage burnout. The entire trajectory remains within the atmosphere, with an apogee altitude of approximately 240 000 feet. During the descent phase, the peak load factor for Configuration 3 slightly exceeded the limiting value of 4 g's, but the difference was so small that the added complexity of mechanizing the program to modulate the angle of attack during this short period was not warranted. The unpowered trajectory was continued to the ground, although the actual mission does include a pullout maneuver and powered return flight to the launch site following deceleration to subsonic velocities.

The aerodynamic heating was evaluated at five positions on the recoverable stage fuselage, and the locations of these points are indicated in figure 23. At apogee, the vehicle angle of attack changes from 0 to 55 degrees; and the stagnation point consequently moves from body point 1 to body point 2. The heating rate histories at the five points are presented in figures 24 through 38 as a function of wall temperature for each of the launch vehicles. Also shown as dashed lines are the corresponding equilibrium wall temperatures at each surface location.

At the time of first-stage separation, the nose of the vehicle is exposed to the freestream air, and the stagnation point experiences its highest heating rate. However, the flow over most of the vehicle is turbulent, and the highest overall heating is in the vicinity of body point 2. As the vehicle gains altitude, transition to laminar flow occurs. The flow becomes laminar over the entire body at an altitude of approximately 210 000 feet. At apogee, there

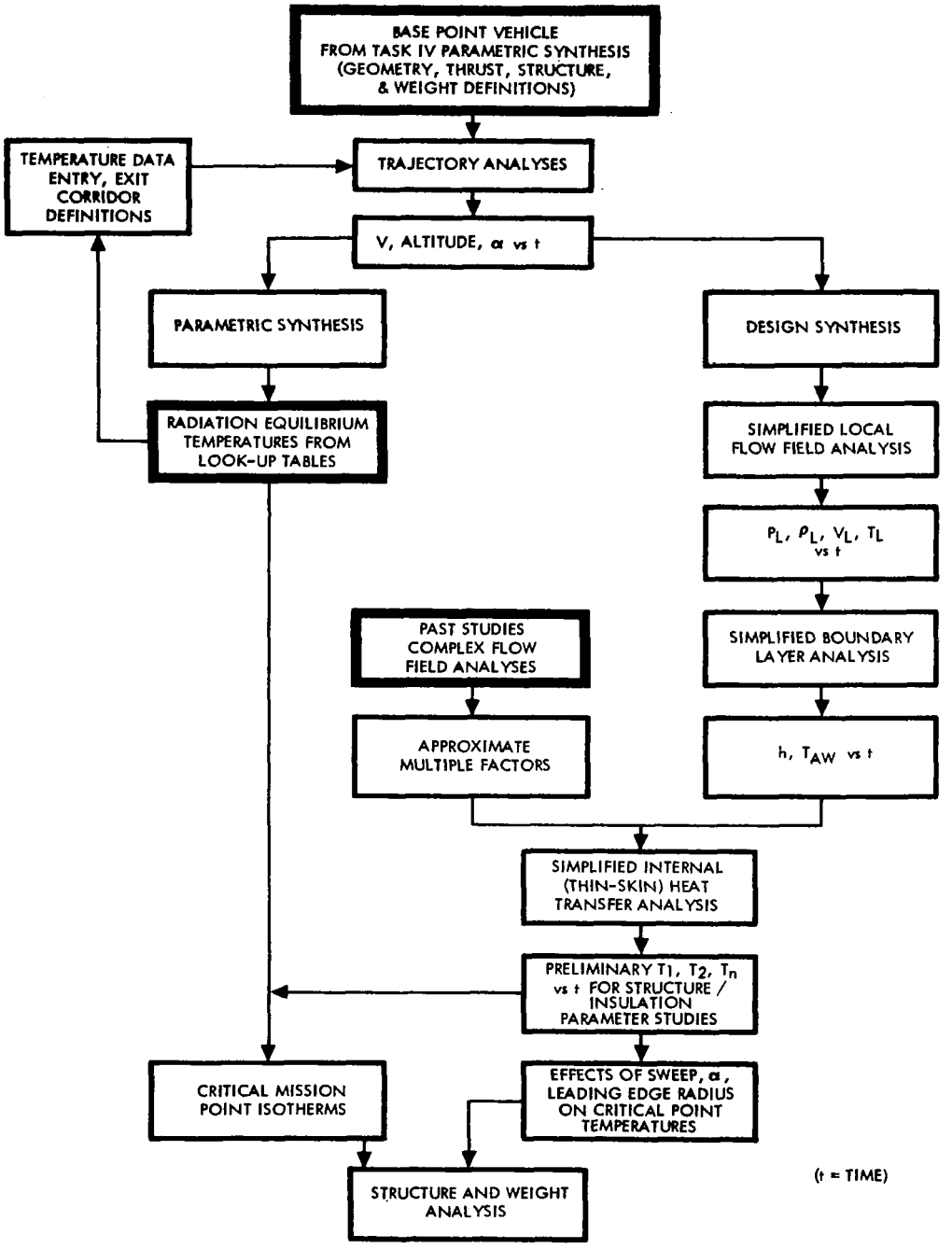

Figure 19. - Estimation of Thermal Environment

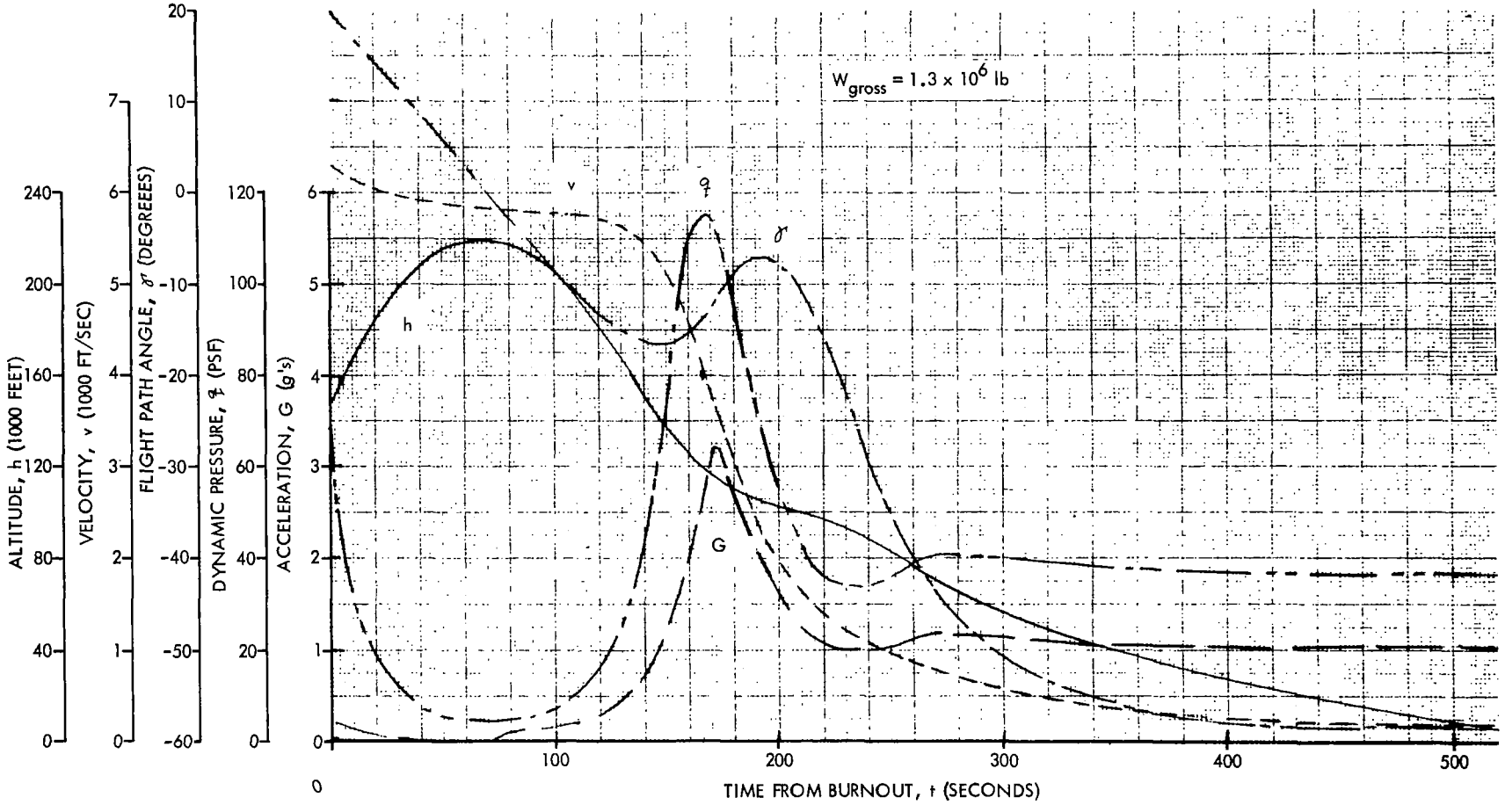

Figure 20. — Recoverable First-Stage Entry Trajectory, Configuration 1

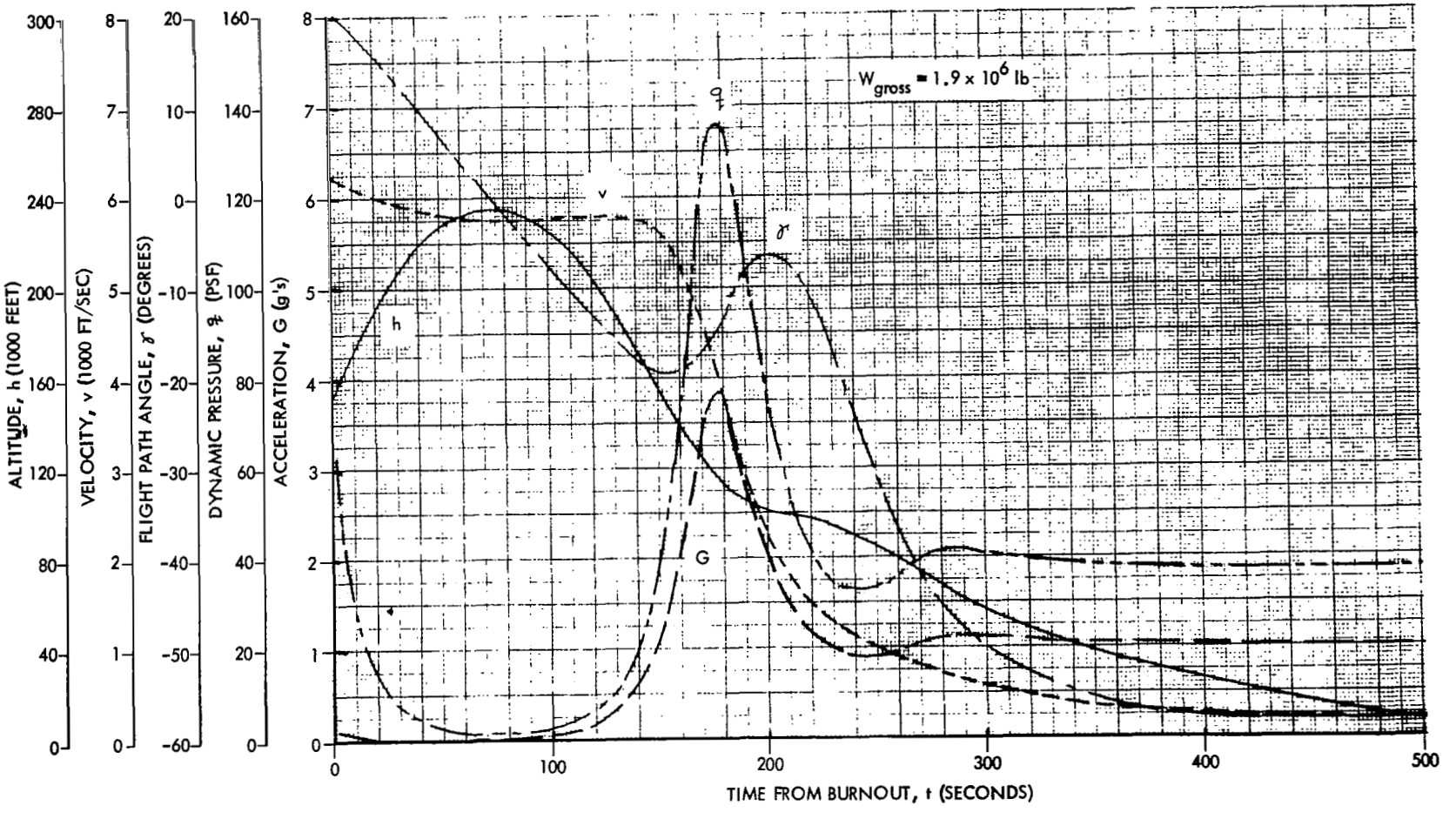

Figure 21. — Recoverable First-Stage Entry Trajectory, Configuration 2

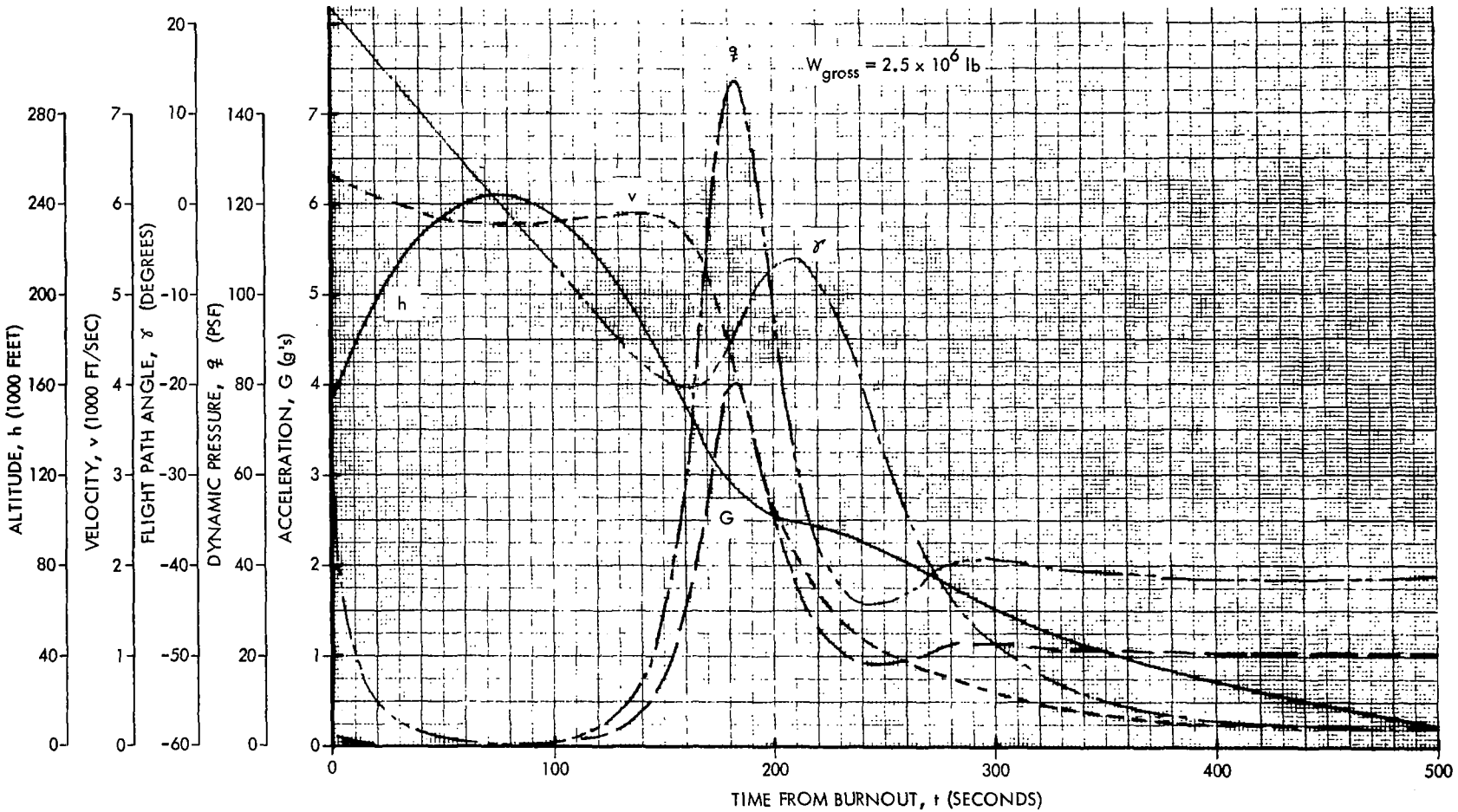

Figure 22. — Recoverable First-Stage Entry Trajectory, Configuration 3

BURNOUT TO APOGEE

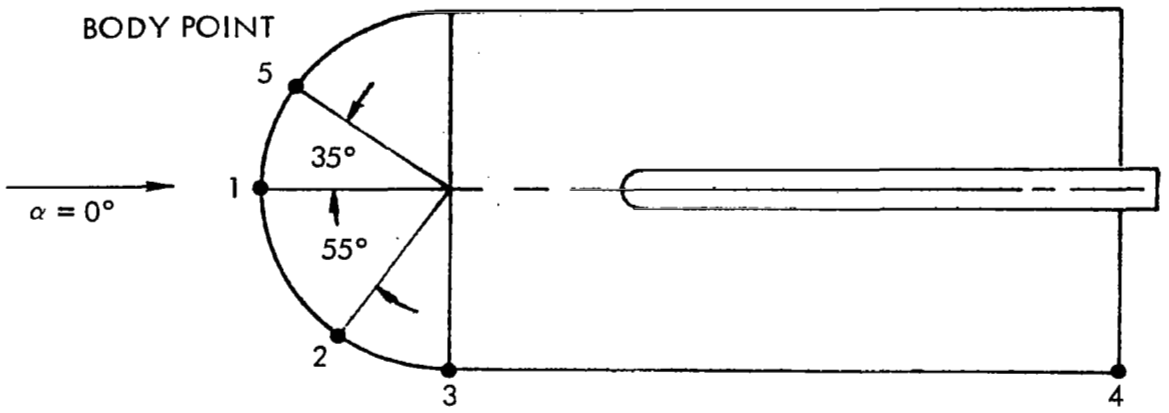

APOGEE TO LANDING

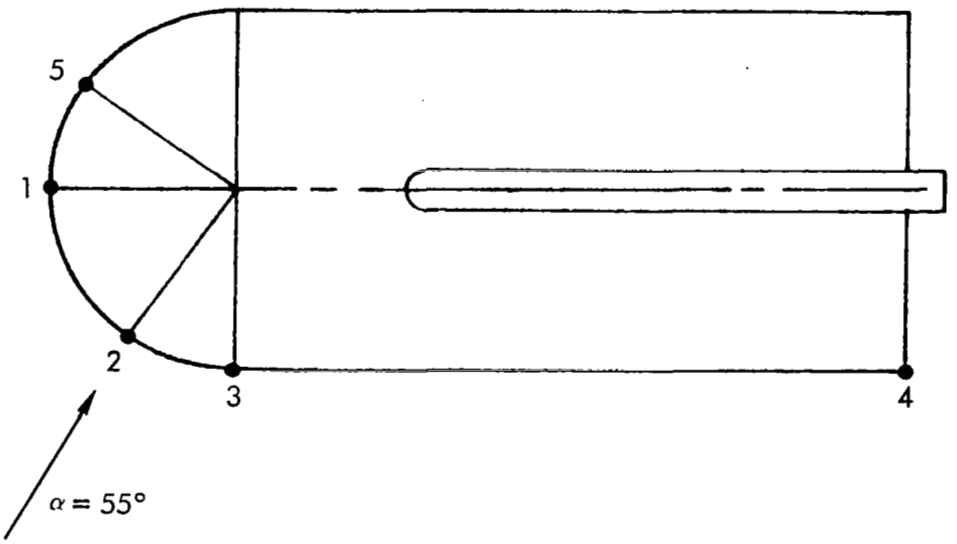

Figure 23. - Body Point Locations for Heating Analysis

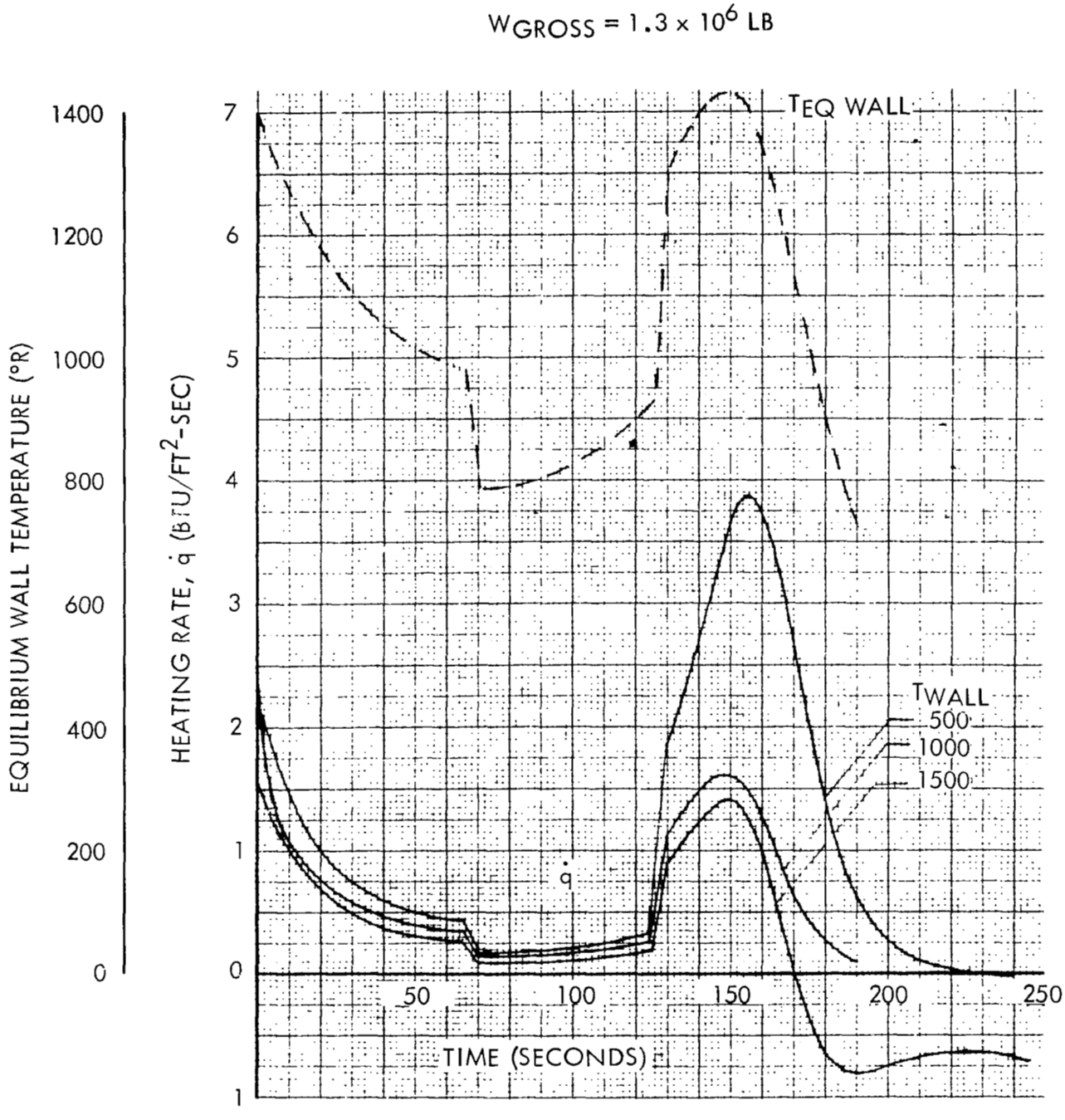

Figure 24. - Recoverable First-Stage Entry Heating - Configuration 1 - Body Point 1

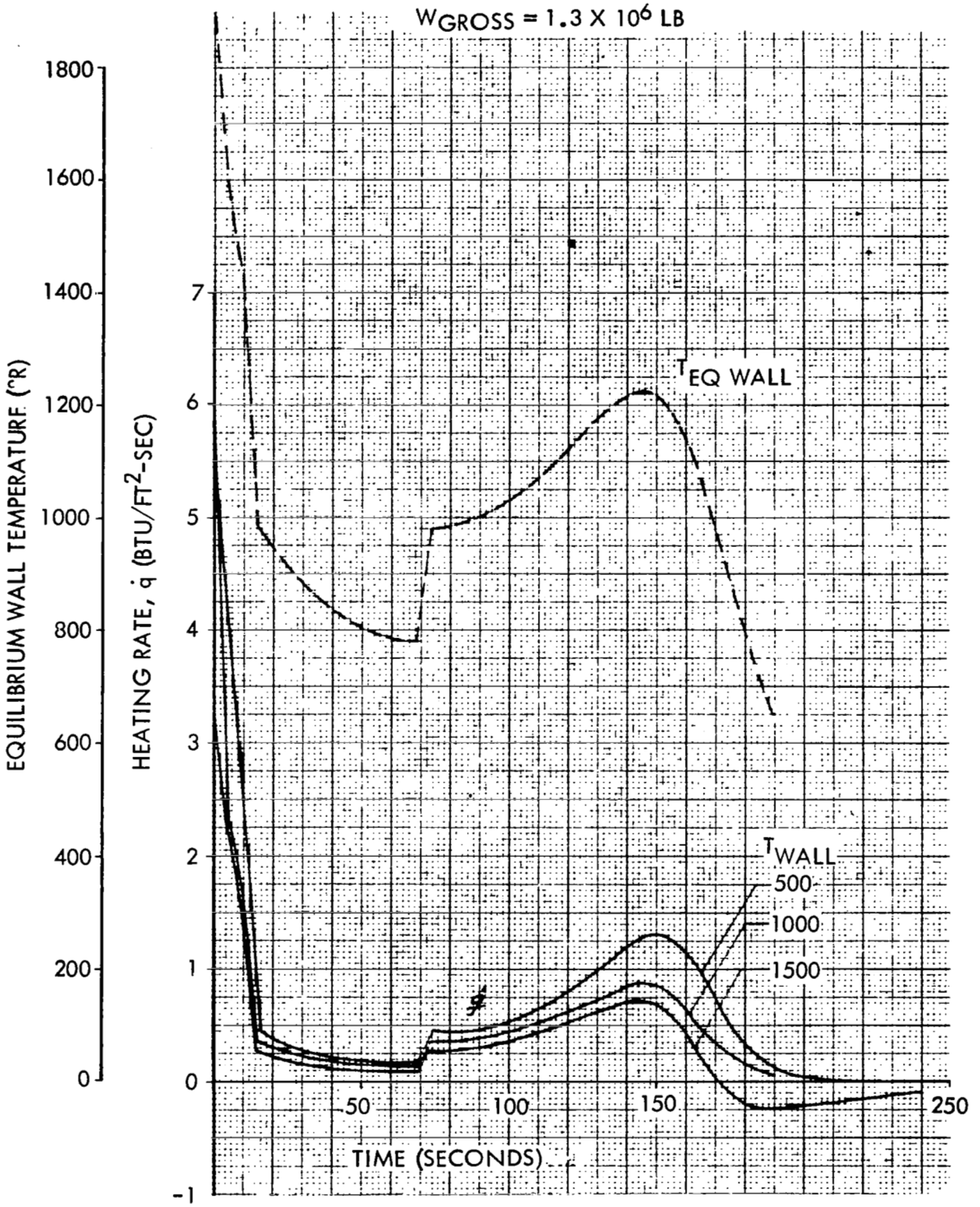

Figure 25. - Recoverable First-Stage Entry Heating - Configuration 1 - Body Point 2

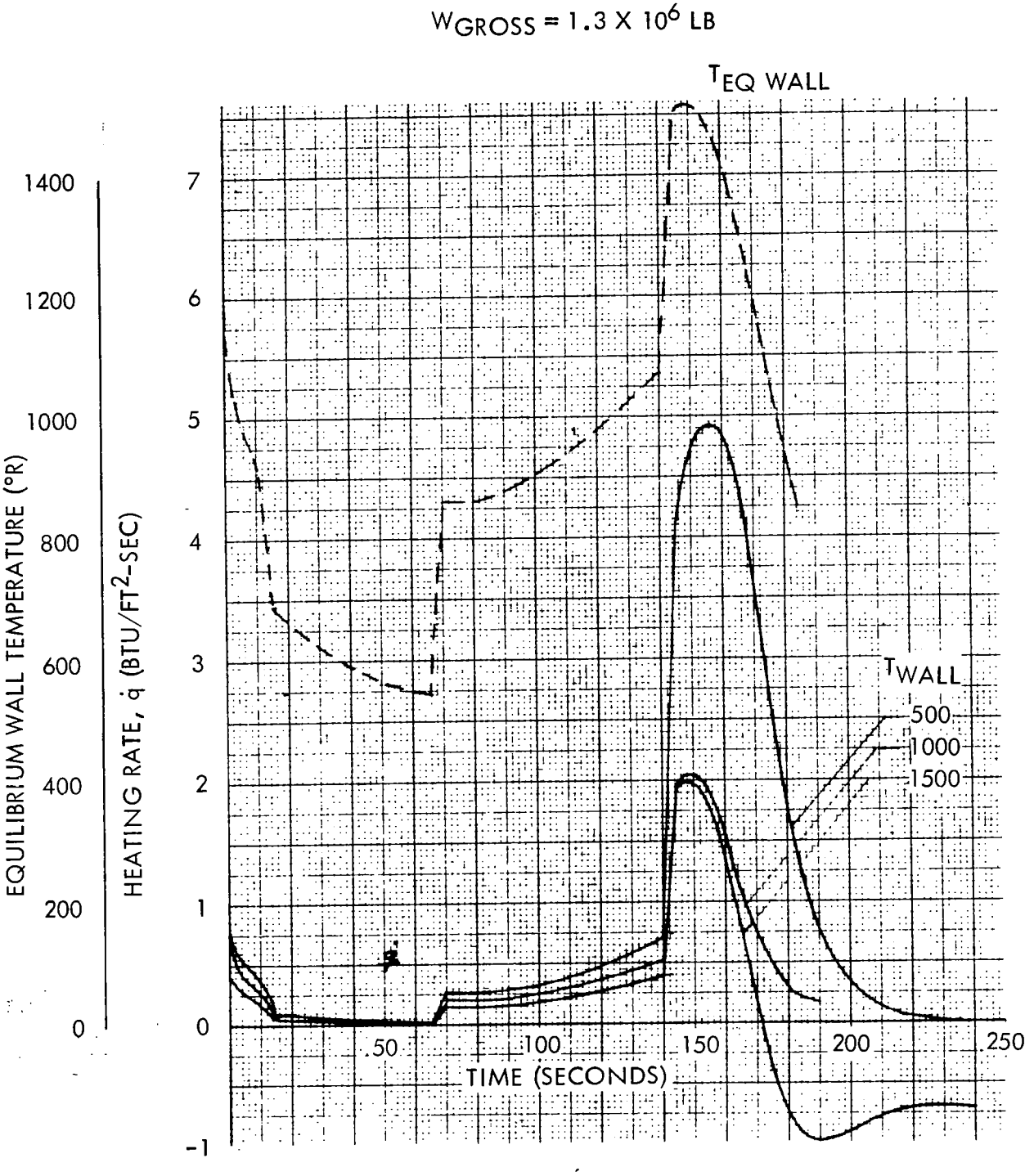

Figure 26. - Recoverable First-Stage Entry Heating - Configuration 1 - Body Point 3

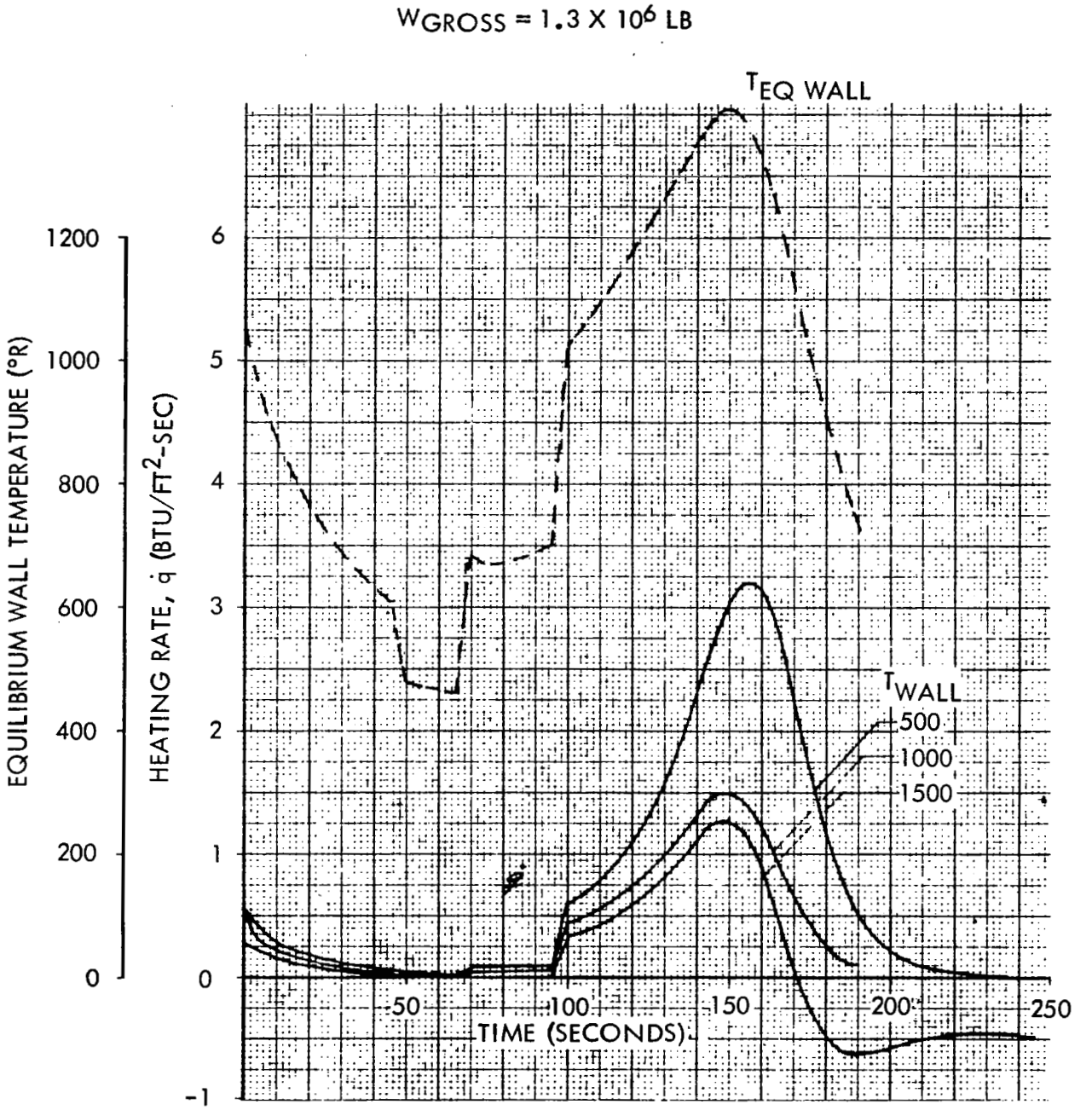

Figure 27. - Recoverable First-Stage Entry Heating - Configuration 1 - Body Point 4

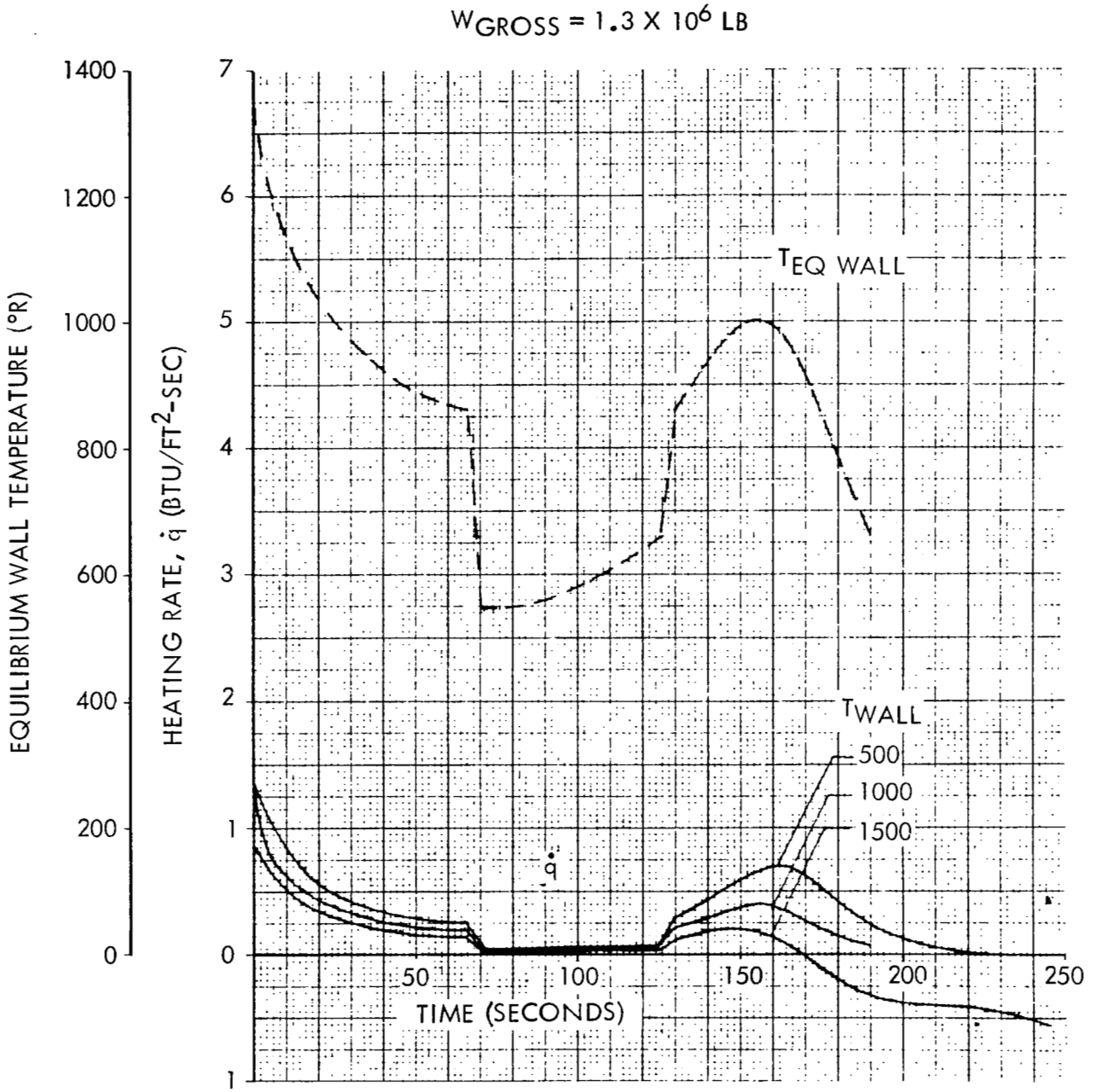

Figure 28. - Recoverable First-Stage Entry Heating - Configuration 1 - Body Point 5

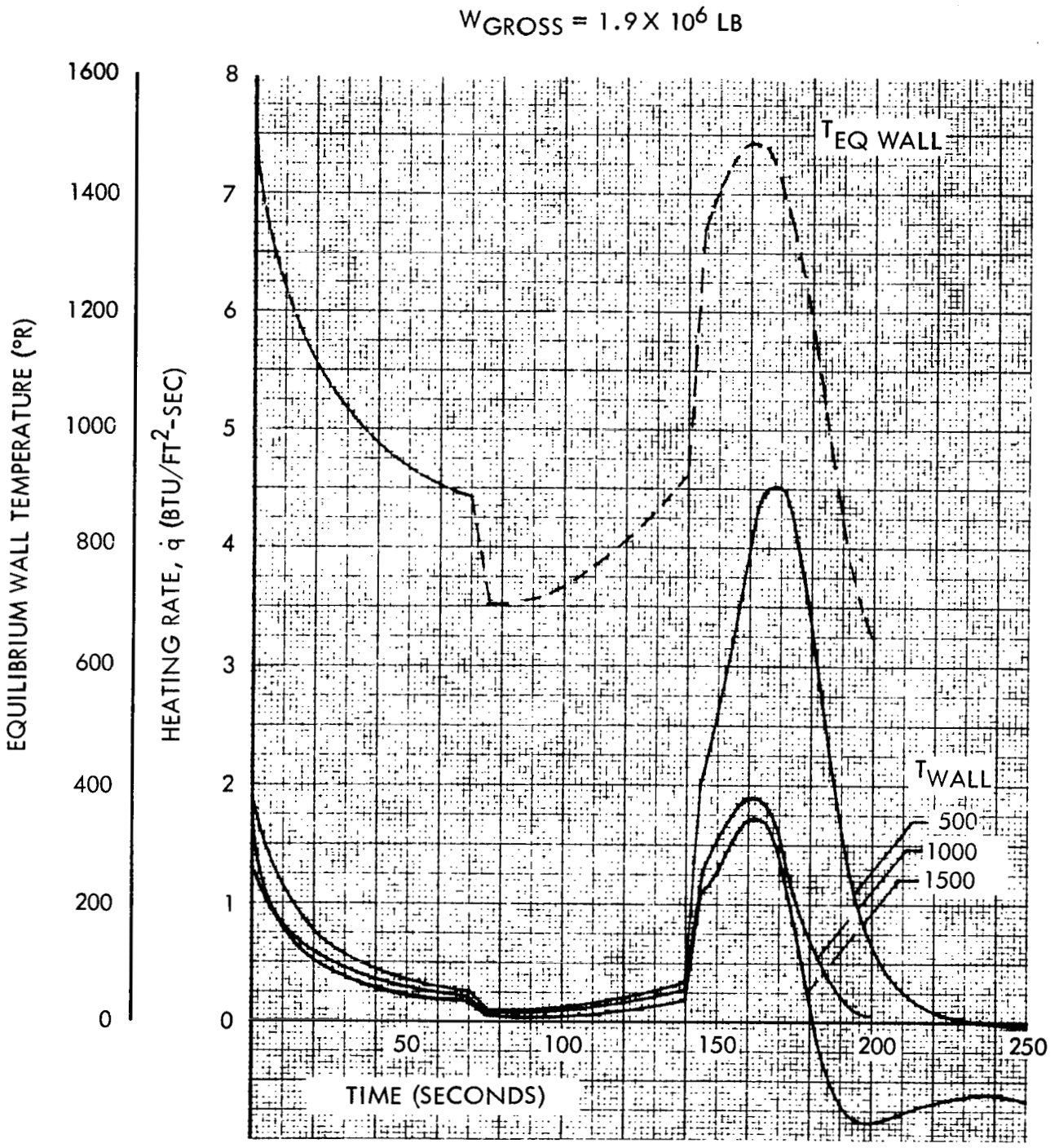

Figure 29. - Recoverable First-Stage Entry Heating - Configuration 2 - Body Point 1

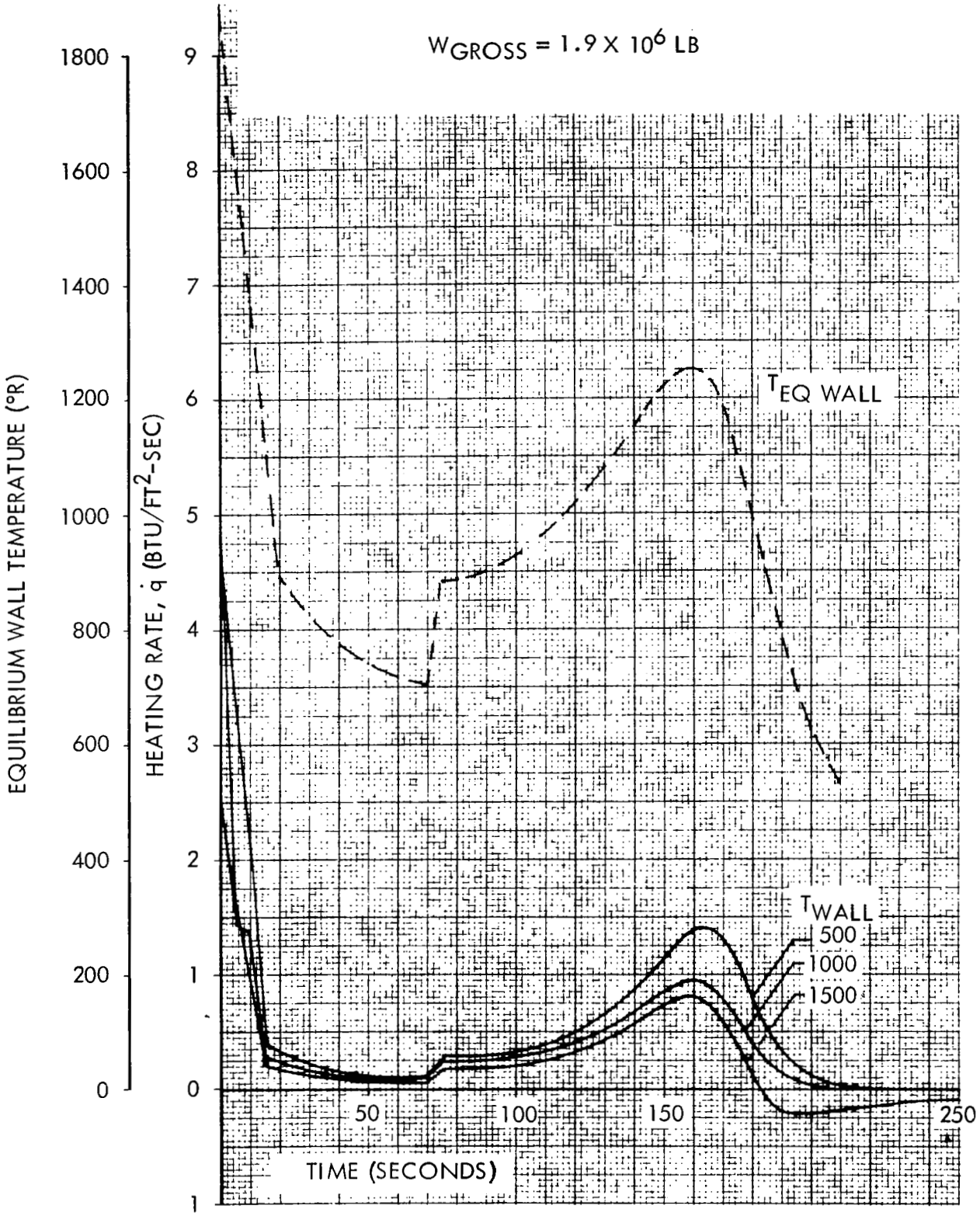

Figure 30. - Recoverable First-Stage Entry Heating - Configuration 2 - Body Point 2

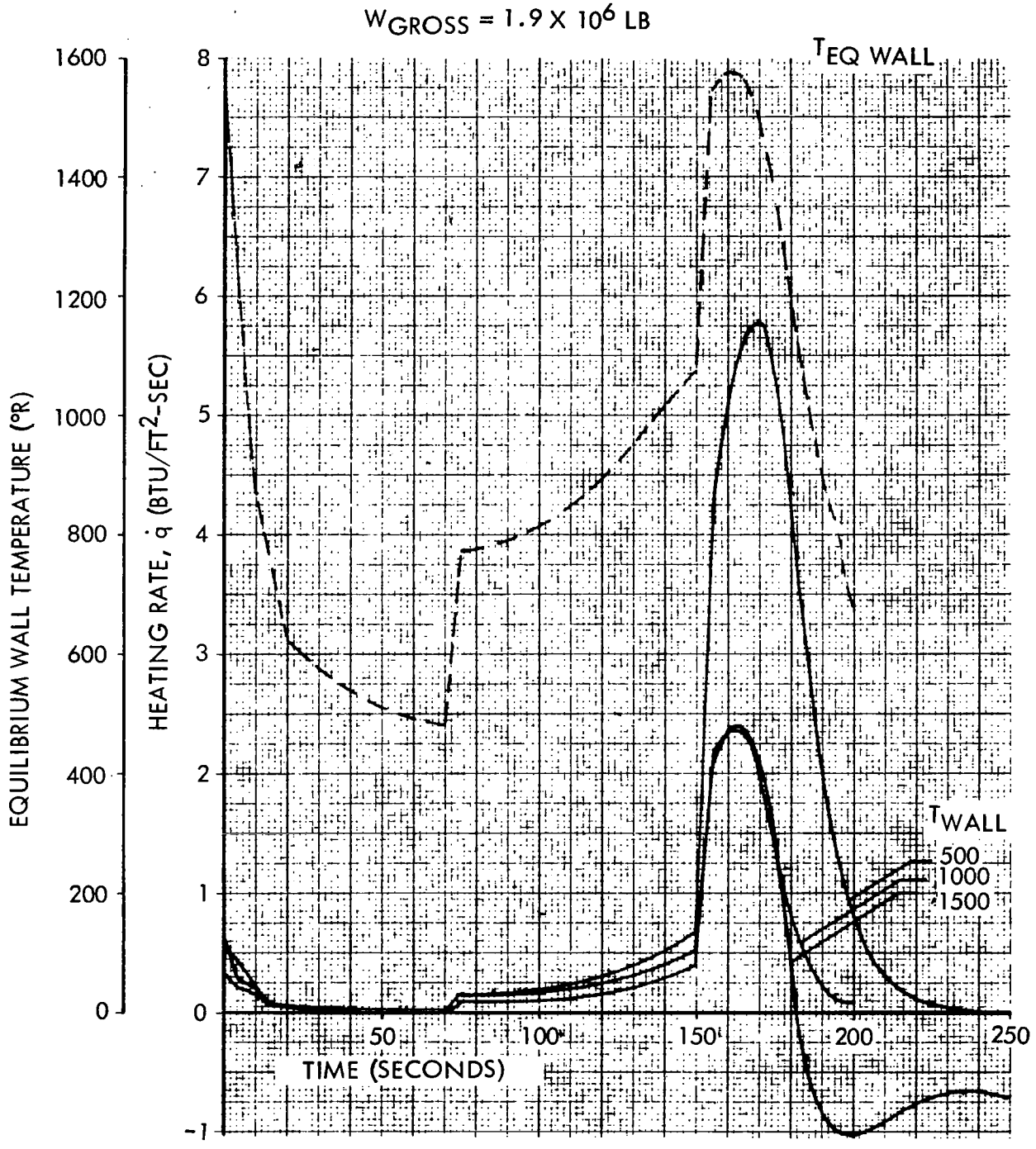

Figure 31. - Recoverable First-Stage Entry Heating - Configuration 2 - Body Point 3

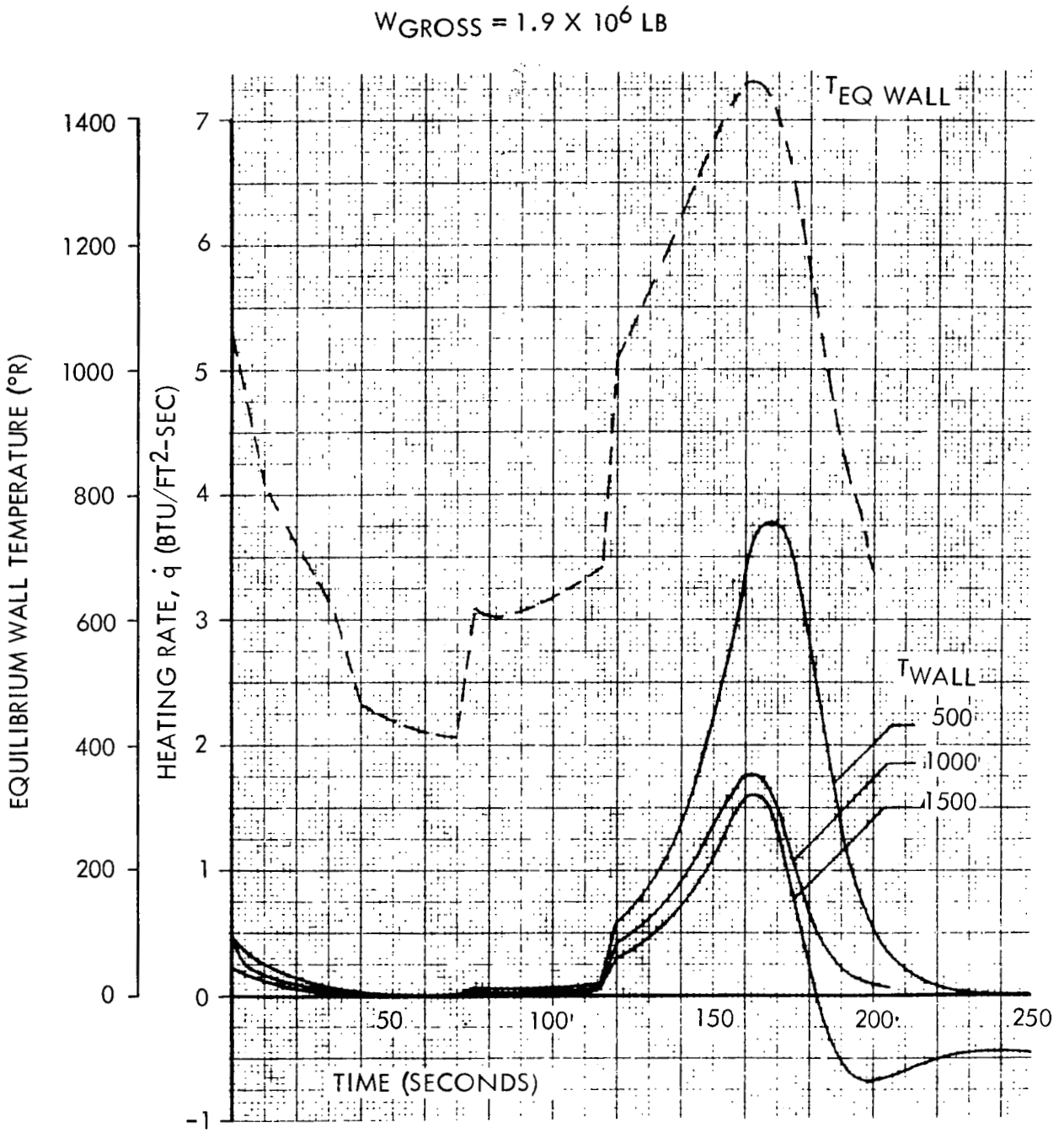

Figure 32. - Recoverable First-Stage Entry Heating - Configuration 2 - Body Point 4

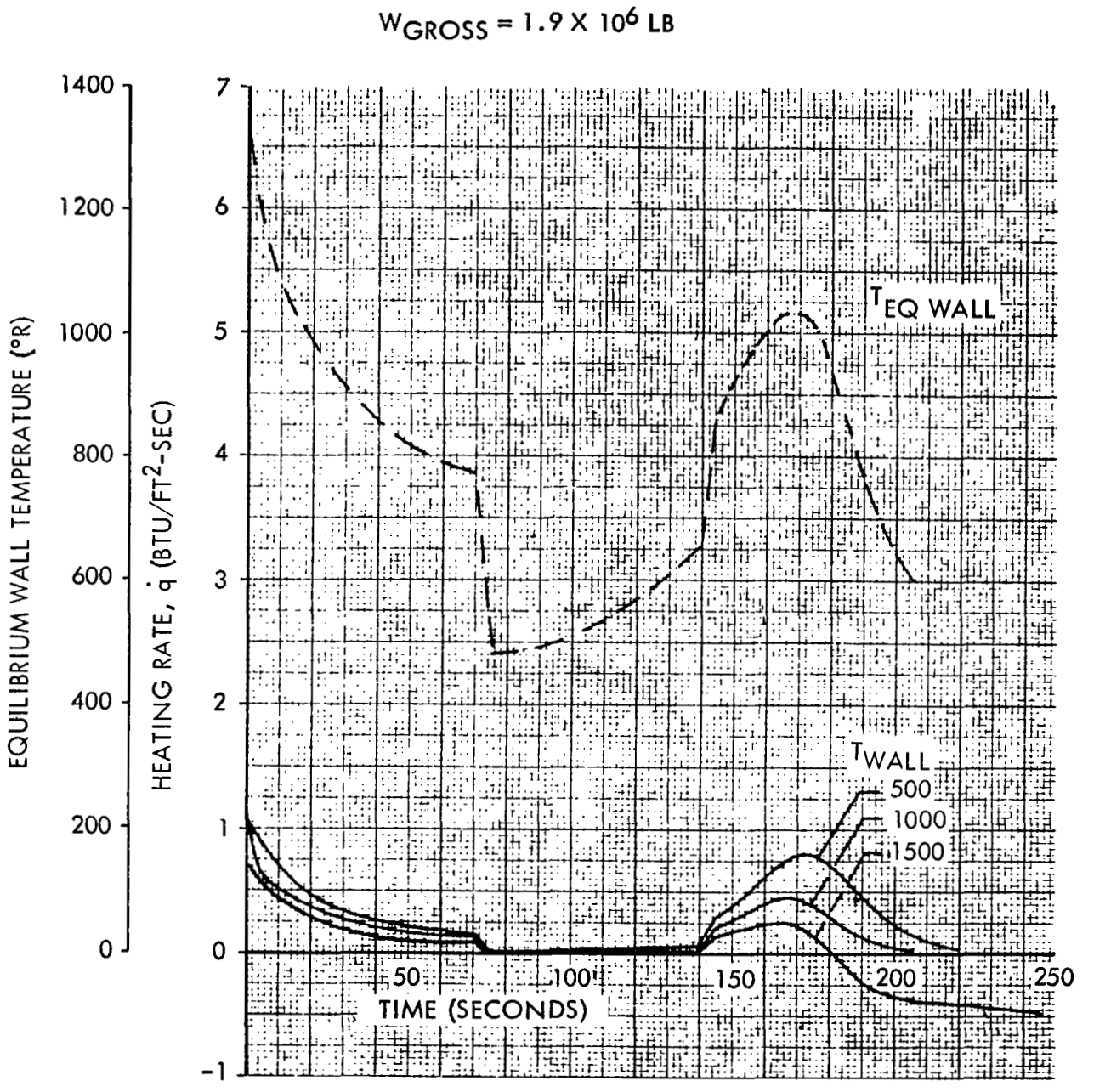

Figure 33. - Recoverable First-Stage Entry Heating - Configuration 2 - Body Point 5

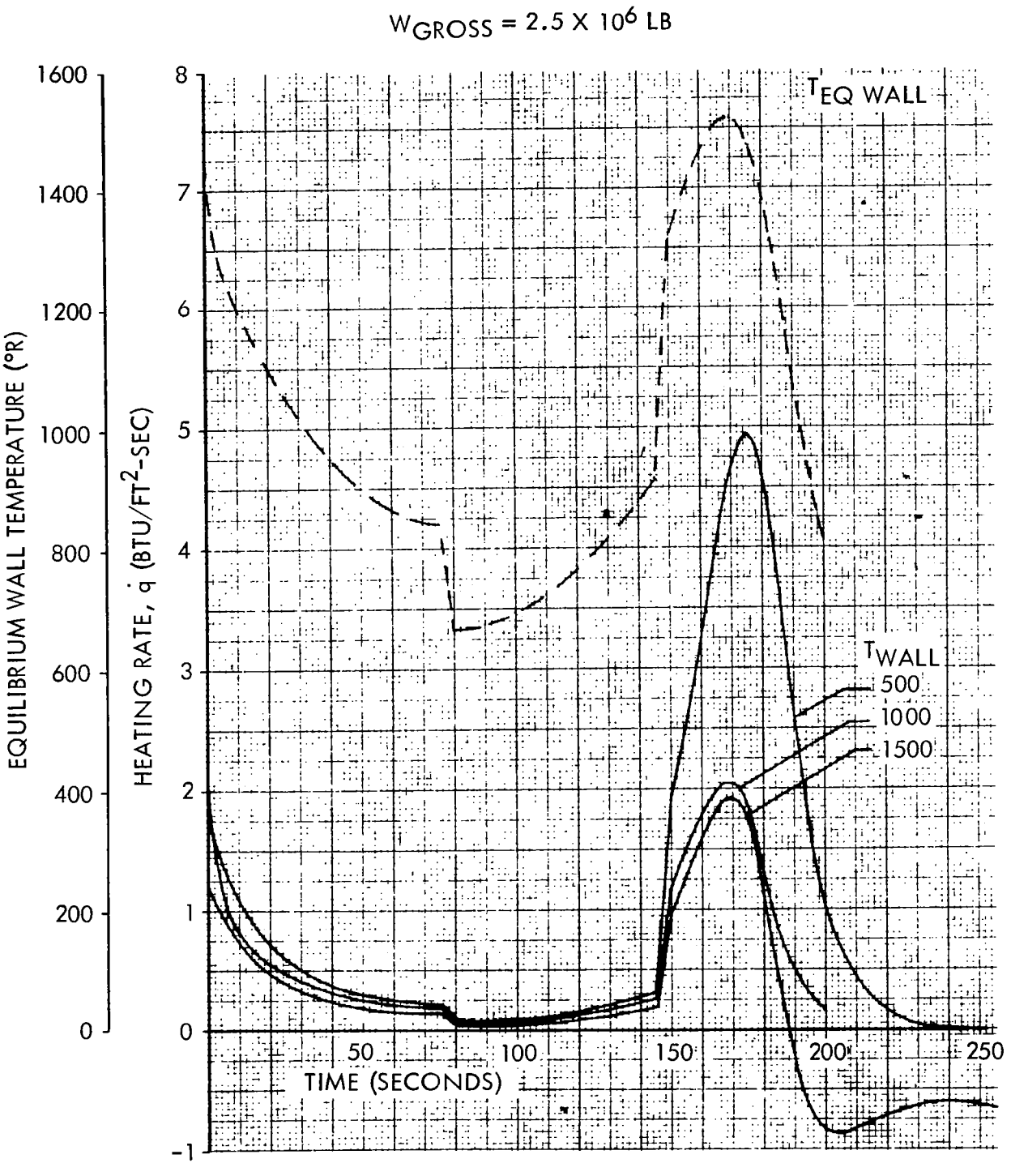

Figure 34. - Recoverable First-Stage Entry Heating - Configuration 3 - Body Point 1

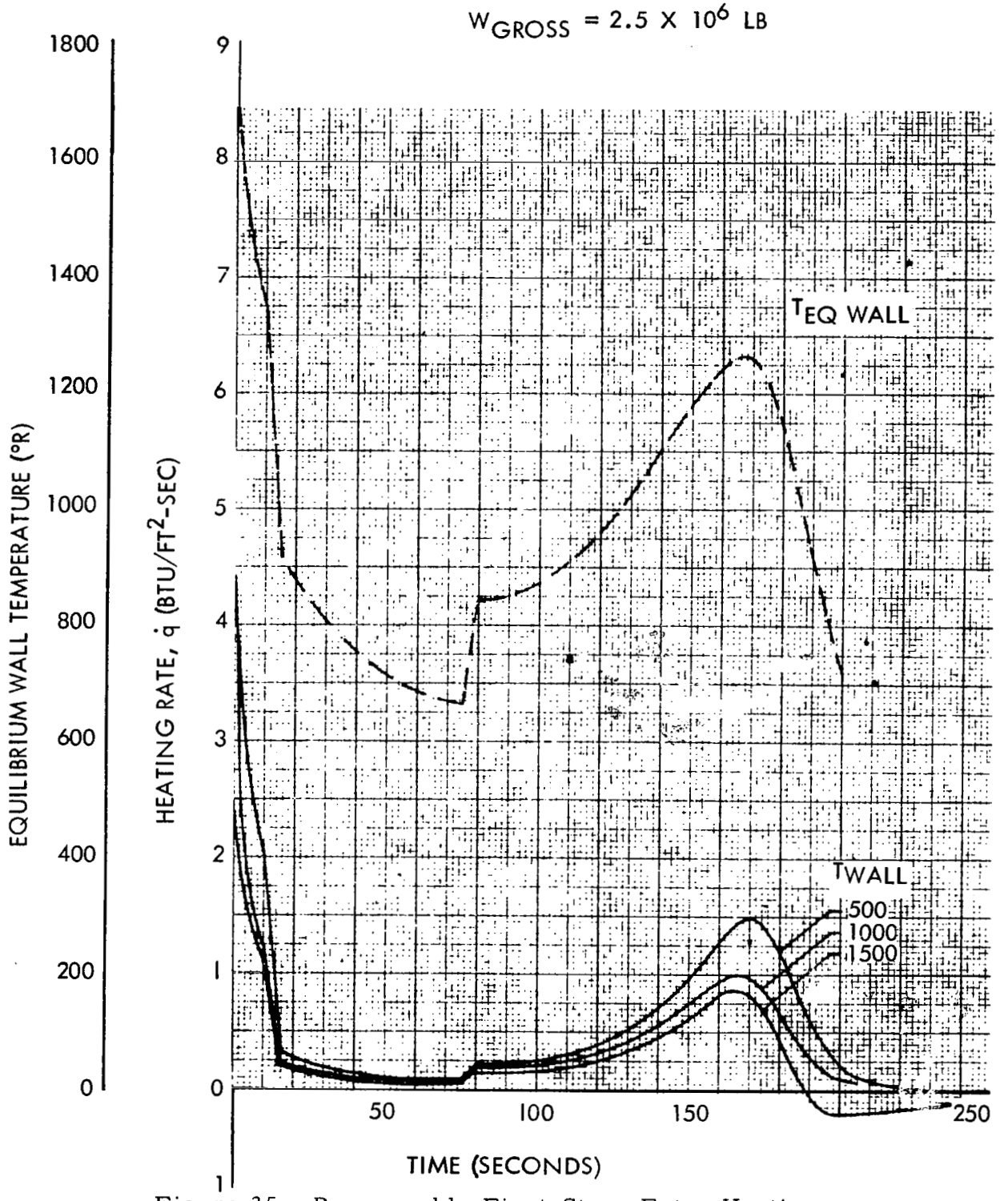

Figure 35. - Recoverable First-Stage Entry Heating - Configuration 3 - Body Point 2

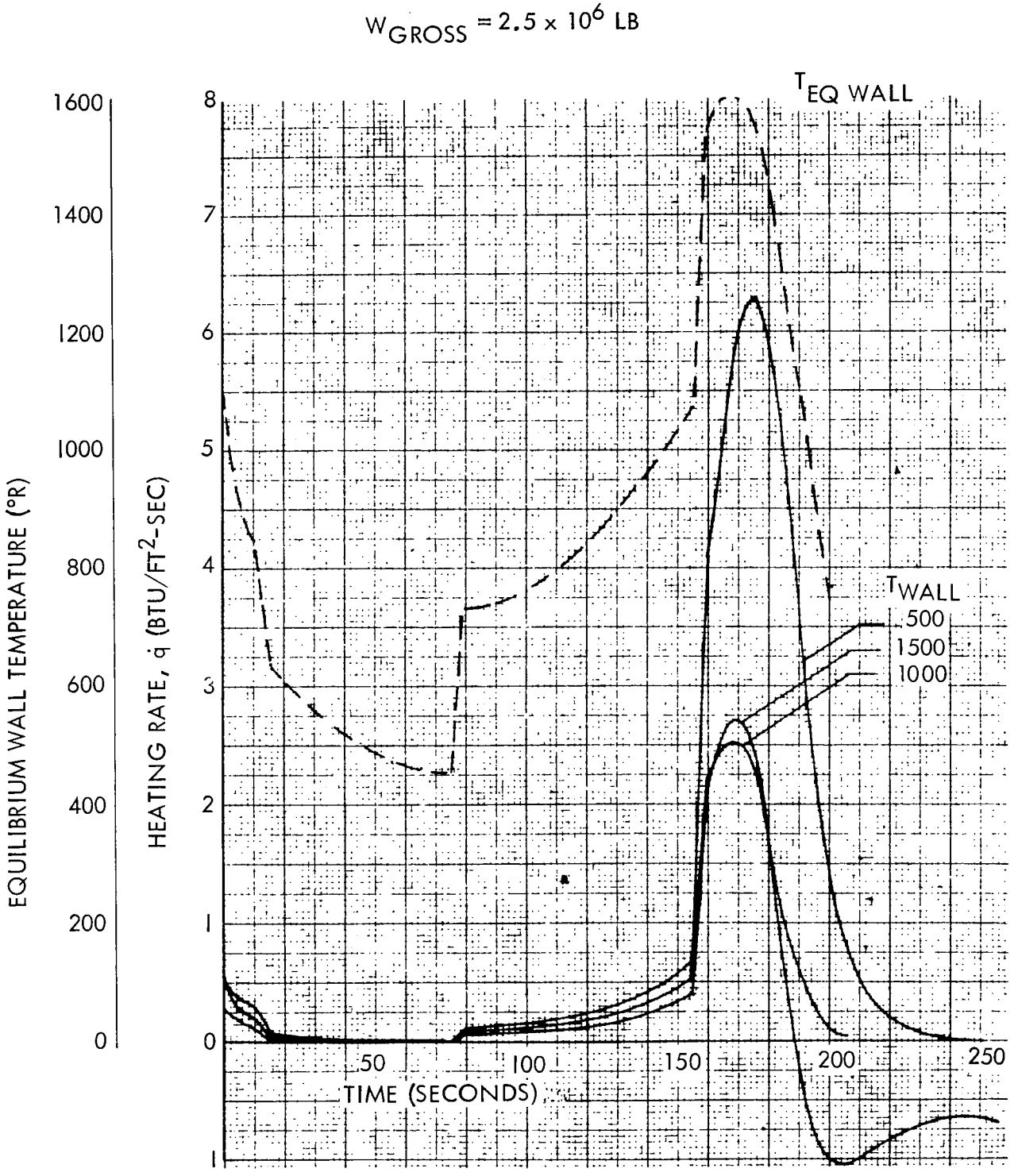

Figure 36. - Recoverable First-Stage Entry Heating - Configuration 3 - Body Point 3

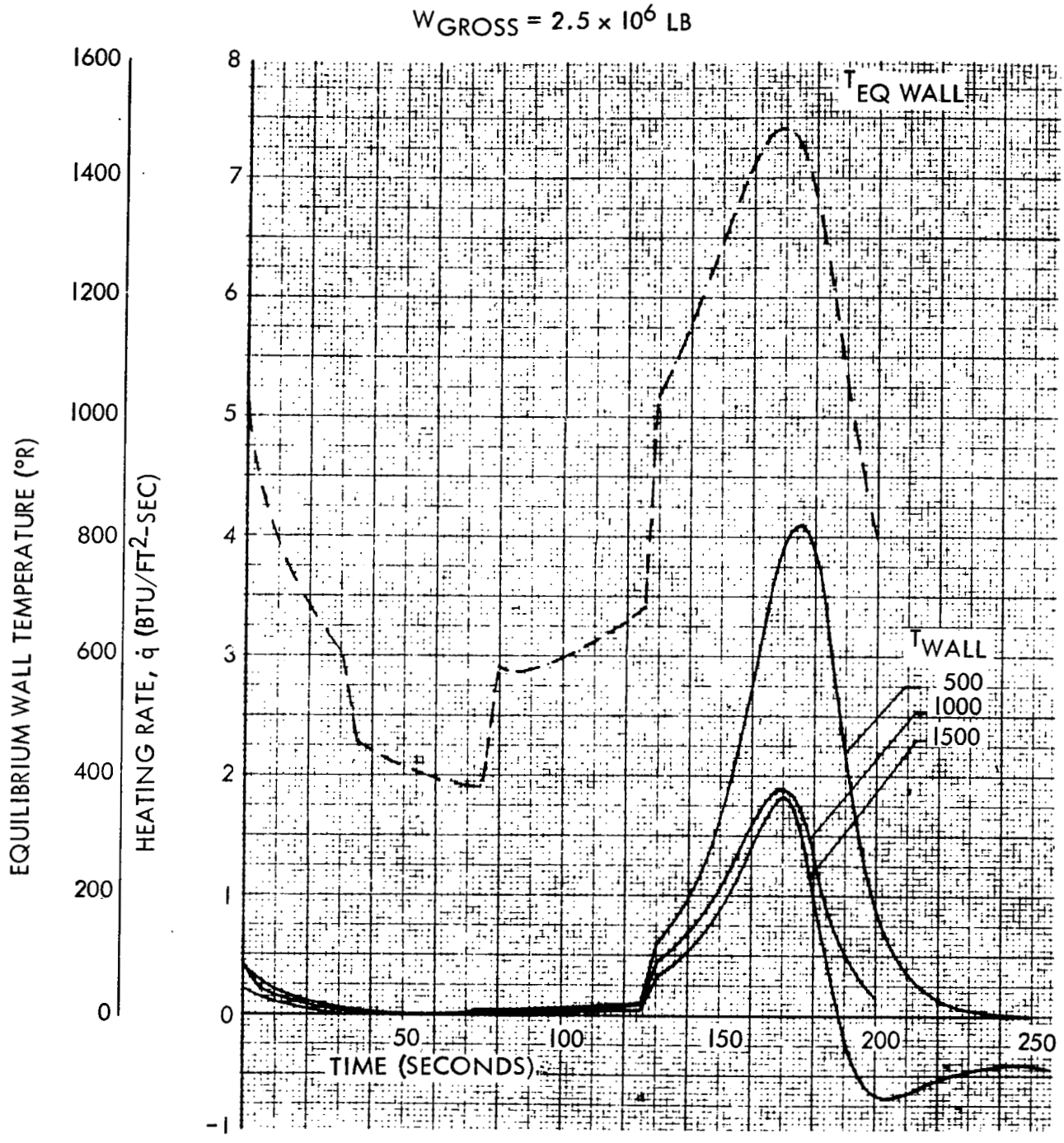

Figure 37. - Recoverable First-Stage Entry Heating - Configuration 3 - Body Point 4

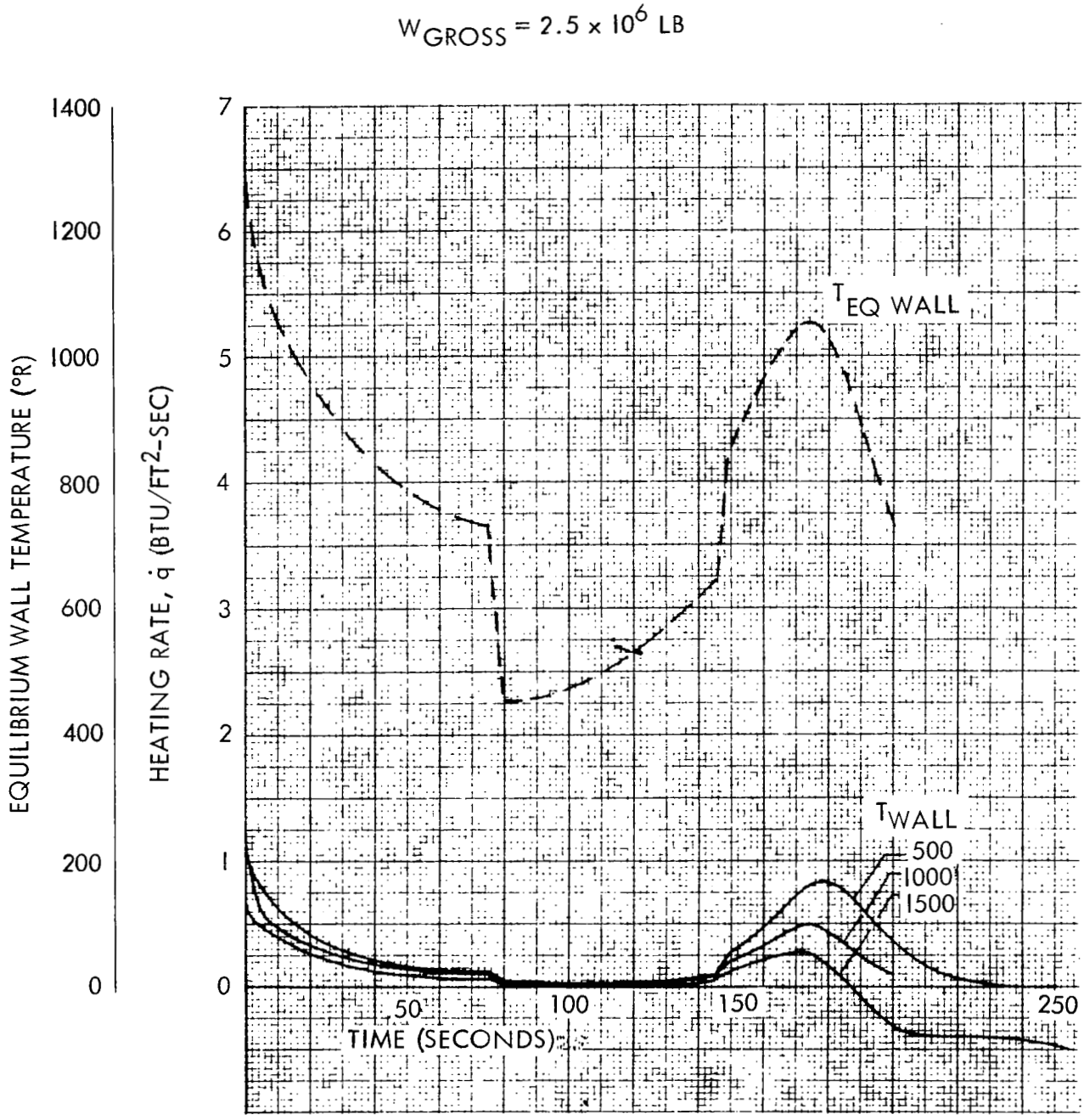

Figure 38. - Recoverable First-Stage Entry Heating - Configuration 3 - Body Point 5

is a jump in the heating at each body point due to the change in angle of attack. During the descent to lower altitudes, the flow once again becomes turbulent over the body, and the heating increases to a second peak value.

The total heat loads experienced from the time of separation to the time at which the heating rate becomes zero are tabulated in table 6 for each of the body points. Maximum cold-wall heat loads are on the order of 200 Btu/ft^2, with the major portion of the heat load occurring during the entry portion of the flight, in contrast to the maximum heating rate conditions, which are encountered at first-stage separation when the velocity is highest.

External Load Evaluation

The major structural shell elements are designed to a series of loading intensities and temperatures occurring at various times throughout the mission trajectory. Of major interest is the overall design envelope for the recoverable first stage. An additional design loading has to be considered for the reentry phase of the trajectory, which could possibly be the most critical, both from the thermal aspect and loading intensity. The entry corridor flown was considered to be at maximum aerodynamic lift with angle of attack of 55 degrees approximately for all size vehicles. The resulting decelerations from this flight profile was 0.5 g's along the flight path and 4 g's normal to the flight path. These deceleration conditions were assumed to prevail when the reentry stage is subjected to its highest heating rates and when the load-carrying structure reaches its maximum temperature. The weight distribution for the reentry vehicle was taken to be that of the stage at stage-one burnout (fig. 7), and the unit distribution along the stage length for the three sizes of vehicles is indicated in figure 39. This weight distribution will produce the design loads, bending moments, and axial loads, during the deceleration. The wing weight was considered to be reacted uniformly along the root chord. The stationwise shear loads due to 1-g normal inertia are shown in figure 40, and the vehicle bending moments from a 4-g normal inertia (maximum deceleration component) is given in figure 41. These bending moments are not balanced yet by any aerodynamic forces, but are conconsidered as a fully fixed condition at station zero. From figures 15 through 17 the hypersonic lift coefficient is obtained, and the resulting lift distribution from both the wing and fuselage was evaluated. The normal force component from the wings was reacted by the front and rear spars into the fuselage section: Based upon the hypersonic center of pressure at 50-percent chord, the concentrated equivalent loads of the two wing spars were derived; the overall stage shear forces due to the aerodynamic forces are shown in figure 42, and the resulting bending moments in figure 43. The aerodynamic

TABLE 6. - RECOVERABLE FIRST-STAGE ENTRY HEATING LOADS

Configuration	Gross Weight	T_{wall}	Body Point	Heat Load, Q, Btu/Ft^2		
				0 to Apogee	Apogee to -$\dot{q}$	Total
1	1.3 x 10^6 lb	500°R	1	60.01	176.69	236.70
			2	67.68	90.33	158.01
			3	9.98	192.44	202.42
			4	9.66	168.23	177.89
			5	34.97	37.08	72.05
		1000°R	1	46.65	70.84	117.49
			2	43.94	61.55	105.49
			3	7.97	71.73	79.70
			4	7.57	77.24	84.81
			5	27.60	19.08	46.68
		1500°R	1	39.98	49.15	89.13
			2	37.50	45.05	82.55
			3	5.15	52.79	57.94
			4	4.77	54.97	59.74
			5	21.37	7.83	29.20
2	1.9 x 10^6 lb	500°R	1	47.65	180.44	228.09
			2	53.70	85.47	139.17
			3	7.85	209.06	216.91
			4	7.10	171.67	178.77
			5	27.73	36.71	64.44
		1000°R	1	38.59	70.09	108.68
			2	37.74	58.88	96.62
			3	6.52	75.19	81.71
			4	5.79	76.39	82.18
			5	22.70	18.81	41.51
		1500°R	1	31.64	52.13	83.77
			2	29.69	43.61	73.30
			3	4.04	61.72	65.76
			4	3.54	57.67	61.21
			5	16.88	7.83	24.71
3	2.5 x 10^6 lb	500°R	1	43.41	192.05	235.46
			2	44.87	83.82	128.69
			3	6.60	219.58	226.18
			4	6.00	173.84	179.84
			5	25.05	37.71	62.76
		1000°R	1	35.18	76.35	111.53
			2	31.00	57.91	88.91
			3	5.47	21.58	27.05
			4	4.87	77.83	82.70
			5	20.53	19.10	39.63
		1500°R	1	28.93	59.27	88.20
			2	25.06	43.64	68.70
			3	3.44	68.61	72.05
			4	3.02	60.58	63.60
			5	15.31	8.76	24.07

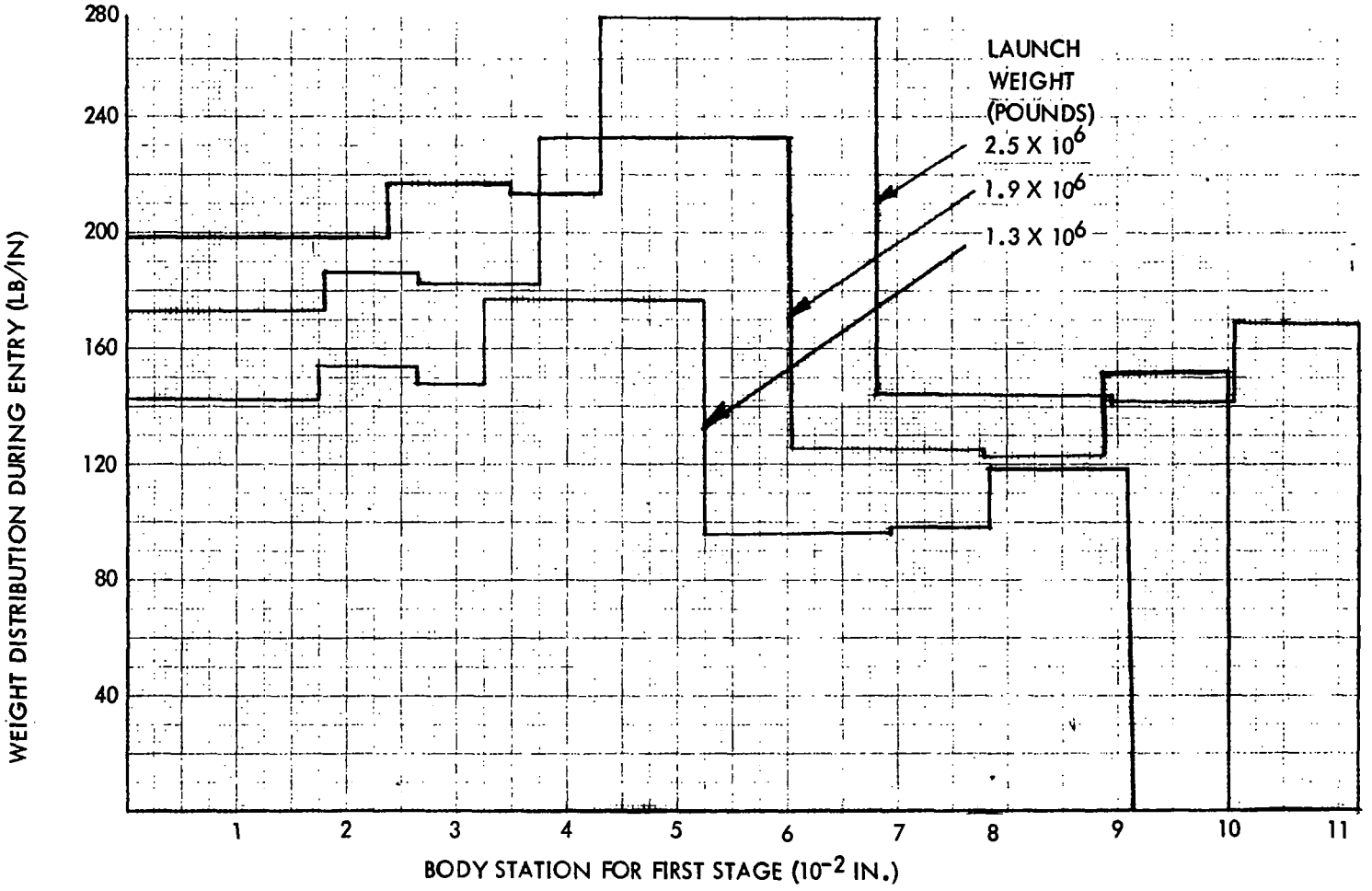

Figure 39. - Stationwise Weight Distribution for Base-Line Vehicles During Entry

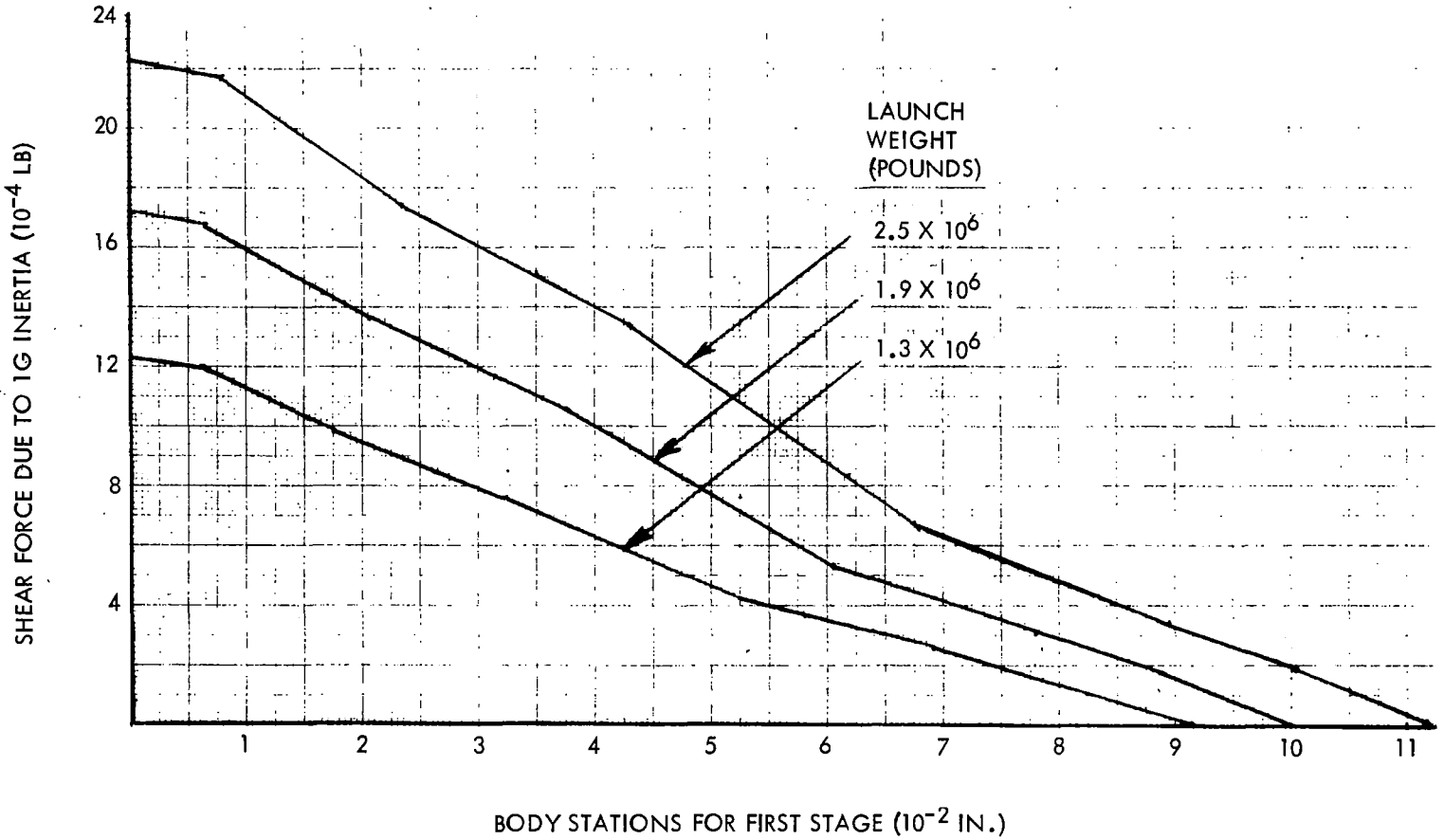

Figure 40. - Station Shear Load Due to Normal Inertia

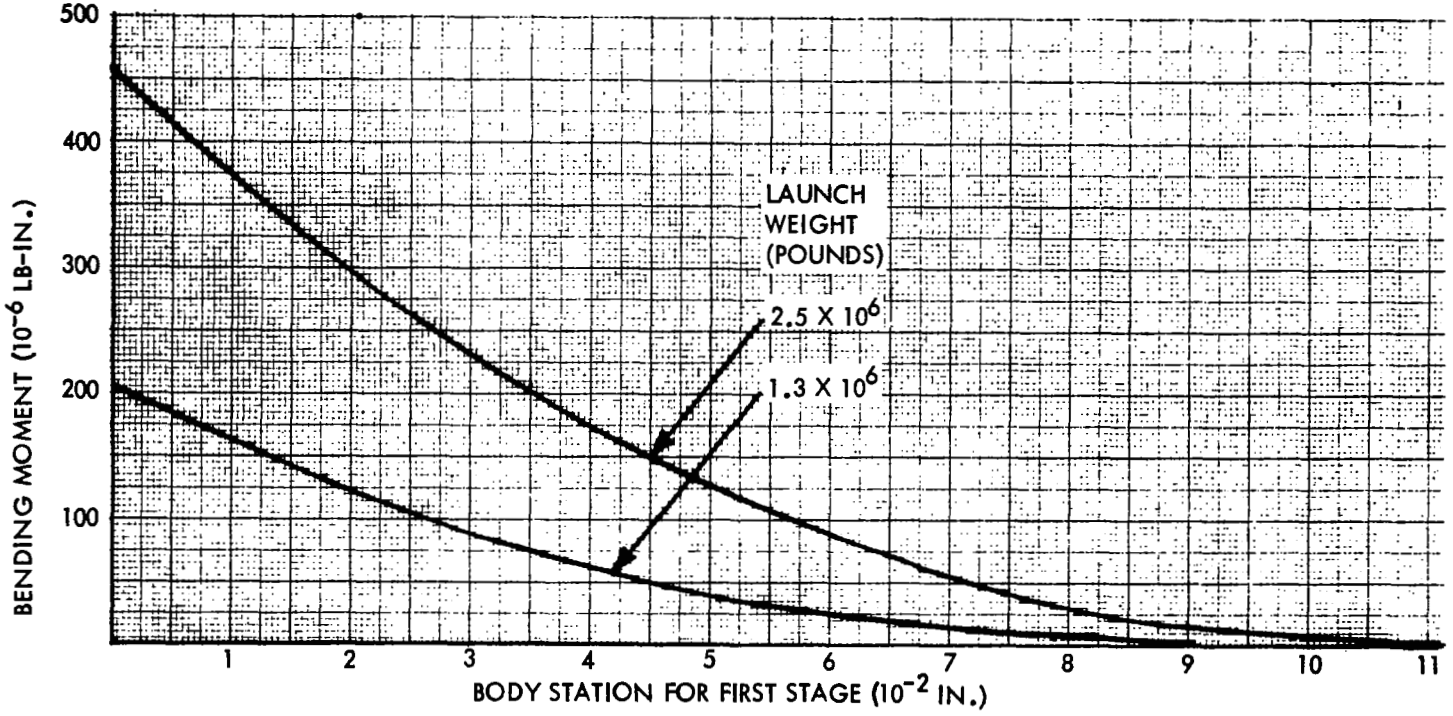

Figure 41. - Vehicle Bending Moments Due to Inertial Loading Only (4-G Normal)

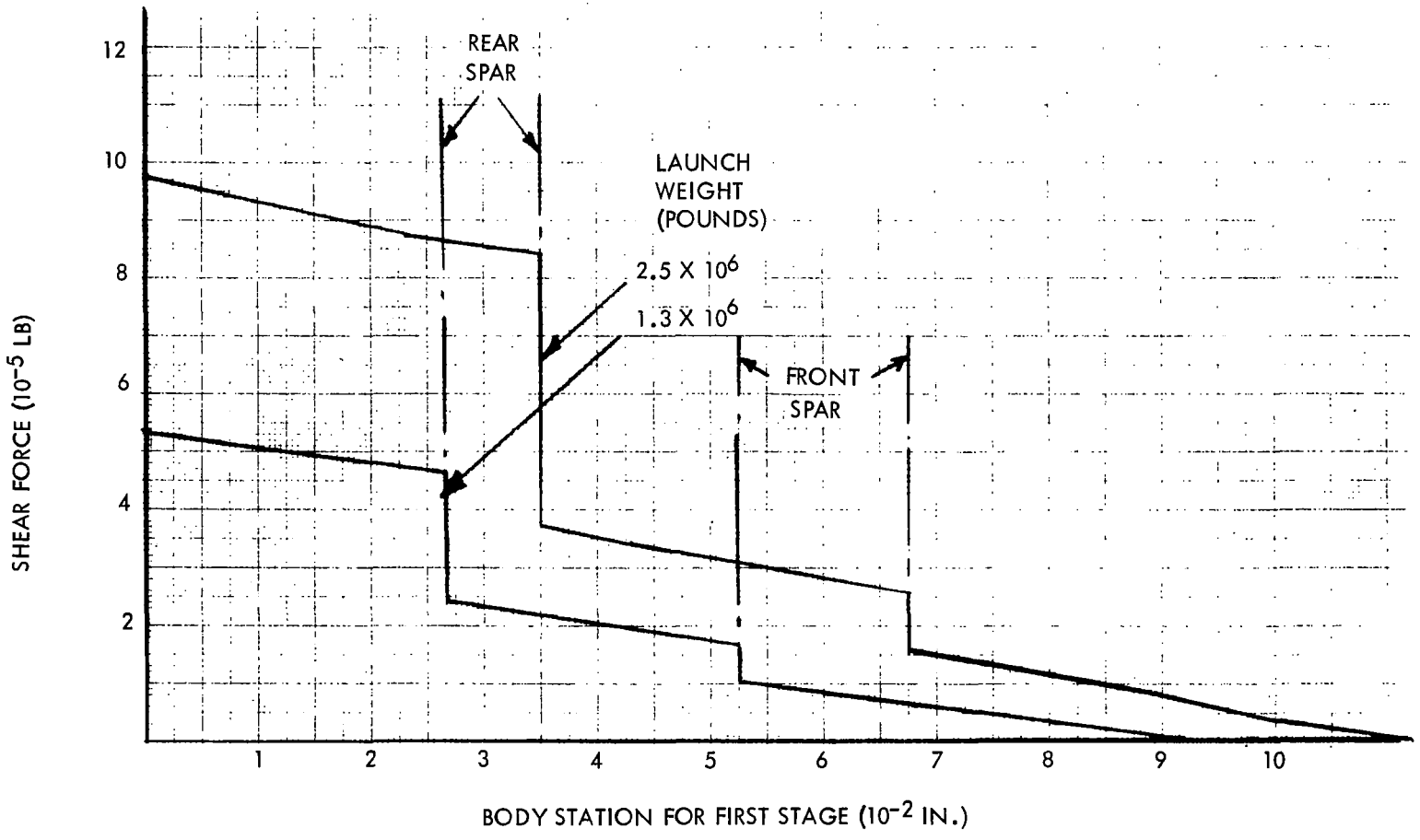

Figure 42. - Vehicle Shear Force Due to Aerodynamic Loading During Entry

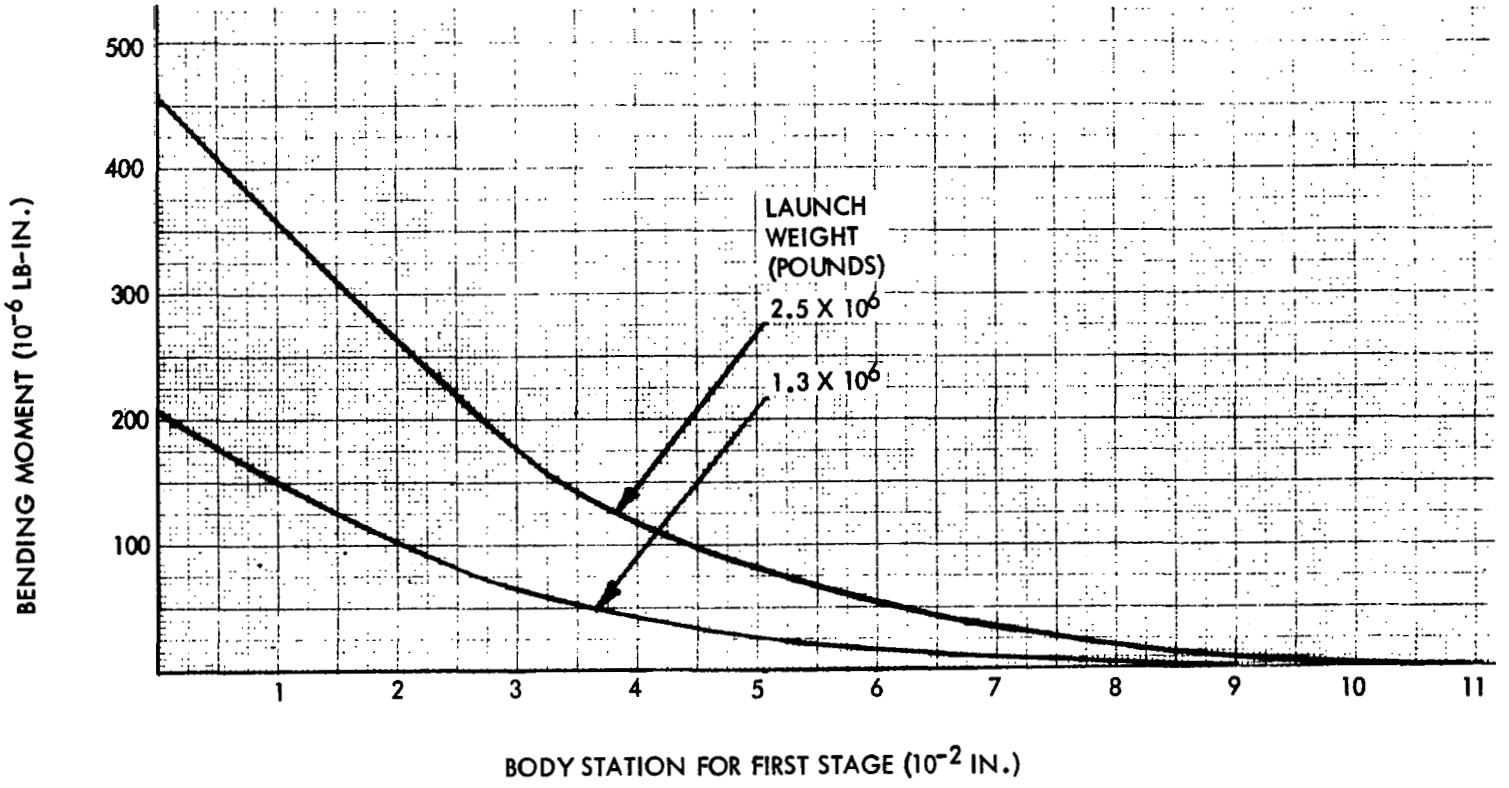

Figure 43. - Vehicle Bending Moments Due to Aerodynamic Forces Only

loading and the inertial loading distributions complement one another for the vehicle to be in balance. Therefore, the resulting net shear force during reentry for stage one is given in figure 44, with the corresponding bending moment in figure 45.

There are other design conditions to be considered. These result from the boost ascent phase of the trajectory. Based upon the trajectory analysis and the vehicle design parameters used in the vehicle synthesis, the bending moment and axial loads were evaluated for the first stage. There were three flight conditions considered: prelaunch at takeoff, maximum dynamic pressure, and end boost of first stage (maximum acceleration). These loads throughout the vehicle length are plotted in figures 46 and 47. Although the bending moment during entry (fig. 46) is of the same magnitude as prelaunch for the center portion of the fuselage, the axial load during entry is considerably smaller. The maximum loading intensity during reentry for the 1.3×10^6 pound vehicle is given by

$$N_{x_{max}} = \frac{66832}{\pi D} + \frac{25 \times 10^6}{\frac{\pi D^2}{4}}$$

where D = diameter of 260 inches

Therefore $N_{x_{max}} = 552$ lb/in.

This load intensity is less than one-quarter of the maximum design load intensity during boost ascent. Therefore, if the load-carrying structure does not get too hot, and the effective stress and modulus allowables are not reduced to one-quarter of their room temperature values, then the load-carrying structural sizing will not be determined by the entry load intensities. The only effect that the entry of these stages have on the structural design is to influence the thermal environment of the material, select the type of material, and dictate the insulation requirements, if required.

During ascent the first-stage propellant tanks are partially filled, and the inertia effects of the propellant contribute as a hydrostatic pressure to the total design pressures for the tanks and bulkheads. A pressure matrix for the six vehicles is given in table 7.

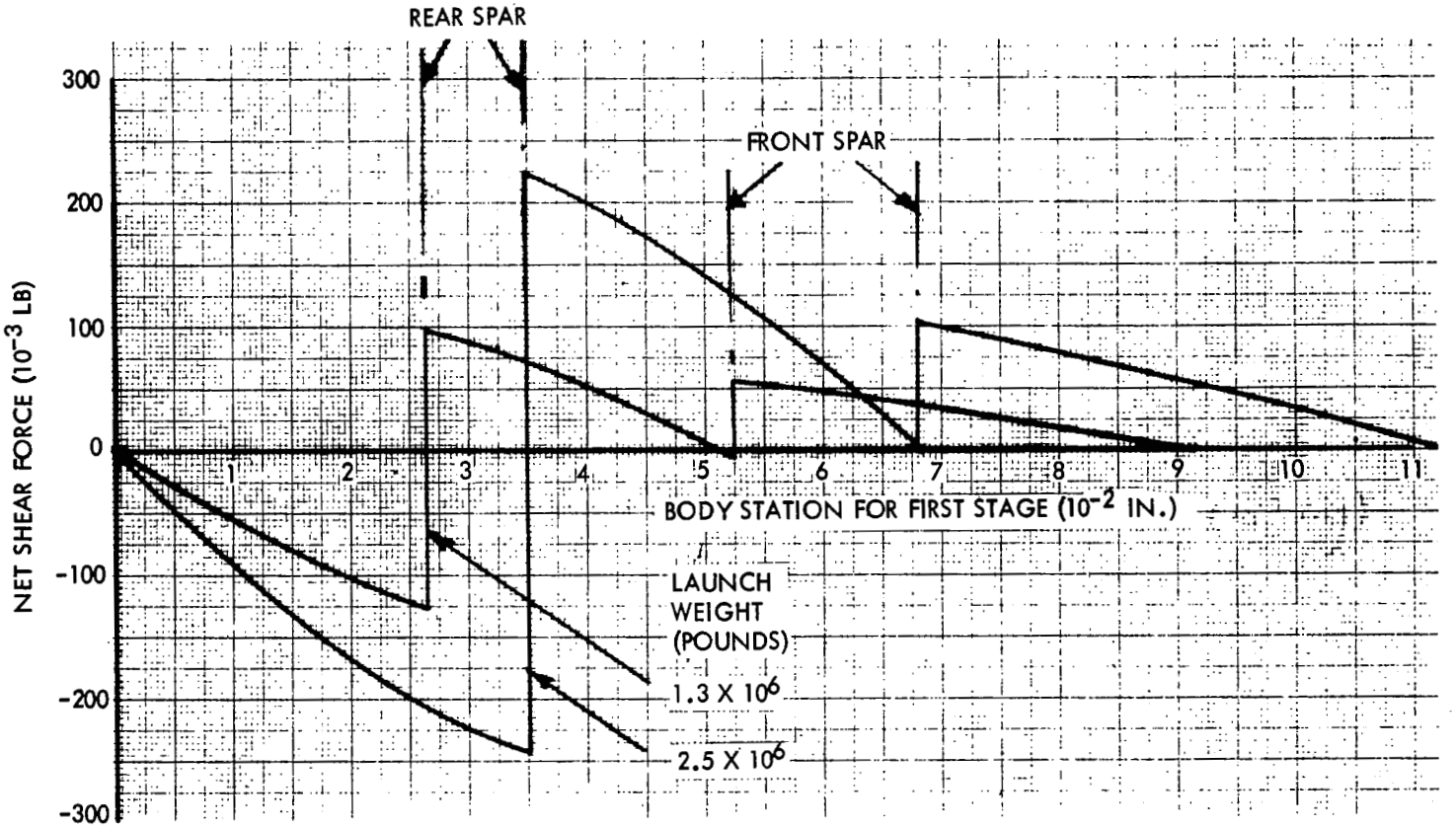

Figure 44. - Vehicle Net Shear Force During Entry

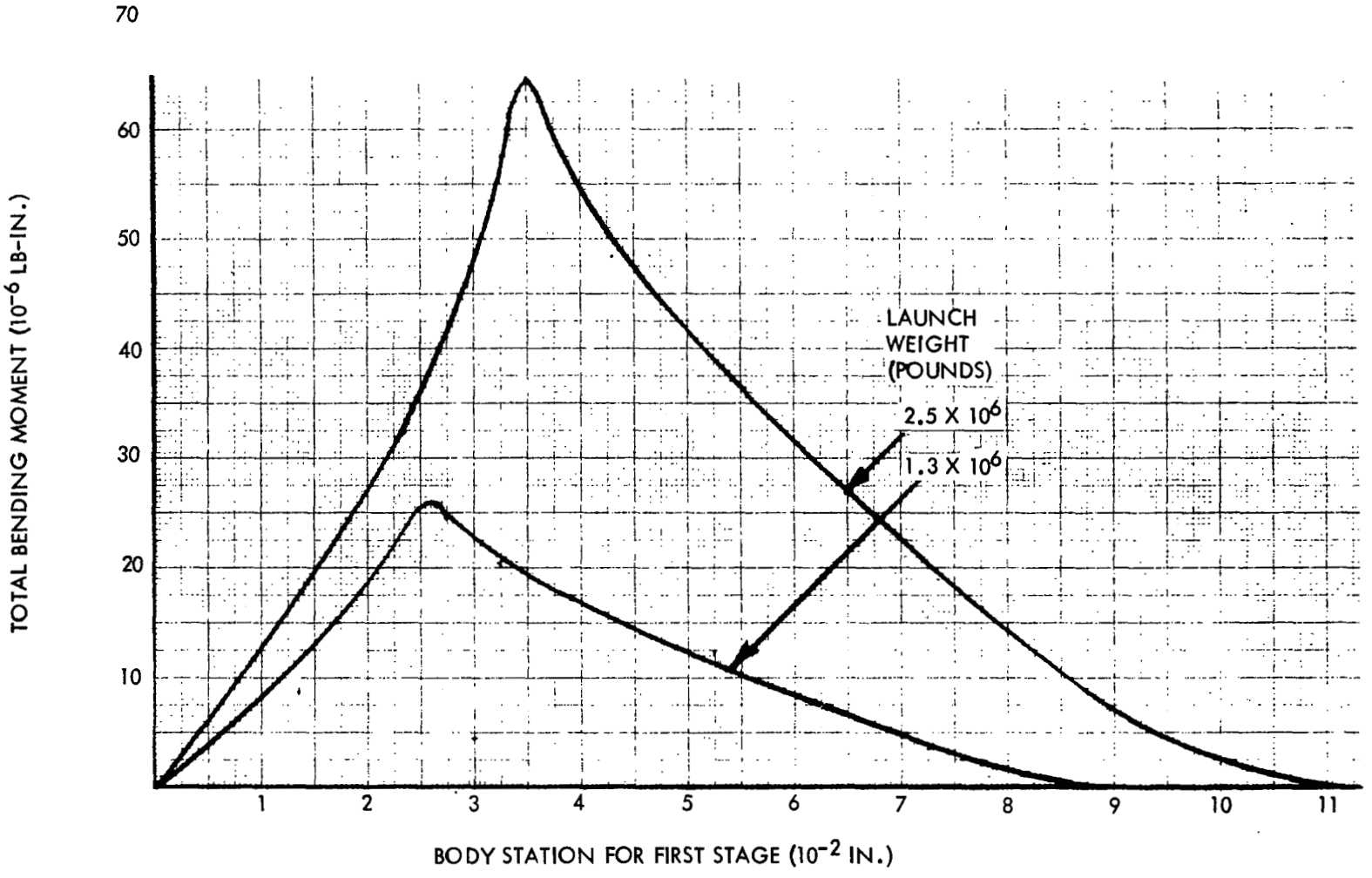

Figure 45. - Vehicle Maximum Bending Moments During Entry Trajectory

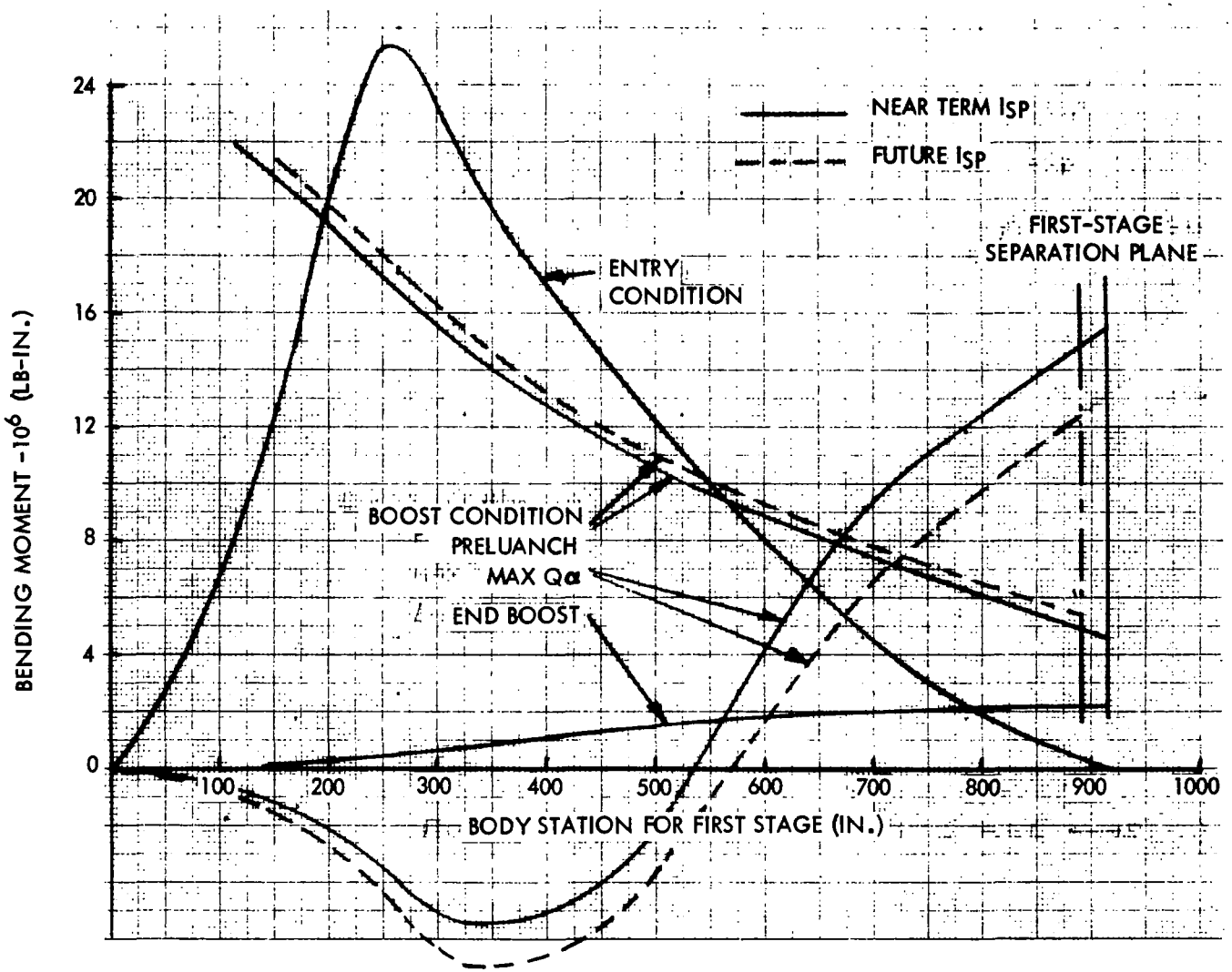

Figure 46. - Bending Moments Experience by 1.3×10^6-Pound Vehicle

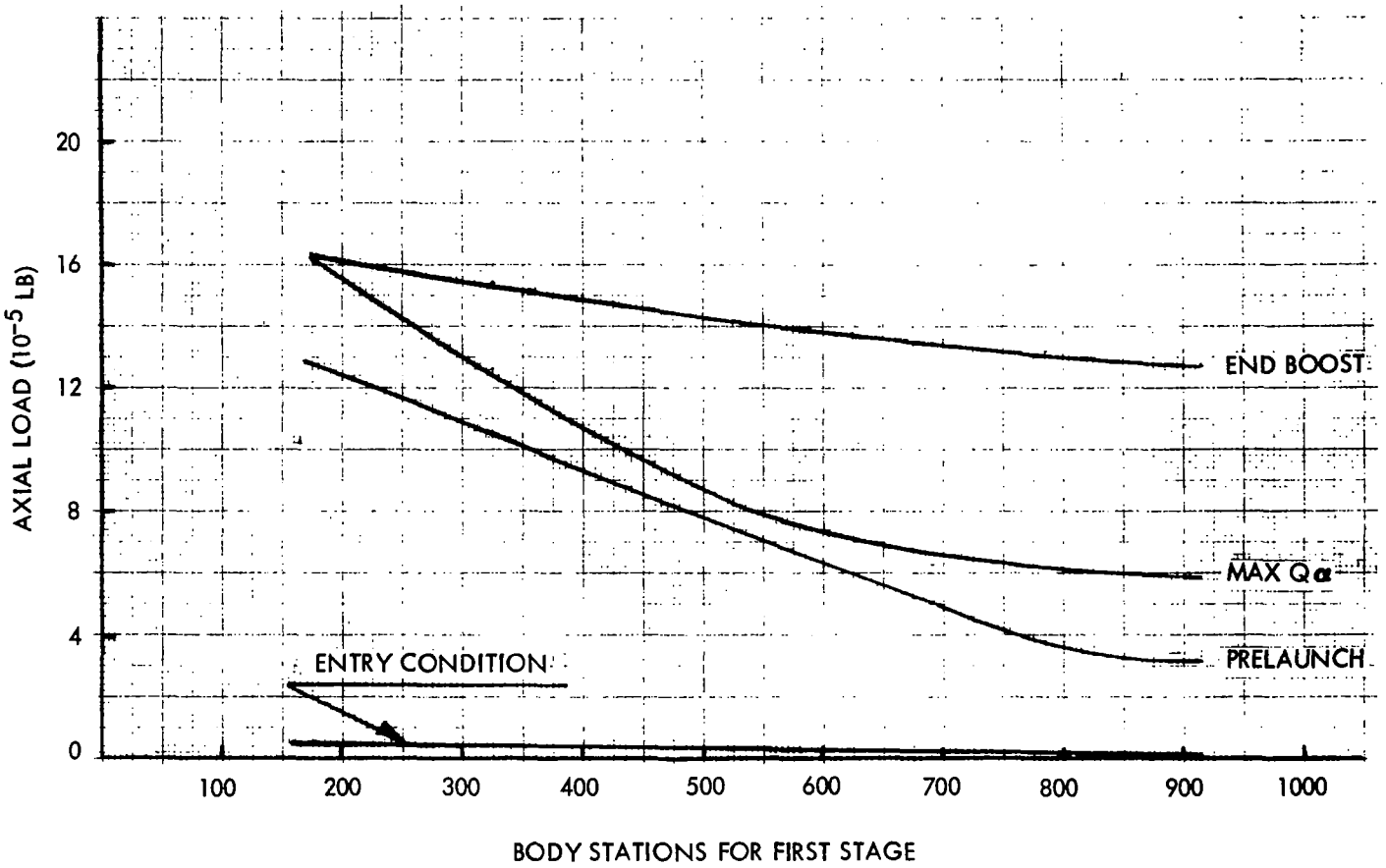

Figure 47. - Axial Load for 1.3×10^6-Pound Vehicle

TABLE 7. - BASE-POINT VEHICLE DESIGN PRESSURE MATRIX (PSI)

	Prelaunch	Max Qα	End Boost
1.3 x 10^6 lb - near-term I_{sp}			
Aft tank	6.3	39.0	39.0
Forward tank	7.6	39.0	39.0
Aft bulkhead		45.8	
Forward bulkhead		39.0	39.0
Aft tank forward bulkhead		39.0	39.0
Forward tank aft bulkhead		43.8	
1.3 x 10^6 lb - future I_{sp}			
Aft tank	5.9	39.0	39.0
Forward tank	7.1	39.0	39.0
Aft bulkhead		45.5	
Forward bulkhead		39.0	39.0
Aft tank forward bulkhead		39.0	39.0
Forward tank aft bulkhead		43.6	
1.9 x 10^6 lb - near-term I_{sp}			
Aft tank	6.8	39.0	39.0
Forward tank	8.3	39.0	39.0
Aft bulkhead		46.9	
Forward bulkhead		39.0	39.0
Aft tank forward bulkhead		39.0	39.0
Forward tank aft bulkhead		44.6	
1.9 x 10^6 lb - future I_{sp}			
Aft tank	6.4	39.0	39.0
Forward tank	7.8	39.0	39.0
Aft bulkhead		46.6	
Forward bulkhead		39.0	39.0
Aft tank forward bulkhead		39.0	39.0
Forward tank aft bulkhead		44.3	
2.5 x 10^6 lb - near-term I_{sp}			
Aft tank	8.0	39.0	39.0
Forward tank	9.7	39.0	39.0
Aft bulkhead		47.4	
Forward bulkhead		39.0	39.0
Aft tank forward bulkhead		39.0	39.0
Forward tank aft bulkhead		44.9	
2.5 x 10^6 lb - future I_{sp}			
Aft tank	7.5	39.0	39.0
Forward tank	9.1	39.0	39.0
Aft bulkhead		47.1	
Forward bulkhead		39.0	39.0
Aft tank forward bulkhead		39.0	39.0
Forward tank aft bulkhead		44.7	

Design Load Intensity

The following strength criteria were used to analyze the shell structures for material failure:

A tensile stress resulting from ultimate pressure loads and/or inertia loads will not exceed the tensile ultimate stress, F_{t_u}, of the material. If the inertia loads are added to the tensile stresses, ultimate inertia loads are used. Limit inertia loads are used if the inertia loads are subtracted from the tensile stresses:

$$F_{t_u} \geq \frac{1}{\bar{t}}\left[\left(\frac{BM}{\pi R^2} + \frac{PR}{2}\right) FSU - \frac{AL}{2\pi R}\right]$$

where t is the equivalent shell longitudinal extensional thickness.

A tensile stress caused by yield pressure and/or limit inertia loads will not exceed the tensile yield stress, F_{t_y}, of the material. If the inertia loads are added to the tensile stresses, yield inertia loads are used. Limit inertia loads are used when the inertia loads are subtracted from the tensile stress:

$$F_{t_y} \geq \frac{1}{\bar{t}}\left[\left(\frac{BM}{\pi R^2} + \frac{PR}{2}\right) FSY - \frac{AL}{2\pi R}\right]$$

A compressive stress resulting from ultimate inertia loads and pressure will not exceed the allowable compressive strength, F_{c_u}, of the material. If the pressure is added to the compressive stresses, ultimate pressure is used. Minimum pressure is used when the pressure is subtracted from the compressive stresses:

$$F_{c_u} \geq \frac{1}{\bar{t}}\left[\left(\frac{BM}{\pi R^2} + \frac{AL}{2\pi R}\right) FSU - \frac{P_{MIN}R}{2}\right]$$

or for collapsing pressures,

$$F_{c_u} \geq \frac{1}{\bar{t}}\left[\left(\frac{BM}{\pi R^2} + \frac{AL}{2\pi R} + \frac{PR}{2}\right) FSU\right]$$

A compressive stress resulting from yield inertia loads and pressure will not exceed the yield compressive strength, F_{c_y}, of the material. If the pressure

is added to the compressive stresses, yield pressure is used. Minimum pressure is used when the pressure is subtracted from the compressive stresses:

$$F_{c_y} \geq \frac{1}{t}\left[\left(\frac{BM}{\pi R^2} + \frac{AL}{2\pi R}\right) FSY - \frac{P_{MIN}R}{2}\right]$$

The ultimate compressive load intensity matrix for the six vehicles is given in table 8 for three phases of the boost trajectory. Values of maximum N_x/R quoted in table 8 are corrected for high temperature at end boost by the changes in the materials modulus with temperature

$$N_{x_{eq}} = N_{x_{\text{End Boost}}} \frac{E_{\text{Room Temp}}}{E_{\text{End Boost Temp}}}$$

Table 8 now represents the design compressive loading intensity matrix for the structural components of the recoverable first stages. Pressure requirements from table 7 will dictate the strength requirements for the pressurized shells and select the allowable skin thickness due to hoop tension for the various components.

TABLE 8. - VEHICLE DESIGN LOAD INTENSITIES

Station	Prelaunch NX LB/IN.	Max Q Alpha NX LB/IN.	End Boost NX LB/IN.	Max NX/R
	1.3×10^6 Pound Vehicle - Near-Term I_{sp}			
173.	2732.	2834.	3058.	23.5239
265.	2401.	-76.	179.	18.4683
325.	2190.	2310.	2920.	22.4585
525.	1541.	-1128.	-63.	11.8571
694.	1054.	1307.	2604.	20.0288
786.	793.	1360.	2547.	19.5901
916.	725.	1413.	2443.	18.7928
	1.3×10^6 Pound Vehicle - Future I_{sp}			
173.	2747.	2834.	3086.	23.7355
265.	2419.	-32.	213.	18.6099
316.	2245.	2398.	2971.	22.8503
515.	1599.	-983.	6.	12.3023
668.	1161.	1309.	2701.	20.7735
760.	900.	1370.	2651.	20.3900
890.	830.	1436.	2559.	19.6838
	1.9×10^6 Pound Vehicle - Near-Term I_{sp}			
207.	3371.	3567.	3867.	25.7768
313.	2949.	245.	505.	19.6570
373.	2720.	3054.	3699.	24.6575
603.	1884.	-917.	197.	12.5584
780.	1311.	1359.	3296.	21.9726
887.	973.	1376.	3222.	21.4789
1002.	911.	1428.	3122.	20.8105
	1.9×10^6 Pound Vehicle - Future I_{sp}			
208.	3387.	3568.	3901.	26.0057
314.	2968.	294.	547.	19.7857
362.	2785.	3142.	3761.	25.0710
592.	1952.	-765.	282.	13.0151
752.	1441.	1597.	3414.	22.7617
858.	1104.	1470.	3349.	22.3276
973.	1040.	1479.	3260.	21.7336
	2.5×10^6 Pound Vehicle - Near-Term I_{sp}			
237.	4158.	4394.	4776.	29.8482
350.	3664.	893.	1122.	22.8989
431.	3320.	3886.	4563.	28.5197
677.	2346.	-420.	744.	14.6635
895.	1584.	1827	4070.	25.4349
1008.	1192.	1679.	3984.	24.9027
1119.	1128.	1582.	3883.	24.2658
	2.5×10^6 Pound Vehicle - Future I_{sp}			
238.	4173.	4396.	4818.	30.1095
351.	3683.	945.	1173.	23.0188
419.	3397.	3982.	4640.	28.9969
664.	2427.	-254.	847.	15.1681
862.	1740.	2101.	4214.	26.3395
975.	1350.	1949.	4139.	25.8704
1085.	1284.	1800.	4049.	25.3037

DESIGN SYNTHESIS

Thermal Evaluation

The additional design environment encountered during the entry trajectory will have an effect on the structural design of the major shell components of the first-stage fuselage. Heating profiles for the three entry vehicles were shown in the previous section, and the heating rates were applied to typical construction concepts to determine the transient thermal response and the maximum tenperature that the load-carrying material experiences. During these high-heating rates there also are associated deceleration loads. The maximum temperature condition does not necessarily coincide with the maximum external loading. For this study, it was assumed to be coincident; this does not impose a design condition that is too severe. The maximum equivalent axial load intensity is only 500 lb/in., which is considerably below the boost ascent design loads.

For the external structural concept, two types of designs are considered:

1. Hot structure - The load-carrying structure is fabricated from super alloys, and the skin material is thick enough to absorb the heat flux and only heats the structure to acceptable design levels.

2. Insulated conventional materials - The primary structure will be conventional materials (aluminum), which are protected by an outer insulation layer with the back-face temperature kept at approximately 300°F.

A numerical procedure was adopted to handle the transient temperature distribution in the material state and the insulation layers. A transient one-dimensional temperature distribution model was used for a composite slab, insulated at the back face, and subjected to thermal radiation at the other face. The slab was assumed to be initially at a uniform temperature. The one-dimensional model below has three different types of elements: (1) an internal element, (2) interface element between two materials, and (3) exterior surface element.

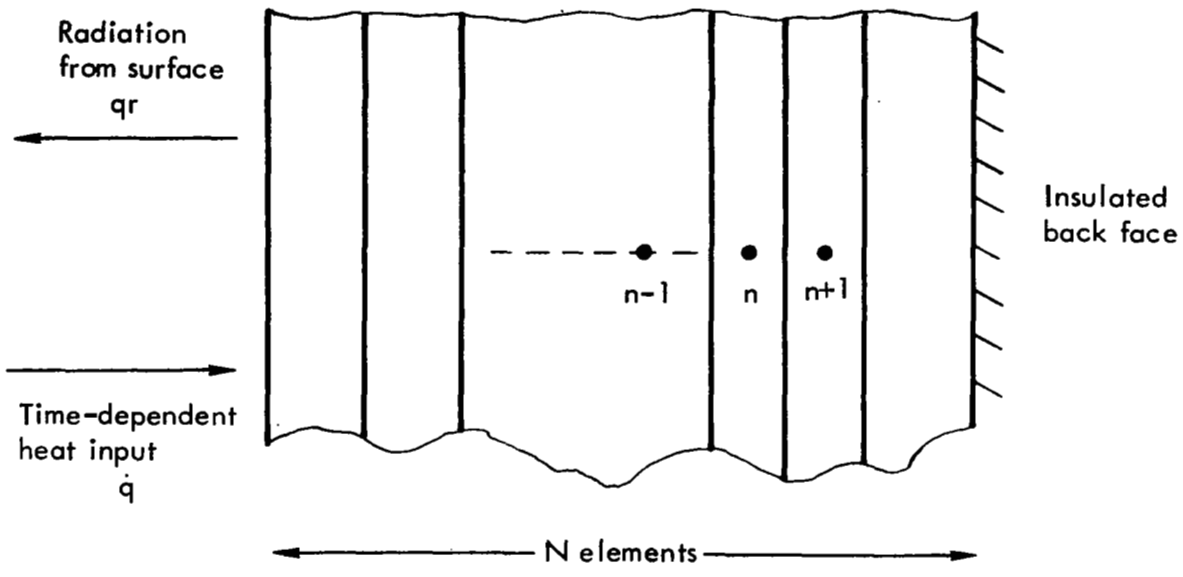

A computer program was generated to handle these transient conditions for the large families of fuselage materials and constructions.

The energy transferred into an arbitrary internal element at any instant of time is given by

$$\Sigma \text{energy in} = k\frac{\delta(1)}{\delta}(t_{n-1} - t_n) + \frac{k\,\delta(1)}{\delta}(t_{n+1} - t_n)$$

$$\Sigma \text{energy out} = 0.$$

where

k = the thermal conductance of the material

t_n = the temperature at the midpoint of the nth element

δ = characteristic dimension of the element

The change in the energy stored in the element is given by

$$\Sigma \text{ energy stored} = \rho\delta^2(1)C\frac{(t'_n - t_n)}{\Delta\theta}$$

where

ρ = the material's density

C = the material's specific heat

$\Delta\theta$ = time increment

t'_n = temperature of the midpoint at the end of the time interval

The conservation of the system's energy requires that the

Σ energy into the system + Σ energy out of the

system = the change in internal energy of the system

Therefore

$$k\,(t_{n-1} - t_n) + k\,(t_{n+1} - t_n) = \rho\delta^2 C\,\frac{(t'_n - t_n)}{\Delta\theta}$$

or

$$t'_n = \Theta\left[(t_{n-1} + t_{n+1}) + \left(\frac{1}{\Theta} - 2\right) t_n\right]$$

where

$$\Theta = \frac{k\Delta\theta}{\rho C \delta^2} \leq \frac{1}{2}$$

Consequently, the temperature at point n at the end of the time interval $\Delta\theta$, is determined from the initial temperatures at points n-1, n, and n+1. When the maximum value of Θ is substituted in the above equation, it reduces to

$$t'_n = \frac{1}{2}(t_{n-1} + t_{n+1})$$

The surface temperature, t_o, is found in a similar manner. The energy transferred into the first element is

$$\Sigma \text{ energy in} = q_{net} + k\,\frac{\delta(1)}{\delta}\,(t_1 - t_o)$$

$$\Sigma \text{ energy out} = 0$$

where

q_{net} is net heat flux into the element

$$q_{net} = q_{in} - q_{radiated}$$

The change in energy stored in the first element is given by

$$\Sigma_{\text{energy stored}} = \frac{\rho C \delta^2 (1)}{2} \frac{(t_o' - t_o)}{\Delta\theta}$$

where

t_o' is the surface temperature at the end of the $\Delta\theta$ time interval

By using the conservation of energy law we obtain

$$q_{net} + k (t_1 - t_o) = \frac{\rho C \delta^2}{2\Delta\theta} (t_o' - t_o)$$

or

$$t_o' = 2\Theta \left[\frac{q_{net}}{k} + t_1 + \left(\frac{1}{2\Theta} - 1 \right) t_o \right]$$

where

$$\Theta = \frac{k\Delta\theta}{\rho C \delta^2}$$

The temperature distribution at the interfaces of the composite material is based on the assumption of negligible heat resistance. Then the heat capacity of the interface element is determined by using a weighted average of heat capacities of the material on each side of the interface (ref. 5). The resulting equation is

$$t'_{(\text{interface})} = \overline{\Theta} \left[t (L, n-1) + t (L+1, 2) + \left(\frac{1}{\overline{\Theta}} - 2 \right) t_{\text{interface}} \right]$$

where

$$\overline{\Theta} = \frac{\overline{k}}{\rho C} \frac{\Delta\theta}{\delta^2}$$

$L = \ell^{th}$ layer of material

$\overline{k}$ = the average thermal conductances of the two materials

$\overline{C\rho}$ = the average volumetric specific heat of the materials

A range of super alloys with no external insulation was considered for the various size vehicles and several different thermal stations around the fuselage. The initial condition of the structure at separation will influence the thermal history. Figure 48 considers the structure being either at room temperature or 300°F, the temperature that various components of the vehicle will reach at maximum acceleration of end boost. The material used was titanium and aluminum with the heat flux experienced by the 1.3×10^6-pound vehicle at Station 3. Figure 48 shows that for relatively thin skins the temperature follows the equilibrium wall temperature during the high heat flux period irrespective of the assumed initial conditions. For the thick section, 0.320-inch, there still is a difference at the maximum temperature, but then the temperature rise is fairly small for both starting conditions. Since the material temperature is a function of its heat capacity, the structural designs were treated as an equivalent skin thickness, except for the honeycomb where only the outer skin thickness was taken for the heat sink. This allowed the back-face temperature estimates to be evaluated for a series of equivalent skin thicknesses irrespective of the type of construction. The second effect considered was that the material heat sink capability changes the surface temperature history. Figure 49 shows the relative temperatures for the Rene' 41 material for a range of thicknesses for the $1\text{-}3 \times 10^6$-pound vehicle at thermal station 3.

To find the difference of the position along the fuselage, point 4 was evaluated and the results shown in Figure 49. The resulting temperature is slightly lower and, therefore, for the design conditions it was considered that the maximum heating, point 3, would be applied to the whole of the fuselage. Heating rates for the largest vehicle, 2.5×10^6 pounds, appeared to be different than the small vehicle, and the variation of the temperature histories between the two vehicles is shown in Figure 50 for two materials. Figure 51 shows that the choice of material as the heat sink also has a noticeable difference on the maximum attainable temperature.

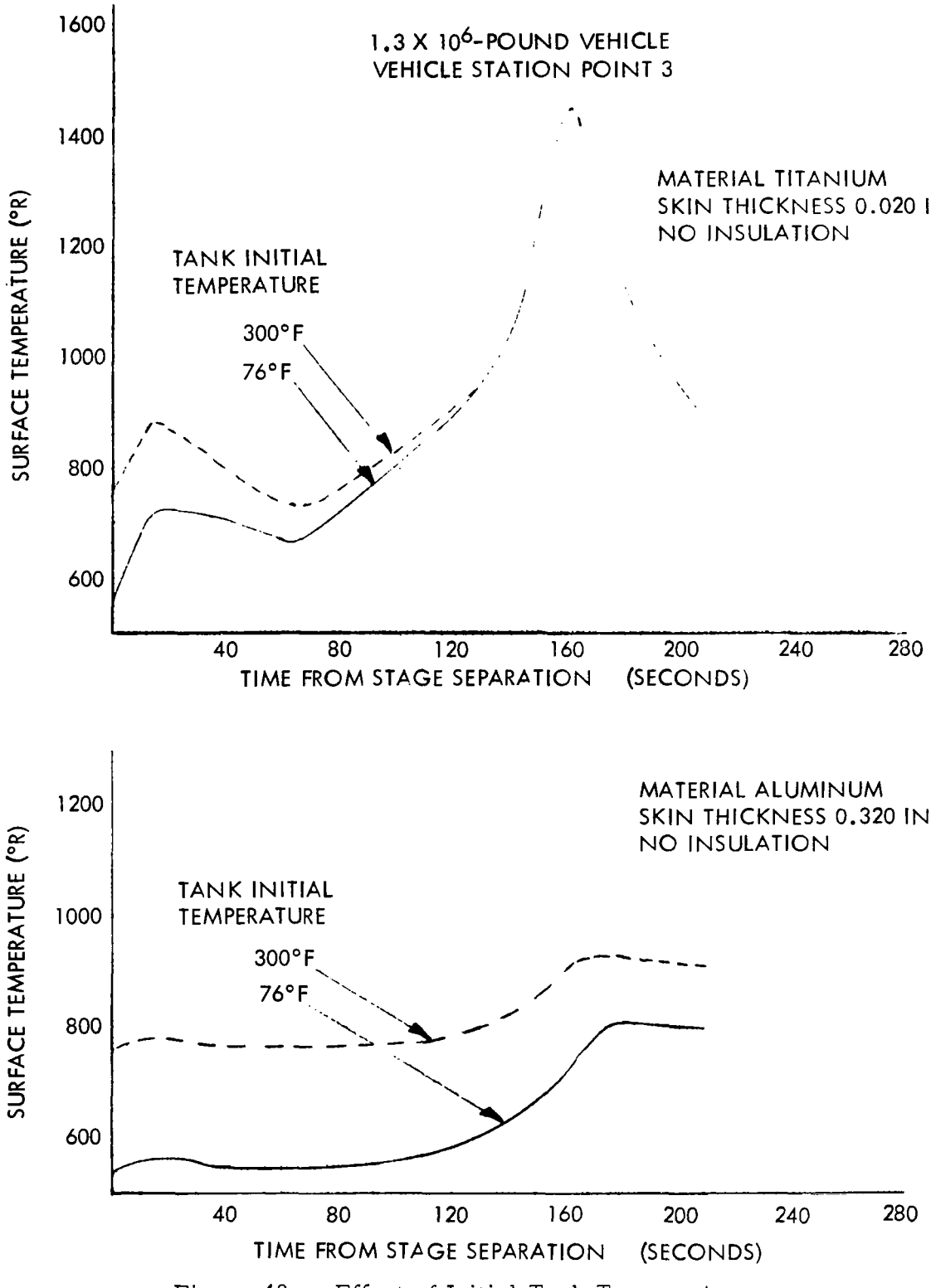

Figure 48. - Effect of Initial Tank Temperatures on Surface Temperature History

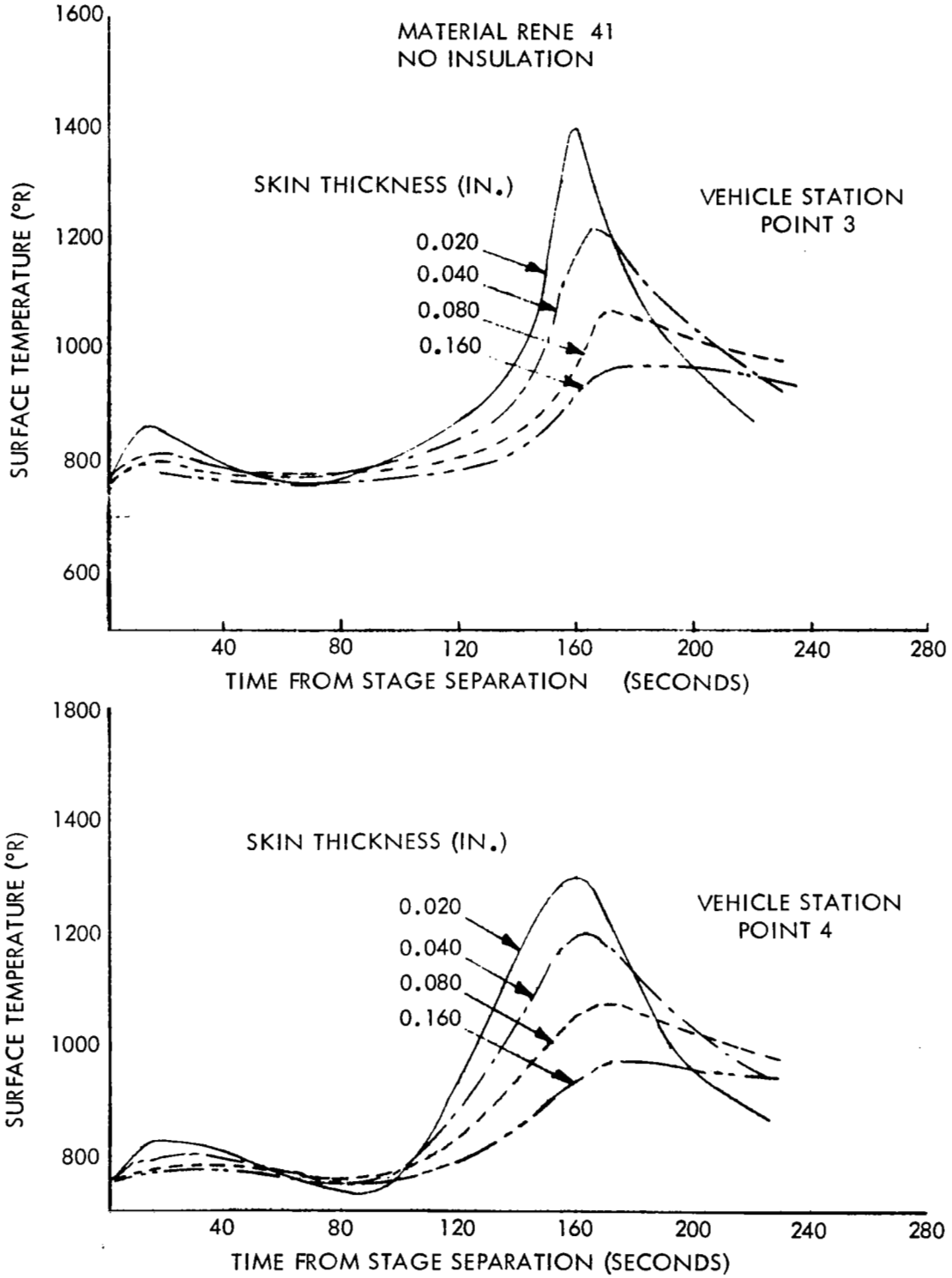

Figure 49. - Surface Temperature History for 1.3×10^6-Pound Vehicle

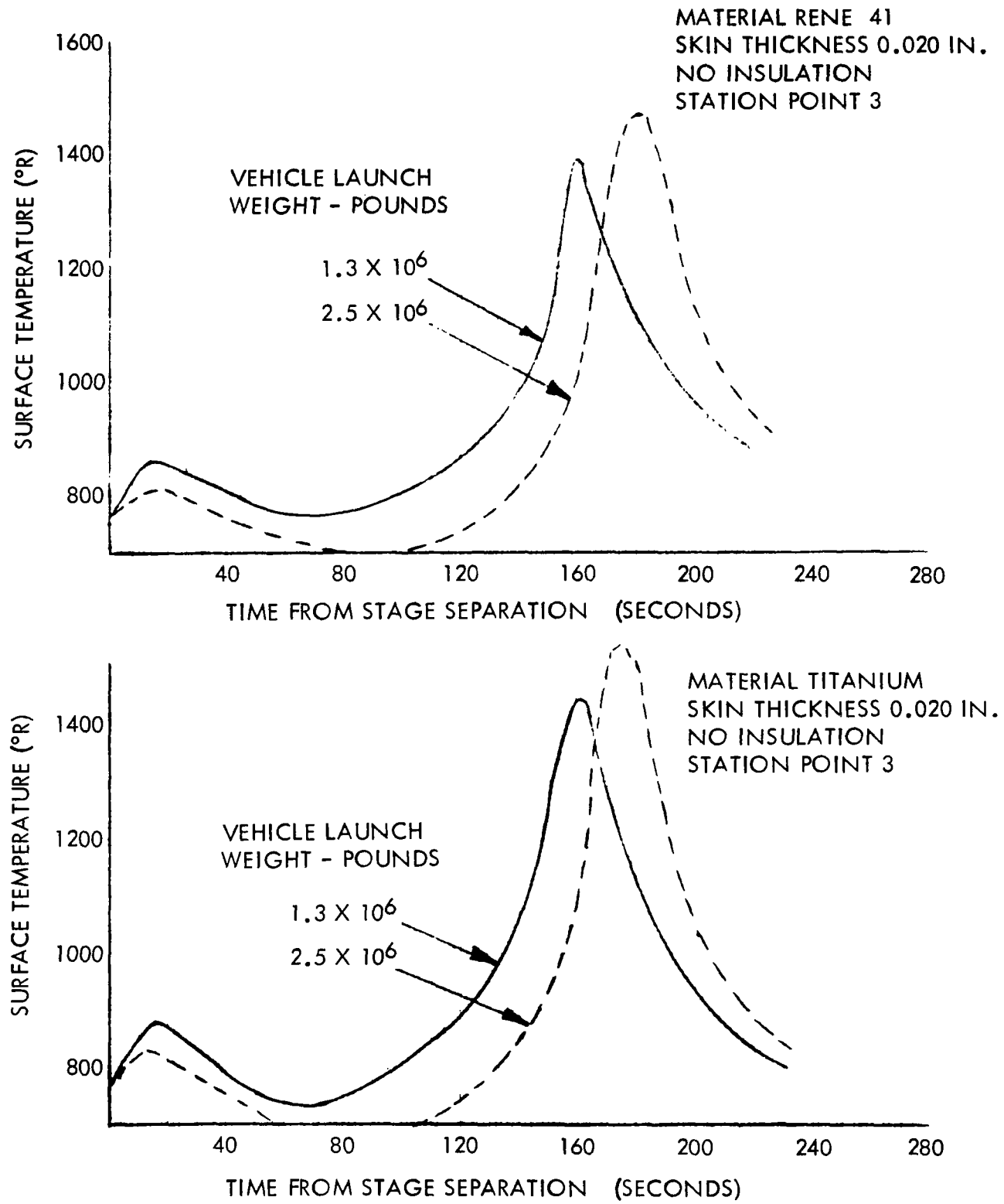

Figure 50. - Effect of Vehicle Size on Surface Temperature History

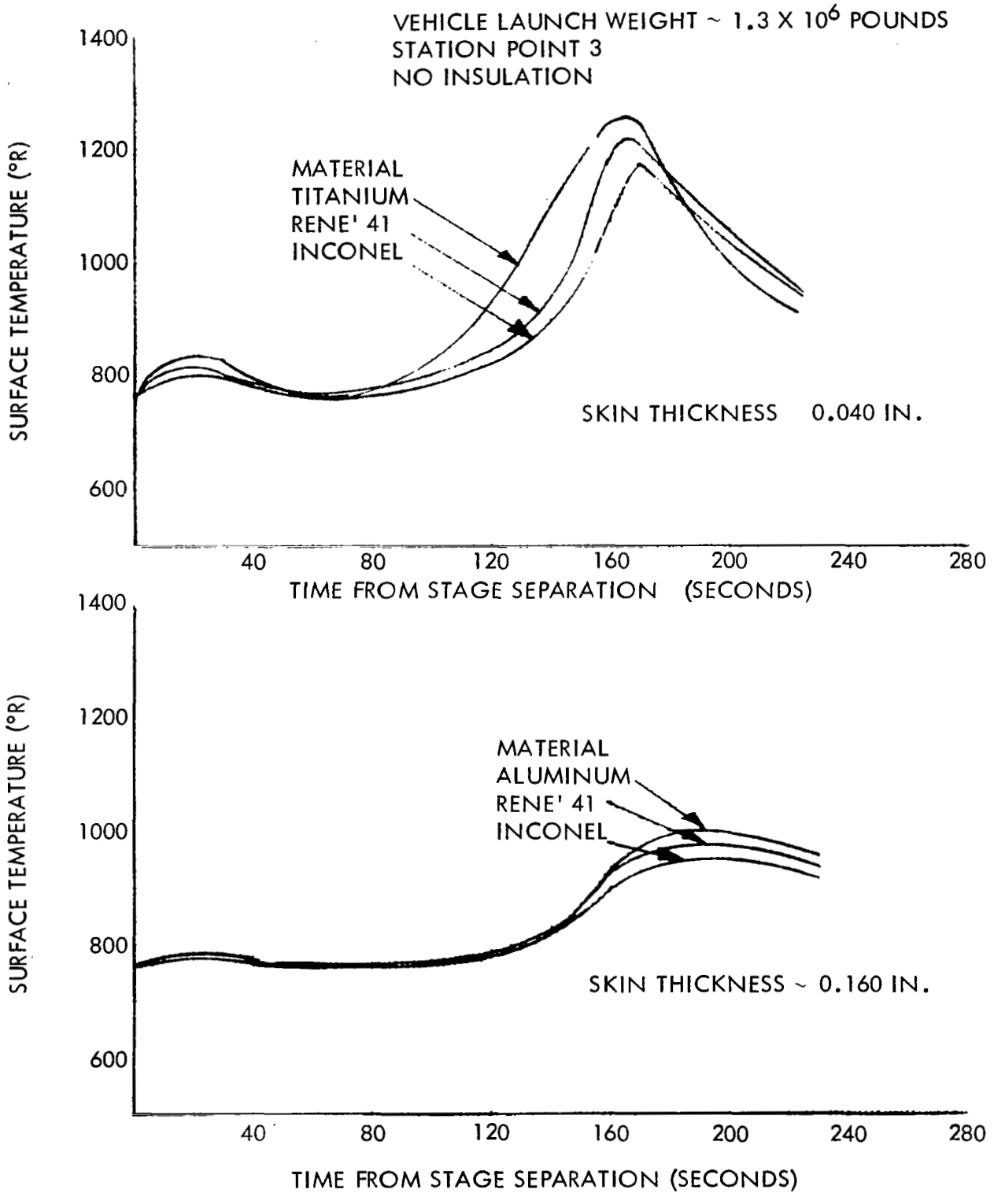

Figure 51. - Effect of Material on Surface Temperature

The program was run for a large series of materials and material thicknesses for both the large vehicle, 2.5×10^6 pounds and the small vehicle, 1.3×10^6 pounds. Maximum temperatures attained by the primary structure were defined and are the material design temperature limits for the structural synthesis study. These maximum surface temperatures for the various equivalent skin thicknesses are shown in Figure 52. Therefore, for any allowable design temperature there must be a minimum skin thickness associated with the construction to act as the required heat sink. These curves show the surface temperature ranging from 1000°R to 1450°R, but do not necessarily imply that the primary material should be subjected to these temperatures. An example is the thinner aluminum skins at 640°F where the strength properties are only 20 percent room temperature values. Other problems might arise with the surface finishes and oxidation at the higher temperature levels.

The insulated primary structure concept was assumed to be an aluminum skin with a layer of microquartz insulation on the front face. For the thermal model; the insulation was treated as 20 elements with a 10-element structure behind the insulation. With the low heat spike considered for the recovery staging conditions, it was found that the back-face temperature rise could be kept to less than 100°F with a minimum insulation thickness of 0.125 inch. Figure 53 shows the thermal profile through the insulation thickness and how the profile varies throughout the entry trajectory. Maximum temperature of 1500°R was developed on the outer surface of the insulation. To retain this insulation concept for the primary structure, an outer heat shield of thin super alloys is required together with the support structure through the insulation.

This outer heat shield was not considered in the thermal analysis of the insulation, but it will in fact reduce the heat input to the insulation. According to Figure 52, for a thin uninsulated sheet of Rene' 41 the maximum temperature would be about 1500°R for an equivalent skin thickness of 0.020 inch.

The outer heat shield is not primary load-carrying, but it must withstand the aerodynamic forces during ascent and reentry. The shield would have to be a light skin-stiffened construction. A single-face corrugated sandwich with 0.010-inch skins is sufficient to take the normal pressure and would weigh approximately 0.85 lb/ft^2. Insulated supports for this heat shield could be designed for about 0.25 pound each and spaced at one foot apart. The total weight for the 0.125-inch insulation material plus the supports and heat shield are assessed at 1.5 lb/ft^2; this additional weight penalty was accounted for with all the insulated concepts considered. Although the thermal evaluation shown in Figure 53 considered only one type of load-carrying

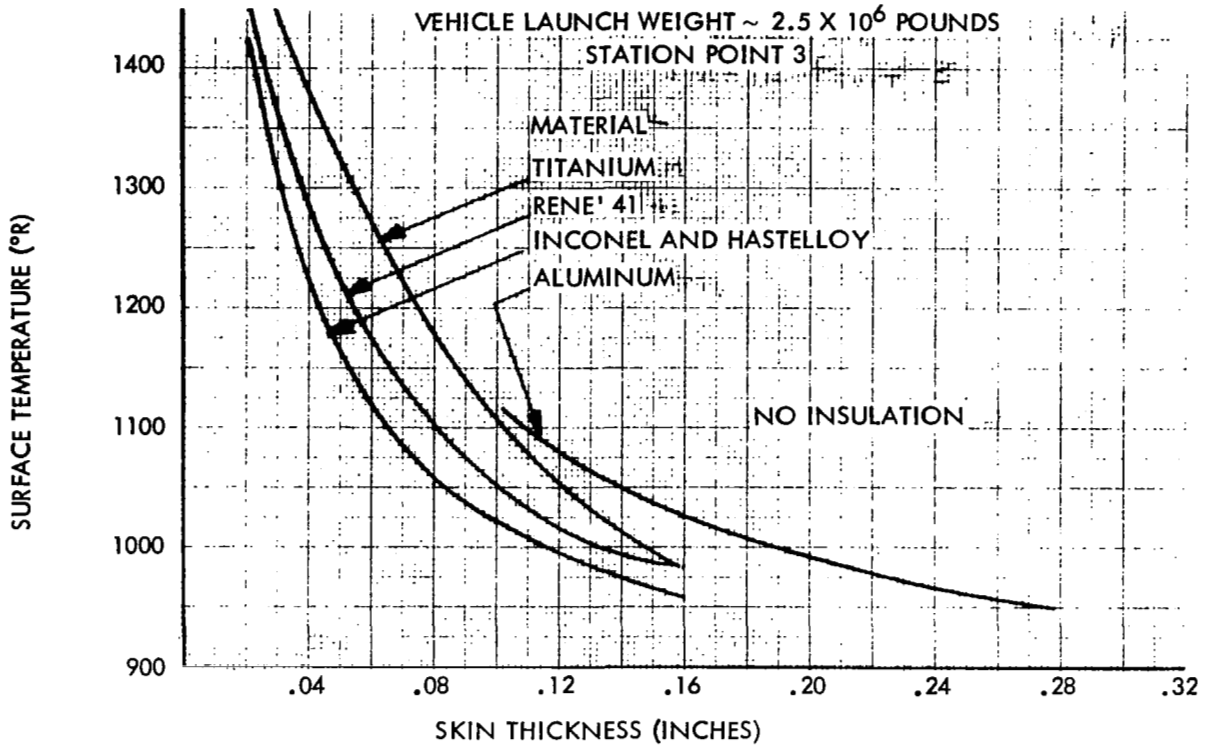

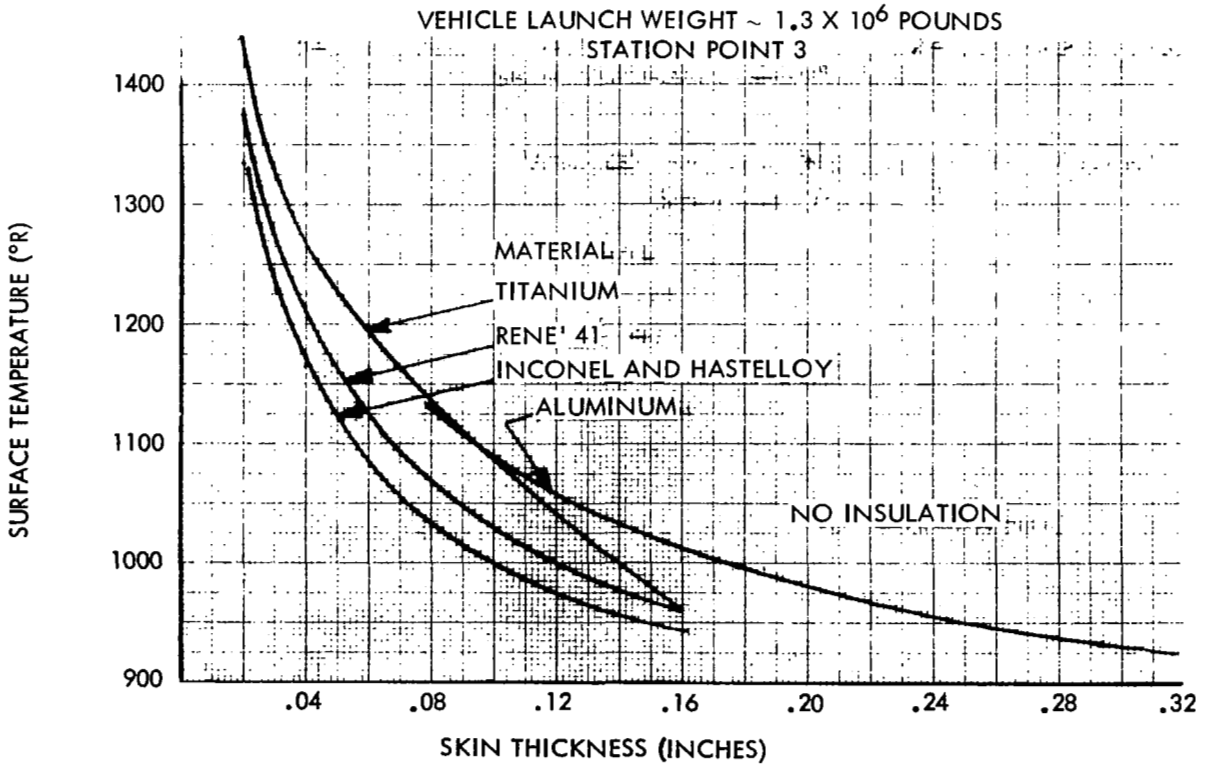

Figure 52. - Maximum Surface Temperature During Entry

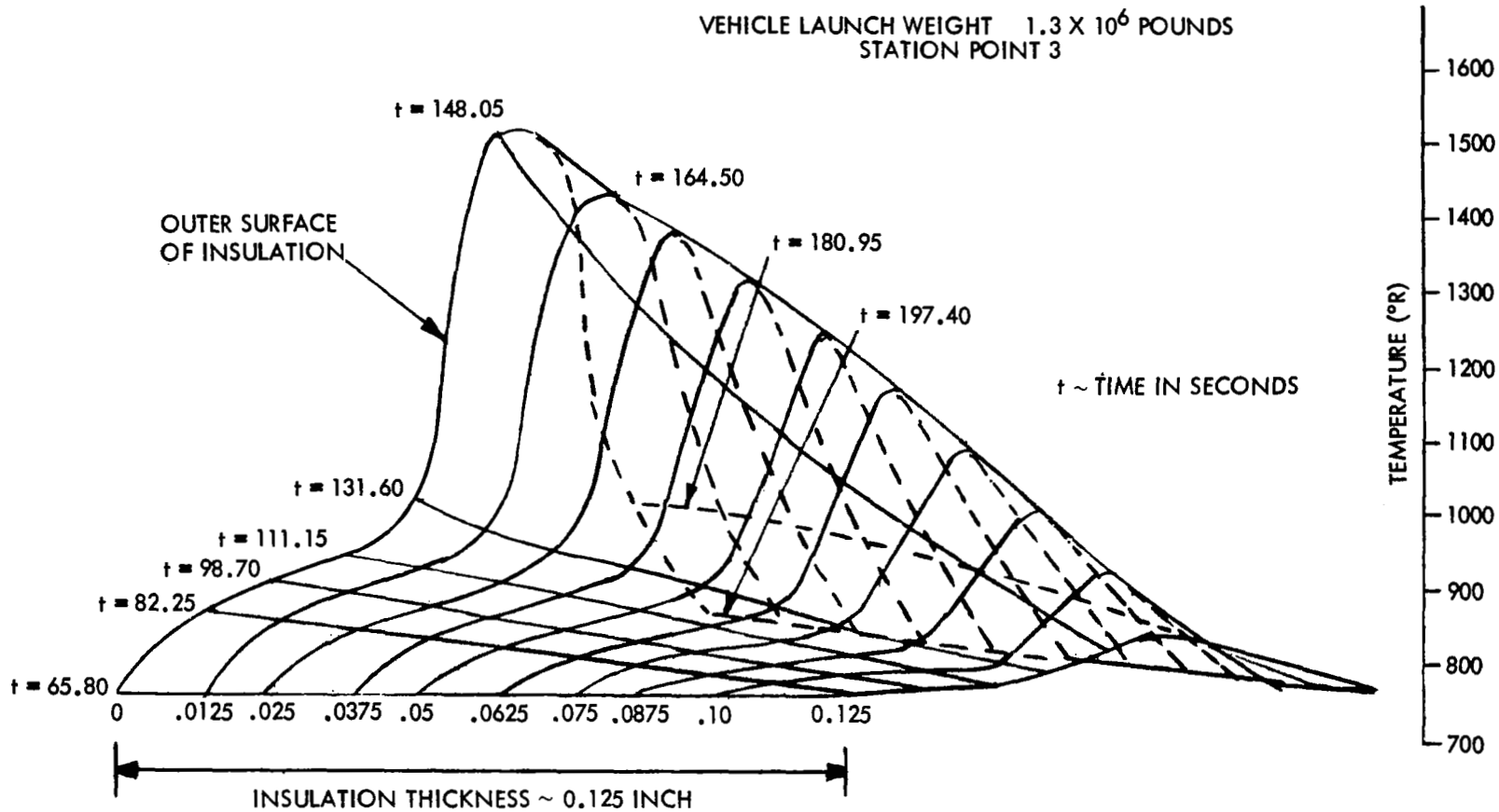

Figure 53. - Thermal History Profile Through Microquartz Insulation

material, the results shown are applicable to all materials because a negligible amount of heat will pass through the insulation and the back face temperature does not rise.

Thermal Stresses

Although the maximum-load intensity during entry is fairly small, less than 500 lb/in., the thermal stresses induced in the primary structure could be significant. The insulated concepts where the back-face temperature does not rise present no significant thermal stress problems to the primary structure. With the hot structure, super alloys, etc., the primary structure will be subjected to a temperature rise and a temperature gradient across the structural elements. The temperature rise will expand the fuselage shell both circumferentially and longitudinally. The latter expansion can be designed to be practically unrestrained and thus reduce the thermal stresses. The temperature gradient through the structure will produce significant thermal stresses if the section elements are constrained. Honeycomb sandwich with its thin skins separated by a one- to two-inch core appears to be the worst design concept for the thermal stress problem. For the thermal stress analysis, the model assumes that the two skins are at a uniform but different temperature. The sandwich construction is treated as a beam with temperatures T_1 and T_2 above the datum on the top and bottom surfaces, respectively. A general solution is given for the stresses and redundant forces in the sandwich beam in terms of its geometry and end fixity.

The geometry property for the sandwich is

$$\bar{y} = \left(\frac{E_1 A_1}{E_1 A_1 + E_2 A_2} \right) h$$

When the sandwich skin's temperatures are changed from the datum temperature, the unrestrained deformations are represented by

W' = change in rotation of cross section per unit distance (curvature) due to thermal loading

$$W' = \frac{\alpha_1 T_1 - \alpha_2 T_2}{h}$$

$\bar{\epsilon}'$ = axial strain at elastic centroid due to thermal loading

$$\bar{\epsilon}' = \frac{E_1 A_1 \alpha_1 T_1 + E_2 A_2 \alpha_2 T_2}{E_1 A_1 + E_2 A_2}$$

and the thermal stresses

$$\delta_1 = \delta_2 = \theta$$

Let

$$e = \frac{E_2 A_2}{E_1 A_1}$$

and

$$a = \frac{\alpha_2 T_2}{\alpha_1 T_1}$$

then

$$\overline{y} = \frac{h}{1+e}$$

$$w' = \frac{\alpha_1 T_1}{h}(1-a)$$

$$\overline{\varepsilon}' = \alpha_1 T_1 \left(\frac{1+ae}{1+e}\right)$$

It can be shown that the general solution for the sandwich beam (ref. 6) is given by:

$$\delta_1 = \frac{-E_1 \alpha_1 T_1}{1+e}\left[\frac{\frac{1+ae}{E_1 A_1 (1+e)}}{K_F} + 1 \quad + \quad \frac{\frac{(1-a)e}{E_1 A_1 h^2 (e/(1+e))}}{K_M} + 1\right]$$

and

$$\delta_2 = \frac{-E_2 \alpha_1 T_1}{1+e}\left[\frac{\frac{1+ae}{E_1 A_1 (1+e)}}{K_F} + 1 \quad - \quad \frac{\frac{1-a}{E_1 A_1 h^2 \left(\frac{e}{1+e}\right)}}{K_M} + 1\right]$$

where K_F is the axial stiffness of the end support and K_M is the rotational stiffness of the end support.

For the typical fuselage shell, the restraint model can be considered as one end fully fixed with the other allowed longitudinal extension but restrained from any rotational deflection. The rotational restraint of the sandwich skin is assumed, since the double skin panels have fairly rigid edge members joining the skin.

Therefore, restraints are assumed to be as follows:

$$K_F = 0 \text{ and } K_M = \infty$$

which will result in thermal stresses equivalent to

$$\delta_1 = \frac{-E_1 \alpha_1 T_1}{1 + e} \left| (1 - a)\, e \right|$$

and

$$\delta_2 = \frac{+E_2 \alpha_1 T_1}{1 + e} (1 - a)$$

Thermal stresses for the shell components were developed from the above formula. The back-face temperature for the honeycomb was considered to be 760°R while the front-face temperature is dependent upon the skin thickness (fig. 52). It was assumed that the honeycomb core was a heat barrier and did not allow the back-face skin to absorb heat from the front face. This large temperature difference resulting from this assumption will give larger thermal stresses and hence a more severe design environment. Figures 54 and 55 show the thermal stresses as a function of the facing sheet thicknesses for the assumed thermal gradient for the 1.3 and 2.5 x 10^6-pound vehicle. For the thin skin honeycomb sandwich designs where there is only manufacturing skin thickness limitations, the thermal stresses are greater than 60 000 psi and will become a design problem. If the external surface temperatures are considered to be less than 1250°R the thermal stresses plus the axial compression due to deceleration are well within the material concept design allowables and will not present a major problem. With thick-skin aluminum sheets without the microquartz protection system, the thermal stress levels are too severe.

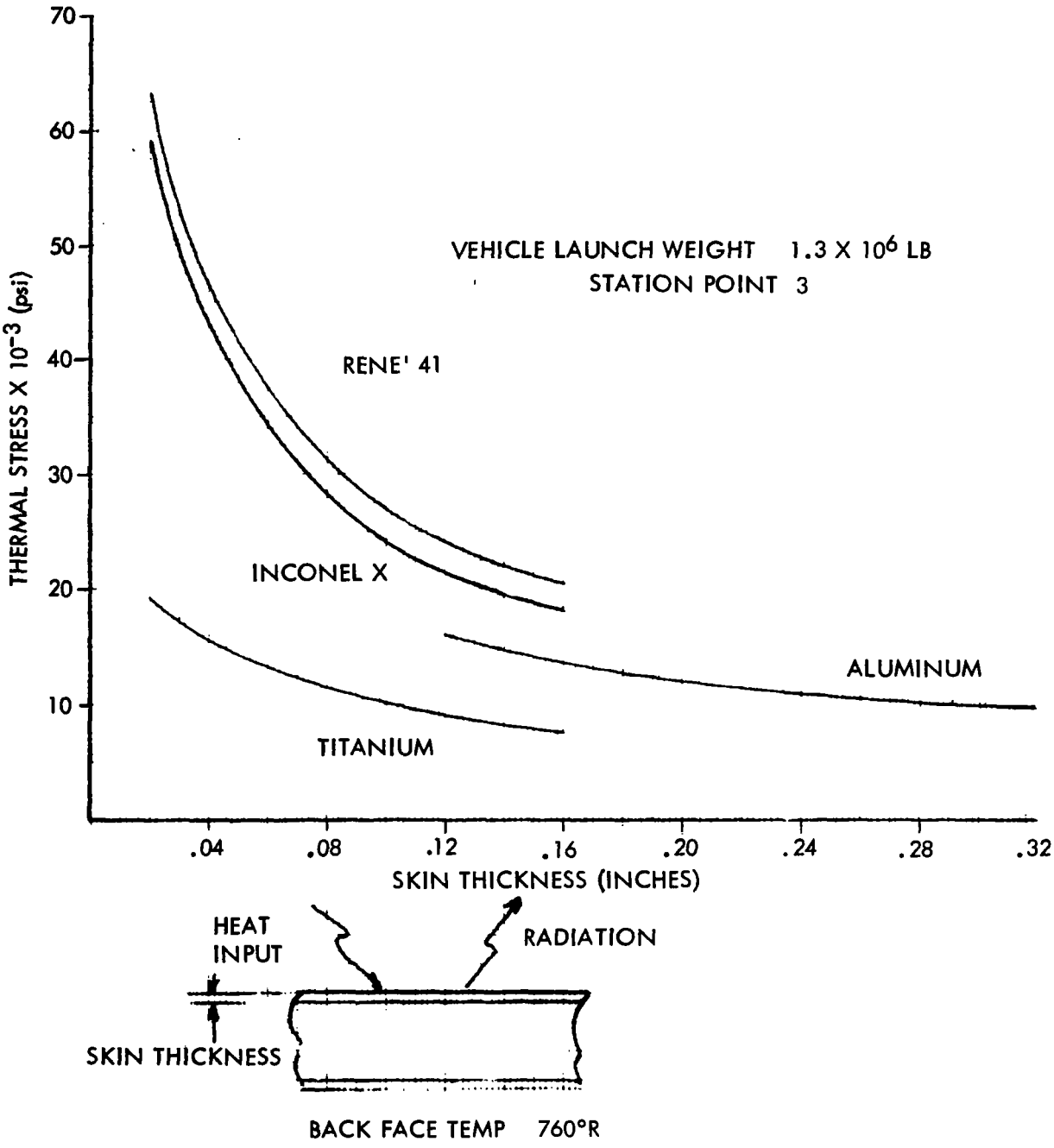

Figure 54. - Thermal Stresses for Sandwich Design on Small Vehicle

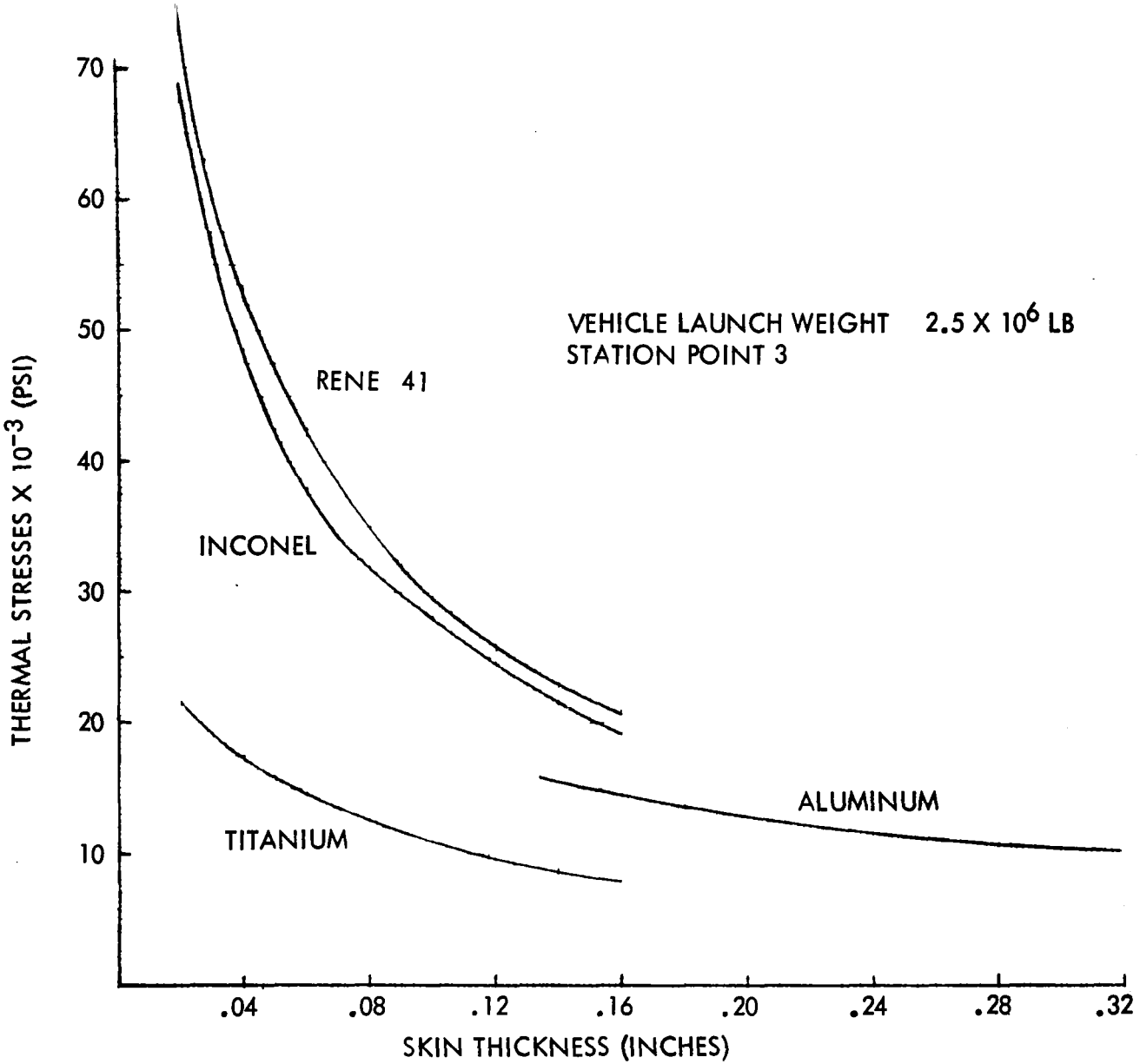

Figure 55. - Thermal Stresses for Sandwich Design on Large Vehicle

Structural Synthesis

During Phase I of this contract, the portion of the program that describes the structural components was separated from the parametric synthesis section. This permitted the structural components to be analyzed individually without associating any of the structural components with a particular launch vehicle. In addition, the assessment of the effects of the substitution of different types of materials, constructions, manufacturing limitations, or analytical methods on the structural components could be obtained by an independent exercise of the design synthesis subroutines. The structural components considered were defined by a range of diameters, lengths, mechanical loads, and thermal environments representative of those associated with the basepoint vehicle systems for the recoverable first stages. The design synthesis determines the resultant unit shell weights for the entire spectrum of radii, mechanical loads, and thermal environments.

In the final assessment of the program, the unit shell weights obtained by the design synthesis subroutines are correlated with various components of specific launch vehicles. A design envelope was specified for each of these components as a function of the vehicle's flight trajectory. One element of the design envelope for an unpressurized shell may be a temperature spectrum which varies from room temperature during prelaunch conditions to 300°F with maximum loading intensity at end boost and to 1000°F during entry with a low load intensity. In addition, various components of the vehicle's stage may be subjected to maximum loading conditions at prelaunch, at the maximum q condition, or at end boost. To evaluate the complete design spectrum, the structural design synthesis was conducted for a range of loading intensities, cylindrical diameters, and thermal environments. The primary temperatures considered were room temperature (prelaunch), cryogenic temperature, and the external temperature associated with the end boost condition. Entry maximum temperatures were handled by considering the equivalent skin heat sink and its associated thickness as being an additional design constraint to control the temperature of the primary structure.

The tensile loading intensity to which a structural component is subjected results from a combination of requirements. The maximum tensile loads for some portions of the propellants tanks result from the ullage requirements for the engine system and the associated bending moment of a particular flight condition. This pressure determines the minimum required skin thickness for the structural component. The maximum compressive loading intensity dictates the required stiffness of the structural component. The maximum compressive stress is determined by the axial acceleration and the

maximum bending moment if the shell is unpressurized. A nominal relief pressure reduces the compressive loading intensities for pressurized components. The relief pressure consists of the ground atmospheric pressure and a nominal differential pressure, which is sufficient to prevent propellant boiloff.

Various safety factors are applied to all these loading conditions. For convenience, the relative magnitudes of these safety factors are established external to the subroutines. This permits consideration in the design synthesis subroutines of only an ultimate tensile or compressive loading intensity. In this study, the ultimate and limit factors of safety are 1.4 and 1.1, respectively.

Numerous alterations of the structural design of a component must be considered to evaluate effectively the significance of technological advances. These include replacing materials to evaluate increases in material allowables; for example, making replacements to increase the compressive yield strength and the ultimate tensile strength of the various baseline materials. In addition, significant weight reductions may be obtained by replacing base-point configuration and material with a different type of construction, material, or both.

Many of the present minimum weight design analysis studies tend to consider absolute minimum weight for single, simple loading conditions. These studies do not take into account restrictions and limitations that can be imposed upon the design philosophy to obtain realistic design concepts. Also, for practical component design, various load conditions make up the overall design load environmental envelope. One flight regime loading will help formulate the design criteria for a specific element of the structure, while other flight regimes might dictate design of the remaining elements.

If consideration is given to absolute minimum weight concepts, the resulting configurations may not be realistic because of overlapping stiffeners, too thin material for skin and stiffener elements, impractical height-to-thickness relationships, etc. To obtain realistic optimum design concepts, the automated computer program for the design synthesis studies must consider the stiffness and stability criteria in depth. These design synthesis subroutines are capable of considering several different types of stability analysis with design sections in both elastic and plastic regimes. Classical buckling analysis for both small and large deflections can be considered for the theoretical minimum weights, but these buckling conditions have to be adjusted by selection of appropriate correction factors which are based on experimental data. The design concepts attained in this study were not results obtained from completely theoretical stability analysis. These results reflect

experience gained from experimental and test development programs. A detailed description of these structural synthesis programs is given in the Users Manual— Volume 2 of this report.

The unit shell weights for the various concepts and materials for a range of design parameters have been summarized in this section. Printouts from the computer programs for the test cases contain significantly more data than shell weights. In fact, the print formats spell out in detail a complete description of the individual structural elements with their thicknesses, lengths, and pitches, sufficient information for the preliminary design. The number of test cases that were synthesized are indicated by table 9. An indication of the elemental detail for the various structural concepts is shown in table 10.

TABLE 9 . - TEST CASES SYNTHESIZED FOR FUSELAGE STRUCTURAL SHELLS

Parameter	Range	Number
Shell component	Forward to aft skirt	5
Vehicle size	1.3 to 2.5 x 10^6 pounds	3
Material		4
Construction		5
Temperature	1000°R to 1300°R	4

The materials considered for the fuselage construction were aluminum with microquartz insulation, titanium, René 41, and Inconel. Since the shells are subject to different design temperatures, the material properties' changes with temperature variation were required for the synthesis programs and are shown in figures 56 through 59. These properties are representative of available grades of material.

One effective method of reducing the weight of structural components is to improve the material properties by alloying current materials. Present-day alloy systems which have performed well in space structures are expected to be used for the next fifteen years, or more. During this period, their design properties are expected to improve significantly. The material property improvements involved the consideration that the magnitudes of both the compressive yield and tensile stress levels were correspondingly increased, but the shape of the stress strain curve was invariant with only a shift in magnitude. Since no detailed knowledge of these advanced materials is obtainable and, at best, most of these advances are postulated, the plasticity factor is assumed to be identical to that for the parent material. When these new

TABLE 10. - STRUCTURAL DESIGN DETAILS

SKIN THICKNESS MINIMUM OF 0.148 INCH

TITANIUM 300 DEGREES 130 RADIUS HAT SECTION STRINGER

RADIUS	NX (LB/IN)	NX/R (PSI)	SKIN THICKNESS	STRINGER AREA	STRINGER SPACING	STRINGER HEIGHT	FRAME AREA	FRAME PITCH	UNIT WT (LB/SQ FT)
130.	3058.	23.523	0.148	0.64	11.0	1.42	0.57	34.77	5.16
130.	2920.	22.462	0.148	0.60	11.0	1.33	0.58	31.88	5.12
130.	2604.	20.031	0.148	0.66	12.0	1.47	0.51	36.66	5.03

SKIN THICKNESS MINIMUM OF 0.102 INCH - HAT SECTION

RADIUS	NX (LB/IN)	NX/R (PSI)	SKIN THICKNESS	STRINGER AREA	STRINGER SPACING	STRINGER HEIGHT	FRAME AREA	FRAME PITCH	UNIT WT (LB/SQ FT)
130.	3058.	23.523	0.102	0.33	7.0	1.08	0.66	25.99	4.06
130.	2920.	22.462	0.102	0.48	8.0	1.55	0.51	41.93	4.04
130.	2604.	20.031	0.102	0.42	8.0	1.36	0.52	36.00	3.92

SKIN THICKNESS MINIMUM OF 0.148 INCH

TITANIUM 300 DEGREES 130 RADIUS Z SECTION STRINGER

RADIUS	NX (LB/IN)	NX/R (PSI)	SKIN THICKNESS	STRINGER AREA	STRINGER SPACING	STRINGER HEIGHT	FRAME AREA	FRAME PITCH	UNIT WT (LB/SQ FT)
130.	3058.	23.523	0.148	0.30	8.0	1.43	0.61	30.90	4.77
130.	2920.	22.462	0.150	0.37	9.0	1.72	0.52	39.60	4.75
130.	2604.	20.031	0.148	0.34	9.0	1.59	0.52	36.01	4.64

SKIN THICKNESS MINIMUM OF 0.102 INCH - Z SECTION

RADIUS	NX (LB/IN)	NX/R (PSI)	SKIN THICKNESS	STRINGER AREA	STRINGER SPACING	STRINGER HEIGHT	FRAME AREA	FRAME PITCH	UNIT WT (LB/SQ FT)
130.	3058.	23.523	0.102	0.20	5.0	1.34	0.60	31.15	3.73
130.	2920.	22.462	0.102	0.19	5.0	1.30	0.60	30.12	3.71
130.	2604.	20.031	0.102	0.20	5.0	1.34	0.55	32.01	3.67

SKIN THICKNESS MINIMUM OF 0.148 INCH - INTEGRAL

TITANIUM 300 DEGREES 130 RADIUS INTEGRAL STRINGER

RADIUS	NX (LB/IN)	NX/R (PSI)	SKIN THICKNESS	STRINGER AREA	STRINGER SPACING	STRINGER HEIGHT	FRAME AREA	FRAME PITCH	UNIT WT (LB/SQ FT)
130.	3058.	23.523	0.148	0.24	8.0	1.99	0.54	39.70	4.43
130.	2920.	22.462	0.148	0.24	8.0	2.01	0.52	40.57	4.42
130.	2604.	20.031	0.148	0.25	9.0	2.07	0.48	42.23	4.33

TABLE 10. - STRUCTURAL DESIGN DETAILS (Continued)

MINIMUM SKIN THICKNESS OF 0.075 INCH

TITANIUM 300 DEGREES 130 RADIUS HONEYCOMB SANDWICH

RADIUS	NX (LB/IN)	NX/R (PSI)	SKIN	CORE HEIGHT	CORE DENS (LB/CU FT)	UNIT WT (LB/SQ FT)
130.	3058.	23.523	0.075	0.54	2.000	3.55
130.	2920.	22.462	0.075	0.52	2.000	3.54
130.	2604.	20.031	0.075	0.48	2.000	3.54

MINIMUM SKIN THICKNESS OF 0.103 INCH - HONEYCOMB

RADIUS	NX (LB/IN)	NX/R (PSI)	SKIN	CORE HEIGHT	CORE DENS (LB/CU FT)	UNIT WT (LB/SQ FT)
130.	3058.	23.523	0.103	0.45	2.000	4.84
130.	2920.	22.462	0.103	0.44	2.000	4.83
130.	2604.	20.031	0.103	0.40	2.000	4.83

MINIMUM SKIN THICKNESS OF 0.055 INCH - HONEYCOMB

RADIUS	NX (LB/IN)	NX/R (PSI)	SKIN	CORE HEIGHT	CORE DENS (LB/CU FT)	UNIT WT (LB/SQ FT)
130.	3058.	23.523	0.055	0.68	2.000	2.64
130.	2920.	22.462	0.055	0.65	2.000	2.64
130.	2604.	20.031	0.055	0.60	2.000	2.63

MINIMUM SKIN THICKNESS OF 0.148 INCH - WAFFLE

TITANIUM 300 DEGREES 130 RADIUS WAFFLE

RADIUS	NX (LB/IN)	NX/R (PSI)	SKIN	WEB	WAFFLE HEIGHT	WAFFLE SPACING	UNIT WT (LB/SQ FT)
130.	3058.	23.523	0.149	0.053	1.72	7.74	3.94
130.	2920.	22.462	0.149	0.051	1.70	7.96	3.92
130.	2604.	20.031	0.149	0.047	1.65	8.39	3.84

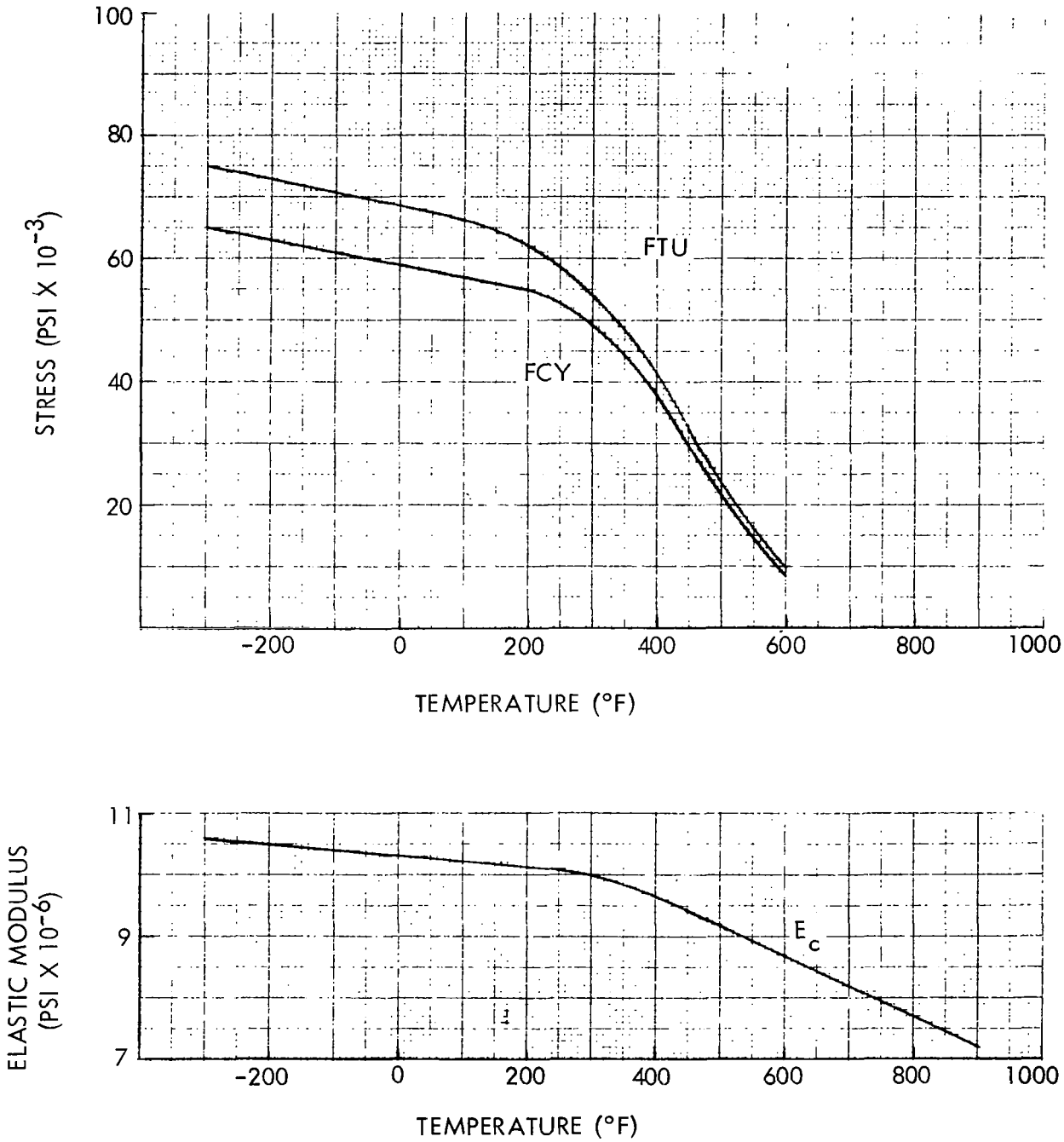

Figure 56. - Material Properties Variation With Temperature - Aluminum

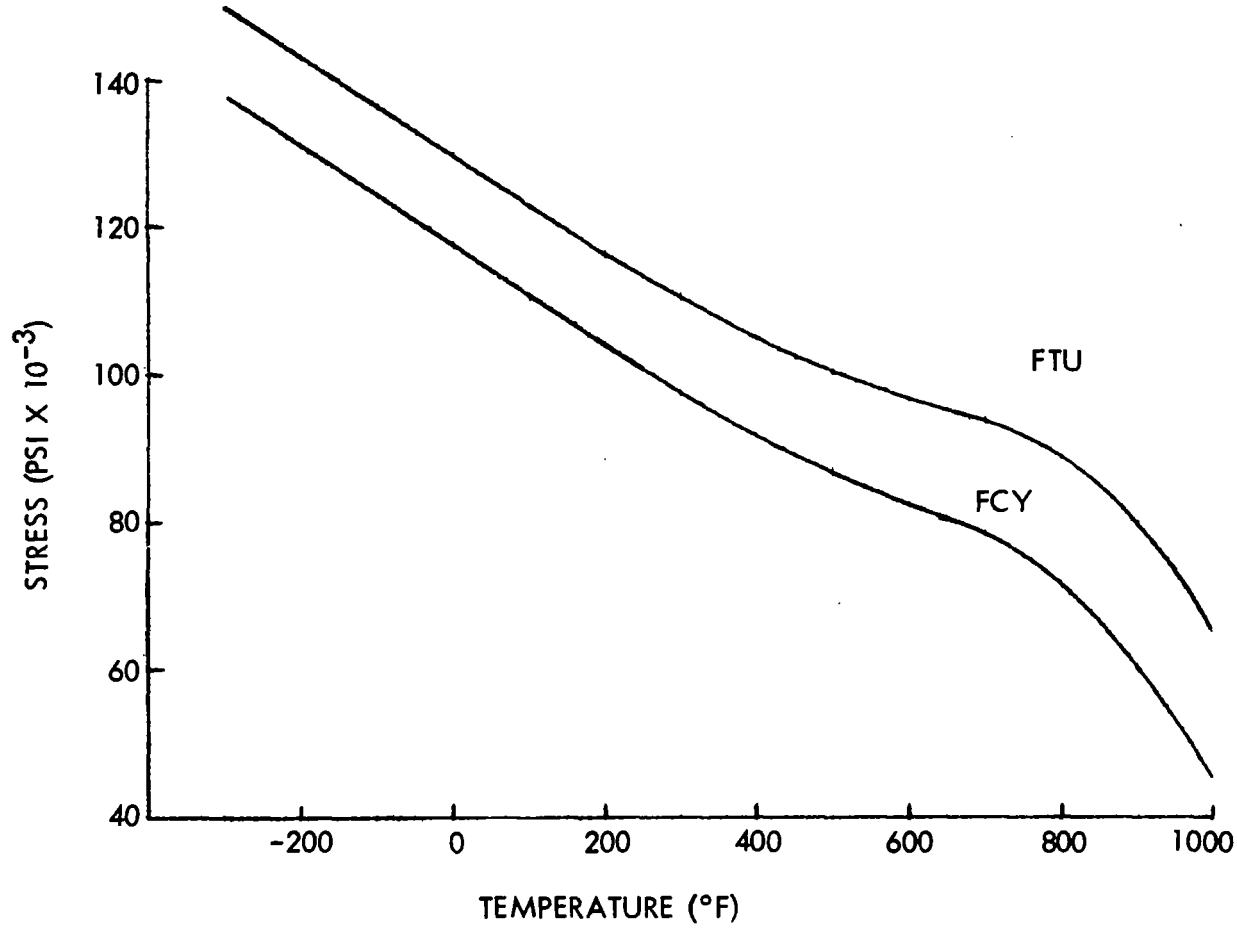

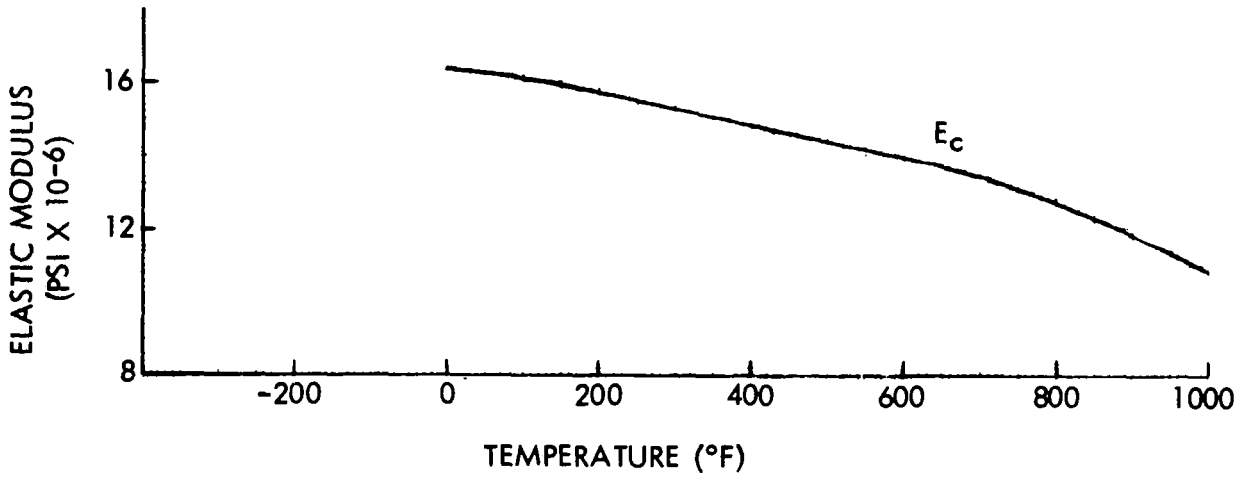

Figure 57. - Material Properties Variation With Temperature - Titanium

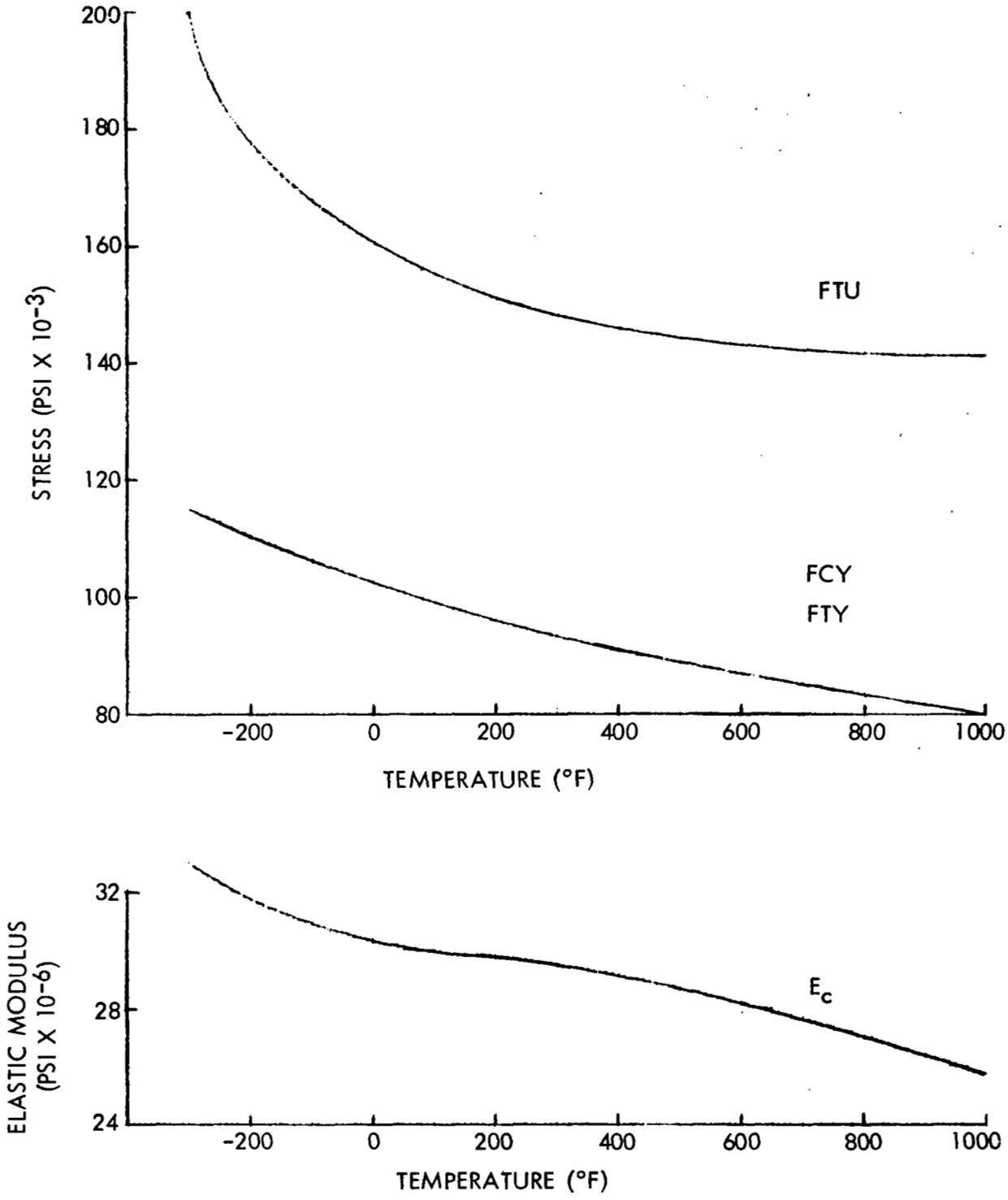

Figure 58. - Material Properties Variation With Temperature - Inconel

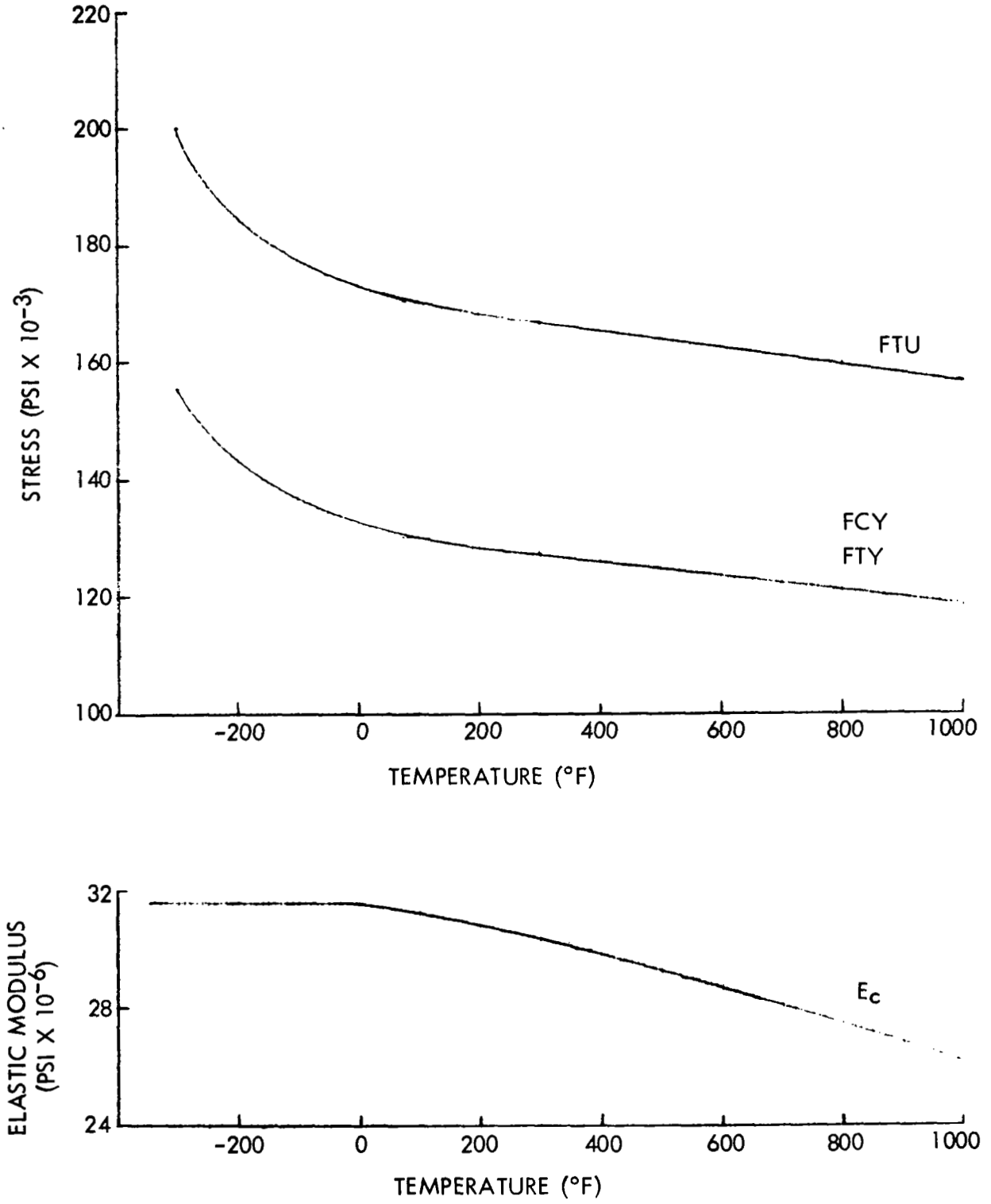

Figure 59. - Material Properties Variation With Temperature - Rene'41

materials have been developed and their properties sufficiently defined, they can again be exercised through the design synthesis programs to obtain further detailed information for design concepts that utilize all the additional, more exact values of the new material properties.

For the design synthesis portion, only improvements in the physical strength and stiffness properties of the material are considered. The effect of the manufacturing difficulties, fabrication limitations, cost considerations, etc., are considered and discussed in other sections of this report where the various structural components and types of materials are associated with specific vehicles in the assessment evaluation. The design synthesis assumes that any of the materials discussed and used in the structural evaluation will be readily attainable and will have the desired and required fabrication properties from which to produce the components. Also, it is assumed that these materials can be welded and joined to form the structural components under discussion. Manufacturing difficulties are discussed in the assessment portion of this study where the relative manufacturing complexity factors are covered.

The material improvements are expressed as a percentage increase of a nominal compression yield and in tensile ultimate strength of current materials. The shape of the stress-strain diagram for the plasticity considerations for advanced alloy materials is assumed to be identical to that of the current material. The plasticity curve of the material is expressed mathematically for inclusion in the computer subroutines to provide access to the plasticity correction factors for the various materials. Design synthesis analyses to evaluate minimum weight for the structural components must consider materials in the elastic and plastic ranges.

The various structural design synthesis programs were exercised to define the minimum practical shell unit weight for the major components of the fuselage. These included unpressurized shells (crew compartment, interstage, and aft skirt) and pressurized shells (forward tankwell and aft tankwall). The types of construction that were considered were

1. Skin - stringer - ring
    a. Top-hat section stringer
    b. Z-section stringer
    c. Integral stringer
2. Honeycomb sandwich

3. Waffle grid pattern

4. Double wall and multiwall

For the designs where minimum skin thicknesses were controlled by available sheet thickness, some of the resulting lightweight designs evolved were for 0.020-inch skins for honeycomb sandwich to 0.115-inch for integral stringer design. When the skins are too thin, there is a very small heat sink capacity; this will result in the average skin temperature being extremely high. With double wall designs the large thermal gradient will produce large thermal stresses. To consider the thermal effects of reentry, a series of predetermined skin thicknesses were supplied to the synthesis program. From the previous section, the maximum skin temperature attained during the entry conditions was influenced by the equivalent skin thickness for the hot structures. Therefore, for a range of operating temperatures of 1300°R to 1000°R, a range of minimum skin thicknesses for René 41, titanium, and Inconel are defined in table 11.

Typical results for several of these constructions applied to the unpressurized shell for the small vehicle, 1.3×10^6-pounds, are shown in table 12.

TABLE 11. MINIMUM SKIN THICKNESSES FOR TEMPERATURE CONTROL

Material	Temperature			
	1300°R	1200°R	1100°R	1000°R
René 41	0.038	0.054	0.080	0.132
Titanium	0.054	0.075	0.102	0.148
Inconel		0.044	0.064	0.112

When these minimum allowable skin thicknesses are imposed on the structural design, the resulting configuration is adjusted to seek a minimum weight within this additional restriction. Therefore, with the stiffened skin designs, the stringer area is reduced; but more noticeably the stringer-pitch is increased in some cases up to 11 inches. Even at this large pitch the skin is thick enough and the stress level low enough to preclude panel instability. The machine program automatically searches for the best pitch for the minimum weight design.

TABLE 12. DESIGN SYNTHESIS PRINTOUT - MINIMUM WEIGHT DESIGN

13 x 10^6-POUND LAUNCH VEHICLE

UNPRESSURIZED COMPONENTS

ALUMINUM 3CO DEGREES 130 RADIUS INTEGRAL STRINGER

RADIUS	NX (LB/IN)	NX/R (PSI)	SKIN THICKNESS	STRINGER AREA	STRINGER SPACING	STRINGER HEIGHT	FRAME AREA	FRAME PITCH	UNIT WT (LB/SQ FT)
130.	3058.	23.523	C.115	0.23	5.0	2.03	0.69	35.75	2.6C
130.	2920.	22.462	0.113	0.22	5.0	1.98	0.68	35.27	2.54
130.	2604.	20.031	C.110	0.20	5.0	1.93	0.63	36.37	2.41

ALUMINUM 3CO DEGREES 130 RADIUS HONEYCOMB SANDWICH

RADIUS	NX (LB/IN)	NX/R (PSI)	SKIN	CORE HEIGHT	CORE DENS (LB/CU FT)	UNIT WT (LB/SQ FT)
130.	3058.	23.523	C.037	1.66	2.000	1.34
130.	2920.	22.462	0.035	1.66	2.000	1.29
130.	2604.	20.031	C.031	1.70	2.000	1.18

A complete array of unit shell weights for the four materials and three vehicles are shown in tables 13 through 16. Table 13 for the aluminum design includes the weight penalty assessed for the insulation. As discussed in the previous section the insulation, heat shield and standoff clips were considered to be about 1.5 lb/ft^2.

Figures 60 through 62 show the effect that entry temperature limitations have on the minimum weights design considerations. When there is no imposed temperature limits, the honeycomb construction is much lighter for all the materials considered. This result agrees with the findings of Phase I of the contract for aluminum, titanium, and beryllium. With the additional requirement for the stage recovery, there is a minimum allowable temperature skin thickness which greatly affects the unit weight. For the lower temperatures of 1000° and 1100° R and using super alloys, the core depth required for stability is at a minimum so that the major portion of the weight is contributed by the two facing sheets. For the design synthesis, it was assumed that the facings were of equal thicknesses and the minimum core depth still acted as an insulated barrier producing appreciable thermal gradient and stresses. In a detailed analysis, which considers the thermal conductivity of the honeycomb core, reflection between the two face sheets would perhaps bring the temperature levels down and allow thinner skins. This detailed thermal analysis of the final honeycomb design sections was not conducted for this phase of the study.

The double wall and multiwall types of construction discussed in Phase II of the contract were considered for the fuselage shells. These concepts all suffer the same weight penalties as the honeycomb concept when temperature limitations are imposed on the primary structure. In fact the double-wall concepts are not competitive with the simple skin stringer concepts for any vehicle component when temperatures are to be less than 1200°R.

For René 41 designs, the minimum unit shell weight for the boost loading will provide a heat sink to constrain the maximum temperature below 1100°R. All the skin-stringer concepts average out at 5-1/2 lb/sq ft and have skin thicknesses of about 0.080 inch. Waffle-type construction is found to be the lightest design throughout the temperature range; this is different from the aluminum designs where the stringer sections are 20 percent lighter. This waffle effect of the lightest design was also exhibited by titanium and Inconel with a 20 percent weight reduction from the top-hat stringer concept when temperature is restricted at 1000°R to a 10 percent reduction at 1100°R and about equal with no temperature restriction. These reductions were the same for the three vehicle sizes and all the fuselage shell components.

TABLE 13. - UNIT SHELL WEIGHTS (LB/SQ FT) FOR INSULATED ALUMINUM DESIGNS

Vehicle	Load Intensity (lb/in.)	Construction Type: Top-Hat Stringer	Z-Section Stringer	Integral Stringer	Honeycomb Sandwich	Waffle Pattern
1.3×10^6 pounds						
Crew compartment	3058	3.80	4.16	4.10	2.84	4.00
Center section	2920	3.75	4.10	4.04	2.79	3.94
Aft skirt	2604	3.64	3.98	3.91	2.68	3.80
Forward tankwall	2401	3.93	3.84	3.74	2.99	3.65
Aft tankwall	1541	3.72	3.56	3.40	2.94	3.24
1.9×10^6 pounds						
Crew compartment	3867	4.18	4.53	4.53	3.16	4.53
Center section	3699	4.12	4.47	4.46	3.10	4.46
Aft skirt	3296	3.98	4.32	4.29	2.97	4.29
Forward tankwall	2949	4.19	4.04	4.01	3.10	4.14
Aft tankwall	1884	3.84	3.69	3.65	3.00	3.73
2.5×10^6 pounds						
Crew compartment	4776	4.60	4.92	4.98	3.49	5.00
Center section	4563	4.51	4.84	4.89	3.42	4.91
Aft skirt	4070	4.31	4.65	4.67	3.25	4.72
Forward tankwall	3664	4.62	4.41	4.35	3.37	4.45
Aft tankwall	2346	4.33	4.11	3.98	3.30	3.85

Note: Unit weights include 1.5 lb/ft^2 for insulation and heat shield.

TABLE 14. - UNIT SHELL WEIGHTS (LB/SQ FT) FOR RENÉ 41 DESIGNS AT VARIOUS TEMPERATURES

Vehicle	No Temperature Restraint (Minimum Weight)					Maximum Entry Temperature (°R) 1000					1100			1200		1300
	⎍	Z	⊥	H	W	⎍	Z	⊥	H	W	⎍	H	W	⎍	H	H
1.3 x 10^6 pounds																
Crew compartment	4.35	5.11	4.82	1.50	4.26	7.82	7.25	6.92	11.2	6.05	5.81	6.98	4.31	4.35	4.74	3.78
Center section	4.30	5.03	4.74	1.44	4.17	7.80	7.21	6.84	11.2	6.03	5.80	6.98	4.24	4.30	4.74	3.38
Aft skirt	4.13	4.81	4.54	1.31	3.93	7.70	7.17	6.80	11.2	6.00	5.79	6.97	4.10	4.13	4.74	3.37
Forward tankwall	3.93	4.61	4.34	1.66	3.70	7.58	7.06	6.71	11.2	5.91	5.69	6.98	3.80	4.13	4.74	3.35
Aft tankwall	3.36	3.91	3.68	1.62	2.96	7.26	6.80	6.57	11.2	5.94	5.54	6.98	3.30	3.88	4.74	3.33
1.9 x 10^6 pounds																
Crew compartment	4.89	5.73	5.43	1.87	5.15	8.24	7.60	7.22	11.2	6.34	5.91	6.99	5.25	4.89	4.77	3.41
Center section	4.81	5.63	5.34	1.80	5.04	8.22	7.57	7.12	11.2	6.28	5.90	6.99	5.10	4.81	4.77	3.41
Aft skirt	4.59	5.39	5.10	1.64	4.75	8.09	7.52	7.06	11.2	6.18	5.89	6.99	4.85	4.59	4.76	3.40
Forward tankwall	4.34	5.09	4.80	1.92	4.40	7.97	7.37	6.94	11.2	6.06	5.84	6.99	4.48	4.34	4.73	3.37
Aft tankwall	3.68	4.31	4.05	1.87	3.52	7.58	7.04	6.69	11.2	5.92	5.78	6.99	3.62	3.98	4.71	3.34
2.5 x 10^6 pounds																
Crew compartment	5.39	6.29	6.01	2.27	5.91	8.62	7.95	7.42	11.2	6.63	6.13	7.01	6.00	5.39	4.79	3.45
Center section	5.30	6.18	5.90	2.18	5.78	8.55	7.92	7.38	11.2	6.56	6.10	7.01	5.89	5.30	4.79	3.44
Aft skirt	5.05	5.91	5.62	1.98	5.46	8.39	7.79	7.32	11.2	6.41	5.96	7.00	5.55	5.05	4.78	3.43
Forward tankwall	4.78	5.60	5.30	2.07	5.07	8.29	7.65	7.16	11.2	6.27	5.94	6.98	5.16	4.78	4.75	3.39
Aft tankwall	4.01	4.73	4.45	2.01	4.06	7.85	7.26	6.85	11.2	6.01	5.83	6.98	4.19	4.21	4.72	3.36

Construction Legend:
⎍ Top-Hat Stringers Z Z Section ⊥ Integral Stringer H Honeycomb Sandwich W Waffle Pattern

TABLE 15. - UNIT SHELL WEIGHTS (LB/SQ FT) FOR TITANIUM DESIGNS AT VARIOUS TEMPERATURES

Vehicle	No Temperature Restraint (Minimum Weight)					Maximum Entry Temperature (°R) 1000					1100					1200		1300
	⎍	Z	⊥	H	W	⎍	Z	⊥	H	W	⎍	Z	⊥	H	W	⎍	H	H
1.3 x 10^6 pounds																		
Crew compartment	3.11	3.65	3.44	1.21	3.27	5.16	4.77	4.43	6.98	3.94	4.06	3.73	3.54	4.84	3.27	3.21	3.55	2.64
Center section	3.05	3.59	3.38	1.17	3.19	5.12	4.75	4.42	6.98	3.92	4.04	3.71	3.48	4.83	3.19	3.15	3.54	2.64
Aft skirt	2.93	3.44	3.23	1.08	3.02	5.03	4.64	4.33	6.98	3.84	3.92	3.67	3.32	4.83	3.02	3.03	3.54	2.63
Forward tankwall	2.66	3.13	2.94	1.26	2.67	4.87	4.49	4.21	6.98	3.72	3.76	3.46	3.20	4.82	2.85	3.11	3.50	2.59
Aft tankwall	2.27	2.65	2.48	1.20	2.14	4.62	4.29	4.06	6.98	3.60	3.54	3.26	3.03	4.82	2.62	2.87	3.50	2.57
1.9 x 10^6 pounds																		
Crew compartment	3.54	4.10	3.90	1.50	3.95	5.48	5.07	4.69	6.98	4.27	4.36	4.11	4.00	4.86	3.95	3.64	3.58	2.69
Center section	3.48	4.03	3.84	1.45	3.86	5.48	4.99	4.67	6.98	4.21	4.32	4.05	3.93	4.86	3.86	3.57	3.58	2.68
Aft skirt	3.32	3.86	3.66	1.34	3.64	5.35	4.92	4.55	6.98	4.11	4.23	3.88	3.76	4.85	3.64	3.42	3.57	2.67
Forward tankwall	2.97	3.47	3.28	1.46	3.18	5.12	4.72	4.39	6.98	3.89	3.99	3.76	3.42	4.82	3.18	3.33	3.52	2.67
Aft tankwall	2.55	2.93	2.75	1.39	2.54	4.84	4.47	4.21	6.98	3.65	3.72	3.43	3.20	4.82	2.72	3.06	3.51	2.67
2.5 x 10^6 pounds																		
Crew compartment	3.94	4.51	4.33	1.75	4.54	5.72	5.28	4.90	7.00	4.62	4.61	4.53	4.56	4.88	4.54	4.03	3.62	2.73
Center section	3.86	4.43	4.25	1.70	4.43	5.69	5.26	4.82	7.00	4.55	4.56	4.44	4.49	4.88	4.43	3.95	3.61	2.72
Aft skirt	3.68	4.24	4.05	1.59	4.18	5.61	5.21	4.76	6.99	4.38	4.47	4.25	4.29	4.87	4.18	3.76	3.60	2.70
Forward tankwall	3.29	3.81	3.63	1.59	3.66	5.33	4.95	4.57	6.98	4.08	4.23	3.92	3.63	4.83	3.66	3.54	3.54	2.64
Aft tankwall	2.81	3.22	3.04	1.50	2.93	5.03	4.63	4.32	6.98	3.76	3.90	3.61	3.29	4.83	3.03	3.26	3.52	2.60

Construction Legend:

⎍ Top-Hat Stringers Z Z Section ⊥ Integral Stringers H Honeycomb Sandwich W Waffle Pattern

TABLE 16. - UNIT SHELL WEIGHT (LB/SQ FT) FOR INCONEL DESIGNS AT VARIOUS TEMPERATURES

Vehicle	No Temperature Restraint (Minimum Weight)					Maximum Entry Temperature (°R) 1000					1100		1200
	⎍	Z	⊥	H	W	⎍	Z	⊥	H	W	⎍	H	H
1.3 x 10^6 pounds													
Crew compartment	4.39	5.15	4.86	1.76	4.31	6.99	6.48	6.10	9.75	5.33	5.01	5.60	3.89
Center section	4.33	5.06	4.77	1.69	4.21	6.90	6.39	6.08	9.75	5.31	5.01	5.60	3.89
Aft skirt	4.13	4.84	4.57	1.53	3.97	6.81	6.32	5.95	9.75	5.23	4.97	5.60	3.88
Forward tankwall	3.87	4.51	4.26	1.76	3.63	6.64	6.16	5.83	9.75	5.13	4.77	5.60	3.93
Aft tankwall	3.30	3.84	3.61	1.69	2.91	6.33	5.91	5.63	9.75	5.01	4.52	5.60	3.88
1.9 x 10^6 pounds													
Crew compartment	4.93	5.77	5.49	2.21	5.20	7.39	6.81	6.38	9.75	5.67	5.27	5.62	3.92
Center section	4.83	5.67	5.39	2.12	5.09	7.36	6.78	6.32	9.75	5.61	5.28	5.62	3.92
Aft skirt	4.62	5.42	5.14	1.92	4.80	7.26	6.72	6.25	9.75	5.48	5.09	5.61	3.91
Forward tankwall	4.26	5.00	4.72	2.04	4.31	7.01	6.49	6.06	9.75	5.31	4.87	5.62	3.92
Aft tankwall	3.62	4.22	3.98	1.95	3.44	6.59	6.12	5.79	9.75	5.09	4.60	5.62	3.89
2.5 x 10^6 pounds													
Crew compartment	5.44	6.34	6.08	2.67	5.97	7.72	7.23	6.69	9.76	6.04	5.50	5.64	3.95
Center section	5.34	6.22	5.96	2.58	5.84	7.68	7.19	6.65	9.76	5.97	5.44	5.64	3.95
Aft skirt	5.09	5.95	5.68	2.33	5.51	7.54	6.94	6.55	9.76	5.79	5.40	5.63	3.93
Forward tankwall	4.68	5.48	5.20	2.21	4.96	7.30	6.81	6.31	9.75	5.51	5.12	5.65	3.96
Aft tankwall	3.95	4.63	4.38	2.10	3.96	6.87	6.35	5.96	9.75	5.16	4.85	5.62	3.91

Construction Legend:
⎍ Top-Hat Stringer Z Z Section ⊥ Integral Stringer H Honeycomb Sandwich
W Waffle Pattern

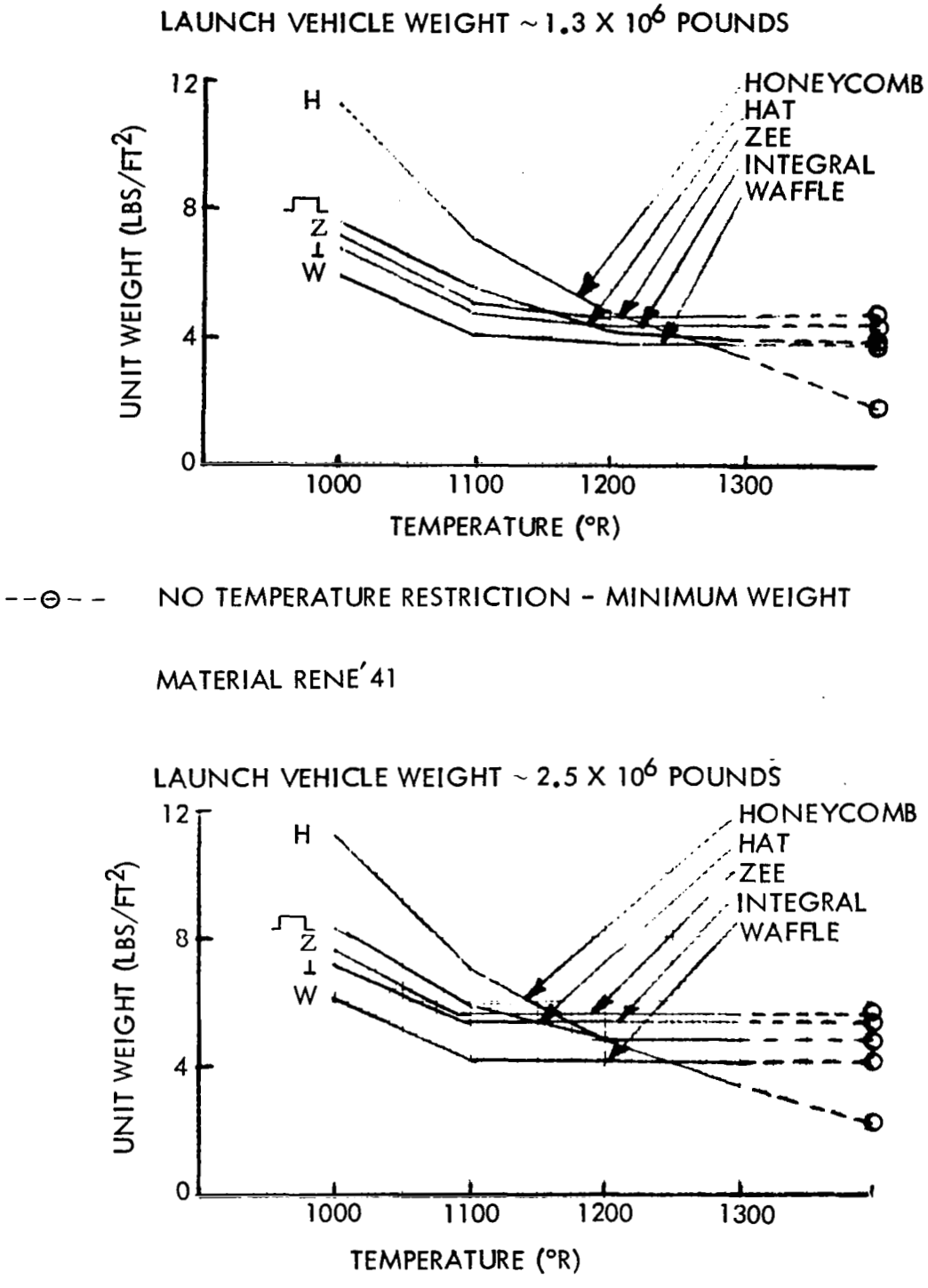

Figure 60. - Effect of Temperature on Unit Weight of Pressurized Forward Tankwall

LAUNCH VEHICLE WEIGHT ~ 1.3 X 10^6 POUNDS

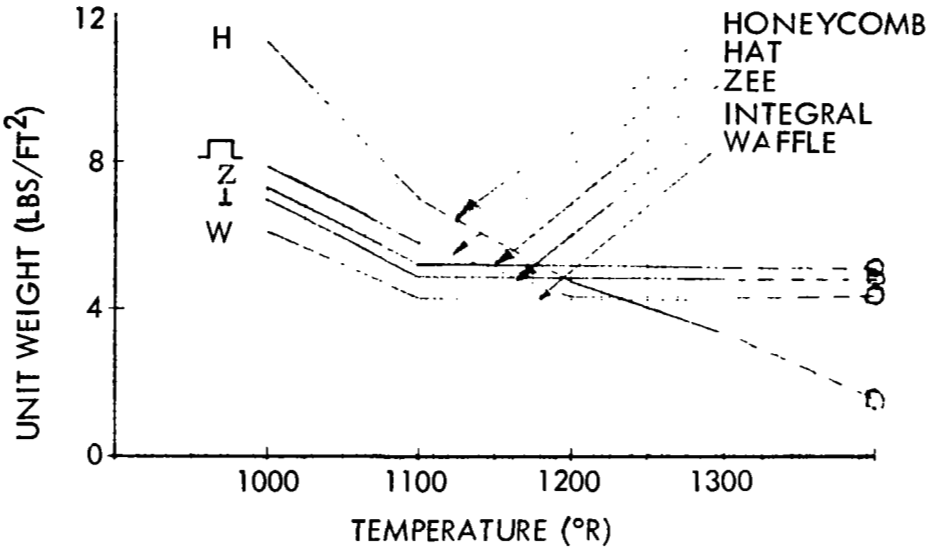

--⊖-- NO TEMPERATURE RESTRICTION - MINIMUM WEIGHT

MATERIAL RENE'41

LAUNCH VEHICLE WEIGHT ~ 2.5 X 10^6 POUNDS

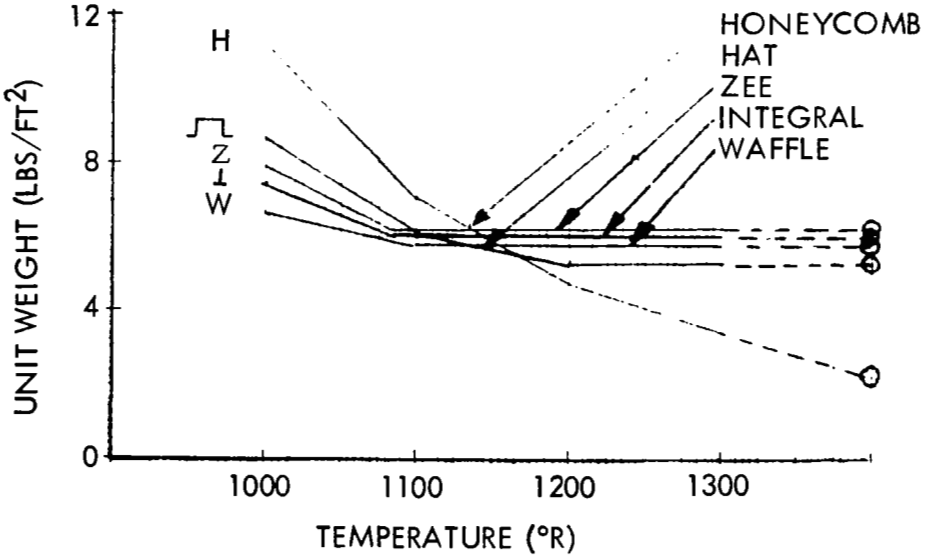

Figure 61. - Effect of Temperature on Unit Weight of Unpressurized Crew Compartment

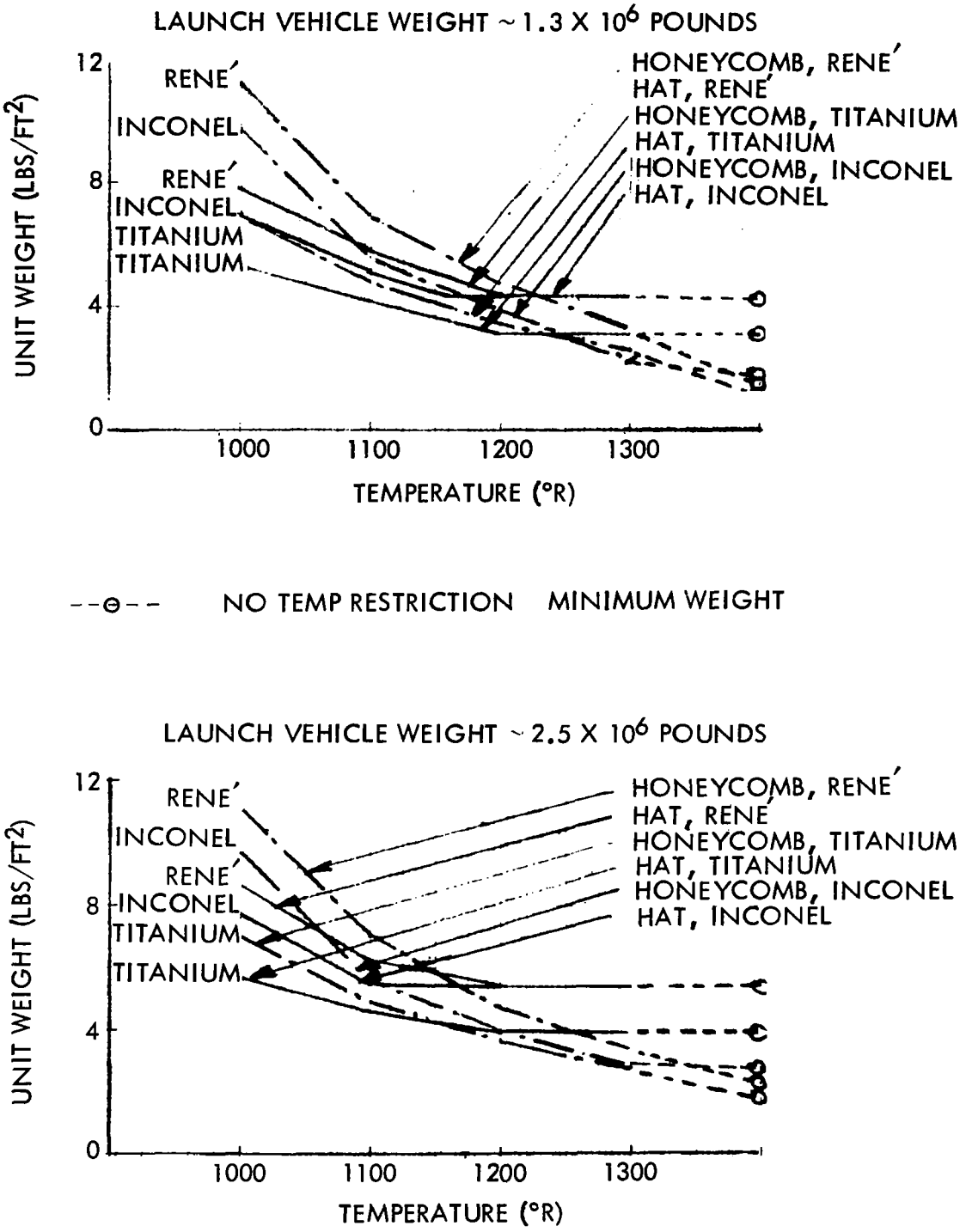

Figure 62. - Material Efficiency With Temperature Restrictions on Crew Compartment

For the expendable vehicle design, it was found that various types of construction working at a high stress level could benefit from improvement of the material properties. These improvements are expressed as a percentage increase of a nominal compression yield and tensile ultimate strength of current materials. The shape of the stress-strain diagram for the plasticity considerations for advanced alloy materials is assumed to be identical to that of the current material. The plasticity curve of the material is expressed mathematically for inclusion in the computer subroutines to provide access to the plasticity correction factors for the various materials. Design synthesis analyses to evaluate minimum weight for the structural components must consider materials in the elastic range and plastic range. Figure 63 shows the weight reduction for the fuselage shells for a range of percentage improvements of the materials compressive yield. It shows that with aluminum skin stringer being used for the unpressurized shells and a design load intensity less than 5000 lb/in., the maximum weight reduction of 3 percent is achieved when the compressive yield is increased 20 percent. For the recoverable fuselage, there is an additional shell weight for the insulation of 1.5 lb/ft^2; therefore, the weight reduction with material improvement is now only 2 percent. For the hot structure concepts where the skin thicknesses are dictated by temperature considerations, the resulting structure unit weight is fairly heavy, i.e., the design is at a low stress level. Therefore, with the allowable working stresses below the yield and ultimate stresses of the material, any improvements in the material strength and stiffness properties will have a negligible effect on the basic unit shell weight.

For the basic shell design with a honeycomb construction with the load-carrying structure of less than 1200 °R, the material preference would be titanium, Inconel, and, finally, René. If the temperature has no constraints imposed, the material rating is titanium, best; then René, and, finally, Inconel. With the honeycomb sandwich designed for temperatures of less than 1100 °R, the sandwich weights are heavier than the single skins with stiffener elements. If the sandwich temperatures are greater than 1200 °R, the thermal stresses are too high for the design concept.

With the single-sheet plus stiffeners, the best weight ordering of concepts is waffle, integral, Z, and, finally, top-hat section for any temperatures less than 1100 °R; at 1000 °R all the designs are at least 50 percent lighter than honeycomb sandwich. When these designs are optimized for the boost condition loads, the resulting skin thicknesses are such that they have sufficient heat capacity to limit the average surface temperature to less than 1100 °R without any thermal weight penalty.

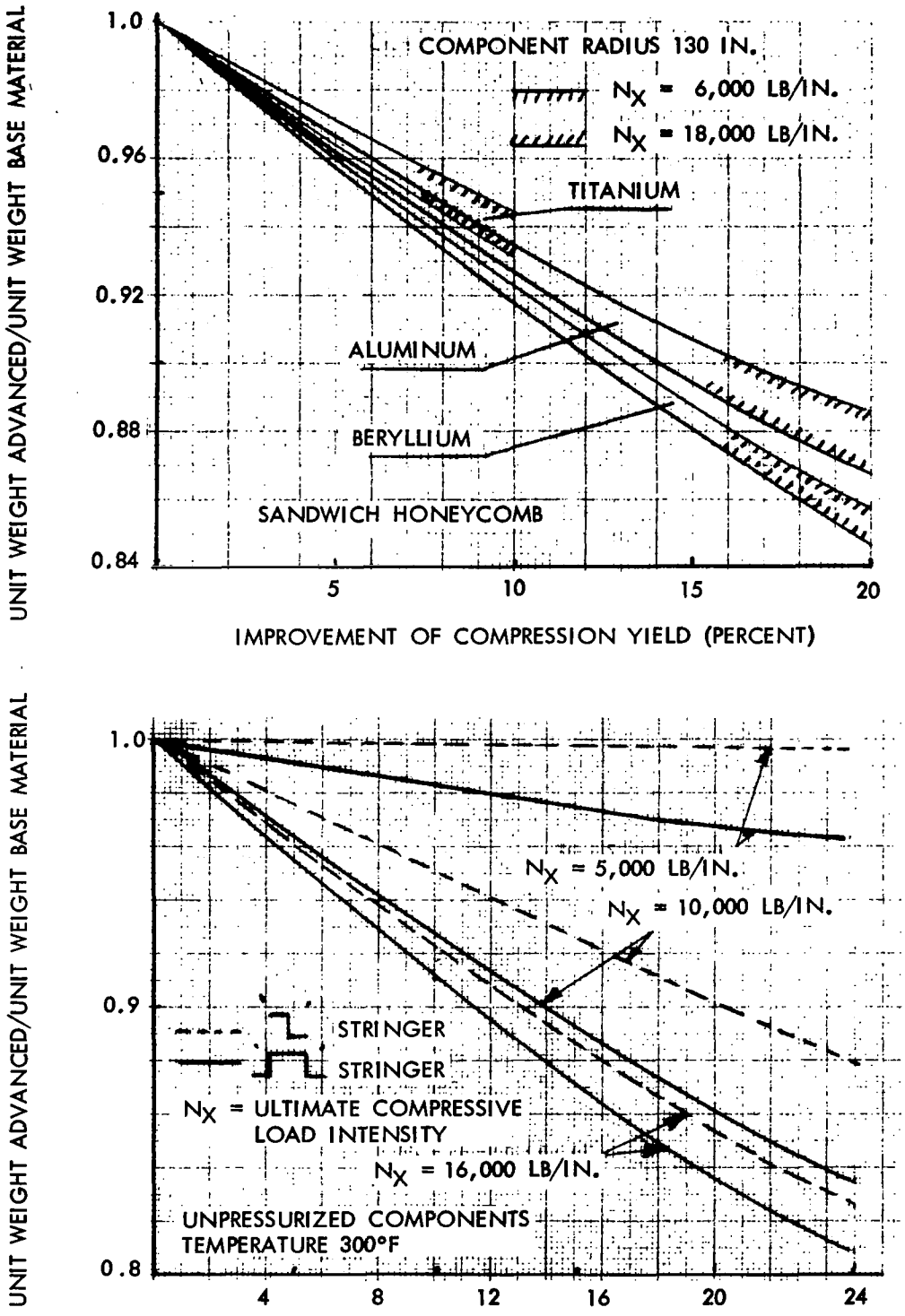

Figure 63. - Unit Weight Reductions With Material Improvements

If the heat sink capacity of the hot structure could be increased to bring the surface temperature down without adding too much weight, then honeycomb designs could be more attractive. A lightweight non-load carrying structure with a good heat capacity or a thermal insulation barrier would allow the honeycomb sandwich to be worked more efficiently and result in a lighter overall design.

With the single-skin designs, if there is a heat sink resulting from the cold propellant in contact with the tank wall, there will be a thermal gradient across the stiffener element. This would induce thermal stresses and deformation. If cryogenic propellants are used, there has to be an insulation system to stop propellant boiloff during ground hold. This cold temperature insulation will act as a thermal barrier also during entry. The load-carrying structure considered as being fully insulated on the back side is a realistic model.

Insulated aluminum design with the weight penalties assumed will be the most efficient structure weightwise. The problem is fabricating the heat shield, insulation, and standoffs within the suggested weight budget. Cost of this thermal protection system might make this concept uneconomical compared with the hot structure.

Assessment

To obtain conclusive evidence as to where and when it is advantageous to achieve material property or construction-type improvements, it is necessary to assess the effects of these improvements on specific structural components in particular vehicle systems. General conclusions cannot be drawn without citing ground rules and criteria for each case in question. To define an effective approach requires a clear definition of the merit functions upon which decisions are to be based. Three merit functions have been indicated in this report. The most obvious of these is the weight reduction that arises from a structures and materials advancement for each of the structural components in a particular vehicle system. This merit function gives a clear indication of the weight savings that can be directly obtained from a structural improvement.

If component weight reduction, per se, is the only merit function used, a true indication of the significance of the weight reduction may not result. Weight reduction effects upon overall system payload performance, schedule, and cost are the governing criteria in the aerospace industry. Component weight reduced and payload (pounds) gained can be translated into a structural cost index which can assist in the economic justification of a specific material

and design for a particular component. The merit functions used during Phase 1—component weight reductions, equivalent payload performance changes, and effective cost ratios—are considered applicable for this phase of the study. An ordering of these merit functions can indicate the relative worth.

Depending upon the circumstances, management decisions can be based on each of these merit functions; however, the objective of this study is to indicate and demonstrate a method wherein these decisions utilize all three merit functions. (Weight reduction, payload gain, and cost index are considered as a set of indices unique to a component change in a particular vehicle base point.) Typical results are indicated, which are limited to three vehicles with recoverable first stages as synthesized during Phase II and defined in a previous section of this report.

Stress analysis results in a definition of the basic shell requirements, while the weight of the component must include complexity factors to assess weight resulting from material tolerances, section closeouts, joining, fabrication techniques, etc. In most standard construction types, where enough historical data is available, these weight factors can be assessed as a percentage increment in component weight. For example, in the advanced titanium tankage parametric study (ref. 7), weight complexity factors of 10 percent were assessed to aluminum and titanium honeycomb sandwich shells for the upper stages of the vehicle system. This percentage was verified by the final full-scale stage design. In the lower stage, this factor was increased to 12 percent. Aluminum skin-stringer factors were 8 percent for upper stages and 10 percent for lower stages while the titanium skin-stringer structure was similar to the sandwich. A survey of the Saturn V launch vehicle weight data confirms these assumptions. Because detail design points for superalloy structures are not available an estimate was included in the parametric synthesis phase of this study for all designs.

The estimated cylindrical shell weight complexity factors included in the parametric synthesis step of this study are given in table 17. These factors were not introduced in the structural design synthesis study and are not reflected in the basic shell data incorporated in that section; however, they were included in the assessment and mass fraction operations in this study. These factors were used in a study where conclusions are drawn from relative weight comparisons. Many unknowns can creep into the weight picture during the hardware design phases, which result in increased weight complexity. However, in this study, it is assumed that these unknowns will influence each construction type to the same relative degree and therefore not change the basic comparative conclusions. Another merit function is the equivalent payload gained from a structural component weight reduction. This can be

thought of as reducing the structural weight and on-loading a fraction of this weight reduction as payload while retaining the same overall vehicle performance capability. The payload exchange ratio provides an expedient and relatively accurate tool for predicting the effects and assessing the effectiveness of any design structural/material/construction changes to the fuselage of the preliminary base point recoverable stages. They assist in indicating the relative merits or penalties in terms of payload performance and, hence, cost effectiveness of structural design decisions, nonoptimum designs, and limitations imposed by manufacturing and fabrication, etc.

TABLE 17.- WEIGHT COMPLEXITY FACTORS (PERCENT)

Material	Type of Construction		
	Skin Stringer	Waffle	Honeycomb Sandwich
Aluminum	10	10	12
Titanium	12	12	12
Beryllium	12	12	14
René 41	12	12	12
Inconel	12	12	12
Steel	10	10	12

These exchange ratios were developed for expendable vehicle systems during Phase I of the study contract (ref. 2). Of particular importance is the ratio due to stage structural weight changes $\left(\frac{dW_p}{dW_{st}}\right)_n$. For expendable systems, the weight of a stage after separation is invariant and inconsequential. With the first stages being recovered, the additional structural weight at burnout has to be augmented with extra fuel for the flyback range and larger wings, engines, landing gear, etc., for the vehicle's touchdown. Therefore, the exchange partial for the recoverable stage structural weight change is the combination of two exchange partials:

$$\frac{dW_{PL}}{dW_{ST_F}} = \frac{dW_{PL}}{dW_{ST}} \cdot \frac{dW_{ST}}{dW_{ST_F}}$$

where

W_{ST_F} is the structural weight of the fuselage

W_{ST} is the stage weight at end boost.

The first ratio dW_{PL}/dW_{ST} is concerned with the ascent boost phase of the trajectory while dW_{ST}/dW_{ST_F} deals with the entry and flyback. The equation for the total velocity gained at burnout can be expressed as follows

$$V = \sum_{i=1}^{N} \Delta V_i = \sum_{i=1}^{N} \left(\Delta V_{I_i} - \Delta V_{g_i} - \Delta V_{L_{a_i}} \right)$$

where

V_I is the impulsive velocity

V_g is velocity losses due to gravity

and

V_{L_a} velocity losses due to atmospheric effects and thrust misalignments

Therefore, the velocity losses can be approximated to develop an expression for the total velocity of the two-stage vehicle as

$$V = \sum_{i=1}^{2} \left[g I_{sp_i} \ln \left(\frac{W_o}{W_{B_{o_i}}} \right) - g t_{B_i} \cos \bar{\beta}_i - \Delta V_{L_{a_i}} \right]$$

For the flyback provision of the first stage, the range is a function of the vehicle burnout condition and design parameters. Using the Breguet equation, the range can be expressed as

$$R = \left(\frac{L}{D} \right) \left(\frac{V}{C} \right) \ln \left(\frac{W_{ST}}{W_{LAND}} \right)$$

C = Specific fuel consumption

Since the burnout velocity is assumed constant the total differential of the velocity is zero and is given by:

$$\sum_{i=1}^{2} \left[\frac{\partial(\Delta V)}{\partial I_{sp}}\right]_i dI_{sp_i} + \left[\frac{\partial(\Delta V)}{\partial Wo}\right]_i dW_{o_i} + \left[\frac{\partial(\Delta V)}{\partial W_{Bo}}\right]_i dW_{Bo_i} + \left[\frac{\partial(\Delta V)}{\partial t_{B_i}}\right] dt_{B_i} = 0$$

The partials of the above equation can be evaluated from the terms in the velocity equation and upon substitution results in:

$$\sum_{i=1}^{2} \left\{ g \ln \left(\frac{W_o}{W_{Bo}}\right)_i dI_{sp_i} + \left(\frac{g I_{sp}}{W_o}\right)_i dW_{o_i} + \left(\frac{g I_{sp}}{W_{Bo}}\right)_i dW_{Bo_i} - g \cos \bar{\beta}_i \, dt_{B_i} \right\} = 0$$

The first exchange ratio to be developed is

$$\left(\frac{dW_{PL}}{dW_{ST}}\right)_1$$

It is assumed that with a change in the stage burnout weight, the propellant weight and specific impulse remain constant, therefore

$$dI_{sp_i} = 0, \quad (1 \leq i \leq 2)$$

$$dW_{o_1} = dW_{ST_1} + dW_{PL}$$

$$dW_{o_2} = dW_{PL}$$

$$dW_{Bo_1} = dW_{ST_1} + dW_{PL}$$

$$dW_{Bo_2} = dW_{PL}$$

$$dT_{B_i} = 0 \ (1 \leq i \leq 2)$$

Therefore, the first partial can be represented by

$$\frac{dW_{PL}}{dW_{ST_1}} = \frac{dW_{PL}}{dV} \cdot \frac{dV}{dW_{ST_1}}$$

$$= \frac{\left(\frac{\partial(\Delta V)}{\partial W_o}\right)_1 + \left(\frac{\partial(\Delta V)}{\partial W_{Bo}}\right)_1}{\sum_{i=1}^{2} \left[\left(\frac{\partial(\Delta V)}{\partial W_o}\right)_i + \left(\frac{\partial(\Delta V)}{\partial W_{Bo}}\right)_i\right]}$$

which upon substitution of partial differentials will reduce to

$$\frac{dW_{PL}}{dW_{ST_1}} = -\frac{\left(\frac{I_{sp}}{W_o}\right)_1 (\mu_1 - 1)}{\sum_{i=1}^{2} \left[\left(\frac{I_{sp}}{W_o}\right)_i (\mu_i - 1)\right]}$$

where

$$\mu_i = \frac{W_{oi}}{W_{Bo_i}}$$

For the flyback provisions taking the total differential of the range will produce

$$dR = \left(\frac{\partial(\Delta R)}{\partial W_{ST}}\right) dW_{ST} + \left(\frac{\partial(\Delta R)}{\partial W_{LAND}}\right) dW_{LAND}$$

where

$$W_{LAND} = W_{ST_F} + W_{ST_{FB}}$$

and $W_{ST_{FB}}$ is the structural weight associated with the recovery features such as wings, flyback engines, landing gear, etc. This recovery weight can be defined as

$$W_{ST_{FB}} \stackrel{\text{EM}}{=} \sigma W_{ST}$$

where σ is a modified structural factor for the recovery system weights. It is assumed that with a change in fuselage structural weight, both the flyback propellant weight and recovery system weights are perturbed

$$dW_{ST} = dW_{ST}$$

$$dW_{LAND} = dW_{ST_F} + \sigma\, dW_{ST}$$

Substituting these equations into the second partial ratio will produce

$$\frac{dW_{ST_F}}{dW_{ST}} = \frac{dW_{ST_F}}{dR} \cdot \frac{dR}{dW_{ST}}$$

$$= \frac{\dfrac{\partial R}{\partial W_{ST}} + \sigma \dfrac{\partial R}{\partial W_{LAND}}}{\dfrac{\partial R}{\partial W_{LAND}}}$$

where

$$\frac{\partial R}{\partial W_{ST}} = \left(\frac{L}{D}\right) \left(\frac{V}{C}\right) \frac{1}{W_{ST}}$$

and

$$\frac{\partial R}{\partial W_{LAND}} = - \left(\frac{L}{D}\right) \left(\frac{V}{C}\right) \frac{1}{W_{LAND}}$$

Therefore, on rearranging, the partial is given by

$$\frac{dW_{ST_F}}{dW_{ST}} = \left[\frac{1}{\mu_{FB}} - \sigma\right]$$

where

$$\mu_{FB} = W_{ST}/W_{LAND}$$

Combining these two effects, we obtain

$$\frac{dW_{PL}}{dW_{ST_F}} = \frac{-\left(\frac{I_{sp}}{W_o}\right)_1 (\mu_i - 1)}{\sum_{i=1}^{2} \left[\left(\frac{I_{sp}}{W_o}\right)_i (\mu_i - 1)\right]\left(\frac{1}{\mu_{FB}} - \sigma\right)}$$

This payload partial has been evaluated for the six-base-point vehicle systems. Recovery systems' weight was assumed to consist of the crew compartment, wing and carry-through, flyback engines and their installations, wing insulation, and landing gears. Table 18 shows the exchange partials for the base-point vehicles and they range from 0.155 to 0.179. These values are representative of recoverable stages, which have a flyback range capability of 300 nautical miles. If the flyback range is varied, the stored propellant required will change. For the condition of propellant weight changes only and assuming that other systems' weight are invariant, the resulting variation of the exchange ratios is indicated in figure 64. The zero-range requirement assumes that the recovery stage has wings, etc., and also flyback engines, but no propellant. This figure clearly shows that the necessity of saving structural weight of the boost system components is significant for recoverable stages. The effect is most noticeable with stages having a large flyback range requirement.

A final merit function that is a good indicator of any subsystem performance is its cost index. The total cost of a structural component is composed of several contributing factors: development, production (fabrication, tooling, and equipment), and testing (static and flight vehicles). For this study, where all components were compared to a base-point design, it was assumed that the development and testing costs were identical for both the improved component

TABLE 18. - BASE-POINT VEHICLE PAYLOAD EXCHANGE PARTIALS

	Near term	Future	Near term	Future	Near term	Future
Vehicle gross weight (pounds) W_{o_1}	1 303 884	1 304 285	1 899 760	1 900 059	2 499 486	2 499 418
Performance fraction ν_1	0.63736	0.60104	0.63736	0.60104	0.63736	0.60104
Performance ratio μ_1	2.75755	2.50651	2.75755	2.50651	2.75755	2.50651
2nd vehicle gross weight W_{o_2}	339 268	389 483	499 895	572 497	663 672	758 624
Performance fraction ν_2	0.73757	0.70793	0.73757	0.70793	0.73757	0.70793
Performance ratio μ_2	3.81053	3.42383	3.81053	3.42383	3.81053	3.42383
Specific impulse I_{sp_1}	.308	.340	.308	.340	.308	.340
Specific impulse I_{sp_2}	460	500	460	500	460	500
$\left(\frac{I_{sp}}{W_o}\right)_1 (\mu_1 - 1)$	.00041516	.00039272	.00028494	.00026958	.00021657	.00020493
$\left(\frac{I_{sp}}{W_o}\right)_2 (\mu_2 - 1)$	.0038107	.0031116	.0025862	.0021168	.0019480	.0015975
Boost Partial $\frac{dW_{pl}}{dW_{st}}$	.09824	.11207	.09924	.11296	.10005	.11370
Stage burnout weight W_{st}	133 492	131 049	188 872	185 590	242 402	238 198
Stage loaded weight W_{land}	118 152	116 040	167 164	164 282	214 522	210 799
Flyback performance ratio μ_{fb}	1.1298	1.1293	1.1299	1.1297	1.1230	1.1230
Recovery system weight $W_{st\ fb}$	33 820	32 109	47 154	46 269	61 801	60 729
Structural fraction δ	.25335	.24501	.24966	.24930	.25495	.25495
Entry Partial $\frac{dW_{st}}{dW_{st_f}}$	.63176	.64049	.63537	.63589	.63552	.63552
Total Partial $\frac{dW_{pl}}{dW_{st_f}}$	.1555	.1750	.1562	.17764	.1574	.1789

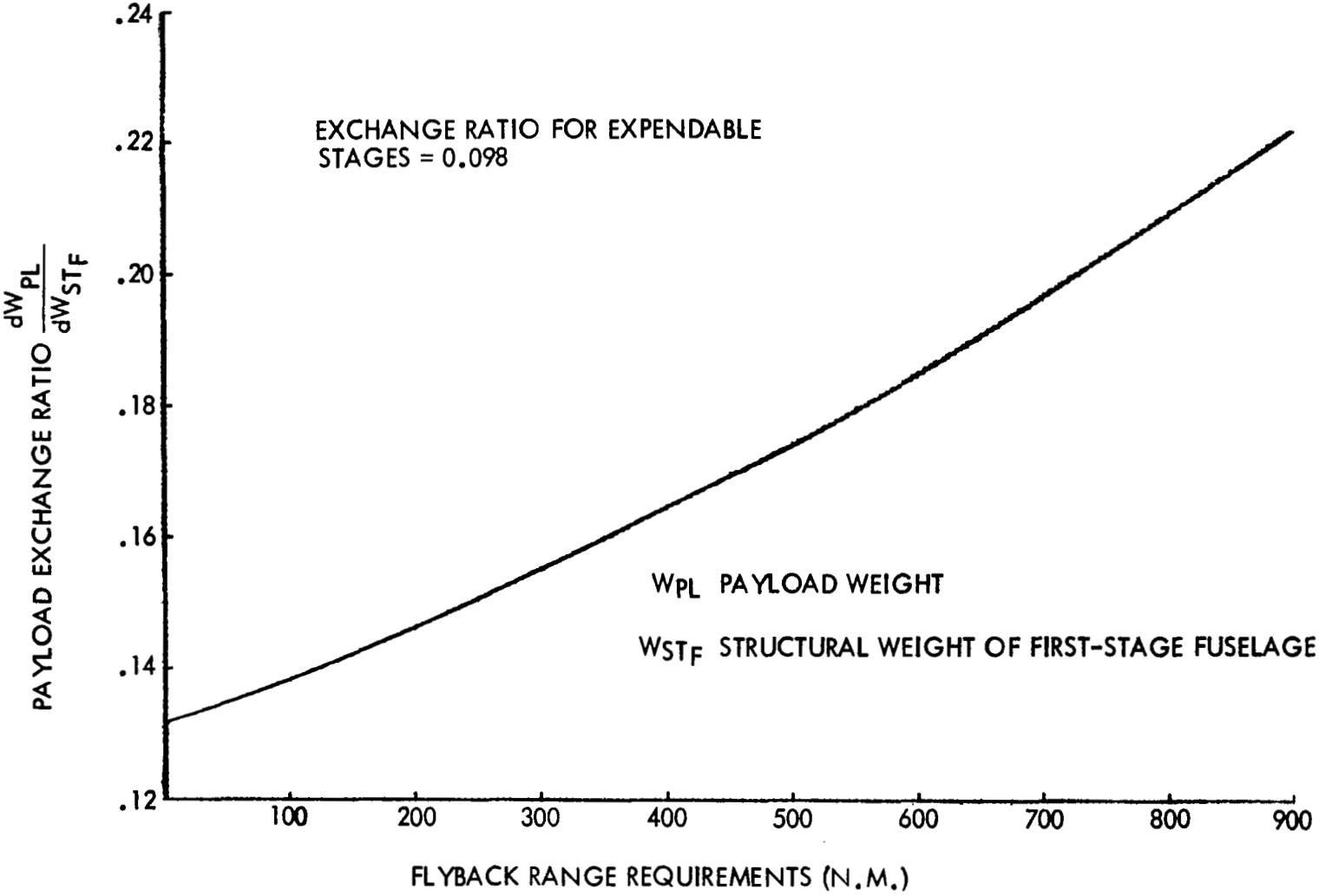

Figure 64. - Exchange Ratios for Recoverable First Stage of 1.3×10^6-Pound Vehicle

and the base-point design; therefore, the only cost differences considered between the two structural components were production costs. The cost figure of merit is the cost difference between the improved and base-point designs and the relative payload gained and uses an index of dollars per pound in orbit for the ordering effectiveness

$$CR = \frac{(\$_{PRODUCTION})_{ADVANCE} - (\$_{PRODUCTION})_{BASEPOINT}}{(W_{PAYLOAD})_{ADVANCE} - (W_{PAYLOAD})_{BASEPOINT}}$$

The basic costing premise in the aerospace industry for structural components is that the cost of an item to be built can be determined by an analysis of the cost of analogous items that have been built. However, when proposed systems differ greatly in basic vehicle characteristics (vehicle size, weight, type of construction, etc.) difficulties arise because of a lack of identical historical data. In the aerospace industry, as in the Phase I study, weight has been used as the basis for cost estimating. This approach uses cost-per-pound, or hours-per-pound, as the relationship between cost and the stage structural weight. Values of cost-per-pound are not constant for all vehicle systems and have a scaling factor introduced to account for the relative sizes and weights of components (ref. 8).

An array of complexity factors for fabrication, was introduced into the following relationship, these factors being in agreement with those contained in reference 9 and one shown in table 19.

$$y = CF\ 4619\ (X)^{-0.322}$$

where

y = first unit airframe cost in dollars per pound of weight adjusted for complexity

CF = total complexity factor of structural component

X = component weight

Added to this cost is the material cost. Material costs such as the following tend to influence the cost ratios in favor of the cheaper material:

Material	Cost (dollars/lb)
Aluminum	0.9
Titanium	30.0
Beryllium	200.0
Rene'	13.0
Inconel	13.0

Also of some significance is the experience (percent learning) used to determine construction costs. Cost dependency is placed upon the number of consecutively produced production units and the slope of this learning curve. Reference 8 defines the experience curve by

$$K_{exp} = A X^{-B}$$

where

A, B = Constants, values of which are selected to express appropriately the relation for a specific situation

K_{exp} = Adjustment factor based on experience

X = Consecutive number of a specific production unit

It has been found that the unit cost decreases for the experience curve by a constant factor as the number of consecutive production units is doubled. This constant factor is referred to as the "percent learning," (P); which for this study was 85 percent. The relationship between learning, (P). the constant B of the experience curve is

$$P = 2^{-B} (100).$$

Total structural cost for the structural component is defined as

$$\text{Cost} = YXK_{exp} + X \$_{MAT}$$

where

$\$_{MAT}$ = dollars per pound for material stock

A digital program for the costing was developed using the preceding approach which systematically considered the effects of numerous construction and material improvements on each and every structural component for

TABLE 19. - COMPLEXITY FACTORS

Material	Construction	Shape and Diameter											
		Flat Plate	Cylindrical				Conical				Spherical			
			10 ft	20 ft	30 ft	60 ft	10 ft	20 ft	30 ft	60 ft	10 ft	20 ft	30 ft	60 ft
Aluminum	Monocoque	0.9	1.0	1.0	1.0	1.0	1.1	1.1	1.1	1.2	2.8	2.9	3.1	3.5
	Integral skin stringer	1.2	1.8	1.6	1.4	1.4	2.1	2.0	2.0	1.8	6.4	6.8	7.2	8.2
	Attached skin stringer	1.0*	1.6	1.4	1.2	1.2	2.0	1.9	1.8	1.6	6.0	6.5	7.0	8.0
	Waffle	1.4	2.0	1.7	1.5	1.5	2.2	2.1	2.1	1.9	6.6	6.9	7.4	8.4
	Honey sandwich	2.8	3.4	3.2	3.0	3.0	4.0	3.9	3.8	3.6	10.0	10.4	11.4	12.4
	Corrugations	3.0	3.6	3.4	3.2	3.2	4.3	4.2	4.1	4.0	10.2	10.6	11.6	12.6
	Double-wall/multiwall	3.4	4.0	3.8	3.6	3.6	4.6	4.5	4.4	4.3	10.6	11.0	12.0	13.2
Titanium	Monocoque	1.4	1.5	1.4	1.3	1.5	1.6	1.6	1.6	1.7	3.4	3.5	3.7	4.1
	Integral skin stringer	4.2	4.8	4.6	4.4	4.4	5.0	4.9	4.8	4.8	13.2	13.6	14.0	15.0
René	Attached skin stringer	4.0	4.6	4.4	4.2	4.2	4.8	4.7	4.6	4.6	13.0	13.5	14.0	15.0
	Waffle	4.4	5.0	4.7	4.5	4.5	5.1	5.0	4.9	4.9	13.3	13.7	14.3	15.2
and	Honey sandwich	8.0	9.0	8.8	8.6	8.6	9.5	9.3	9.2	9.2	18.0	18.4	19.0	20.0
	Corrugations	8.4	9.4	9.2	9.0	9.0	9.8	9.6	9.4	9.4	18.4	18.8	19.2	20.2
Inconel	Double-wall/multiwall	9.0	10.0	9.8	9.6	9.6	10.4	10.2	10.0	10.0	19.0	19.4	19.8	20.8

*Base point

the family of base point vehicles. The cost merit functions are identified for the individual components. Each material and structural change from the base point design was considered to apply to the total vehicle simultaneously for reasons of computer time economy; however, this change could have reflected a single component.

The component weight and cost ratio program developed during Phase I of this study was utilized in assessing the relative merits of the various designs and materials. Typical computer printouts (table 21) show the weight for the base-point component, aluminum integral skin stringer, and the structural cost breakdown. It can be seen that the material cost for the base point is significant. This is because the type of construction requires a thick billet of material which is subsequently milled out to the required shape. For the small vehicle shown, the initial material thickness was greater than two inches. This material cost effect will be extremely noticeable for the more expensive materials with waffle and integral skin stringer construction. Table 21 shows that when the alternative design of top-hat section skin stringer is considered, the material cost drops considerably and is only 10% of the fabrication costs. For the production fabrication evaluation, the number of units considered was 20 at a production rate of 4 a year. This allowed for a fabrication reduction due to the learning proficiency. A list of the three merit functions associated with the alternative design is indicated in the last array of table 21. This array shows the changes from the base-point design in terms of weight, payload, and cost ratio. The relative effectiveness of the cost ratios are indicated in table 20.

TABLE 20. - RELATIVE COST RATIO EFFECTIVENESS

Equivalent Payload Change	Component Cost Change	Cost Ratio	Remarks
Positive	Positive	Positive	Good design, but is it worth it. Cost ratio better nearer to zero value
Positive	Negative	Negative	Better design than base point. Cost ratio better when more negative.
Negative	Positive	Negative	Poorer design than base point. Cost ratio better nearer to zero value.
Negative	Negative	Positive	Does reduced cost warrant reduced payload? Cost ratio better when more positive.

TABLE 21.- COMPUTER PRINTOUTS FOR COMPONENT MERIT FUNCTIONS

BASE-POINT COMPONENT WEIGHT

VEHICLE	1300000. POUNDS		
MATERIAL	ALUMINUM		
CONSTRUCTION	INTEGRAL SKIN STRINGER		
LAUNCH RATE	4.	NUMBER OF UNITS	20.
NUMBER OF TEST VEHICLES	2.	NUMBER OF TOOLS	1.
YEARS IN PRODUCTION RUN	5.		

STAGE	COMPONENT	AREA	NX (P)	UNIT WT BASEPOINT (NOTE)	CORR COEF	UNIT WT ALTERNATE (NOTE)	WEIGHT ALTERNATE
1							
	INTERSTAGE	0.511CE 03	0.3058E 04	0.4100E C1	0.1692E 01	0.4100E 01	0.3544E 04
	FWD TANKWALL	C.959CE 03	0.1541E 04	0.3740E C1	0.1110E 01	0.3740E 01	0.3983E 04
	CENTER SECTION	0.1131E C4	C.2920E 04	0.4040E C1	0.1205E 01	0.4040E 01	0.5505E 04
	AFT TANKWALL	0.3440E 03	0.1541E 04	0.3400E C1	0.1446E 01	0.3400E 01	0.1691E 04
	AFT SKIRT	0.511CE 03	0.2604E 04	0.3910E C1	0.1281E 01	0.3910E 01	0.2559E 04

NOTE-UNIT WT FOR SHELLS-TOTAL WT FOR BULKHEADS

BASE-POINT COMPONENT COSTS

STAGE	COMPONENT	WEIGHT PER UNIT	FABRICATION COST PER UNIT	MATERIAL COST PER UNIT	TOTAL COST PER UNIT
1					
	INTERSTAGE	3544.	38830.	25744.	64574.
	FWD SKIRT	0.	0.	0.	0.
	FWD TANKWALL	3980.	30524.	27372.	57896.
	CENTER SECTION	5505.	42219.	38737.	80956.
	AFT TANKWALL	1691.	12971.	11448.	24419.
	AFT SKIRT	2559.	19620.	18600.	38220.

ALTERNATE DESIGN COMPONENT WEIGHT

VEHICLE	1300000. POUNDS		
MATERIAL	ALUMINUM		
CONSTRUCTION	HAT SECTION SKIN-STRINGER		
LAUNCH RATE	4.	NUMBER OF UNITS	20.
NUMBER OF TEST VEHICLES	2.	NUMBER OF TOOLS	1.
YEARS IN PRODUCTION RUN	5.		

STAGE	COMPONENT	AREA	NX (P)	UNIT WT BASEPOINT (NOTE)	CORR COEF	UNIT WT ALTERNATE (NOTE)	WEIGHT ALTERNATE
1							
	INTERSTAGE	0.511CE 03	0.3058E 04	0.4100E C1	0.1692E 01	0.3800E 01	0.3285E 04
	FWD TANKWALL	0.959CE 03	0.1541E 04	0.3740E C1	0.1110E 01	0.3930E 01	0.4183E 04
	CENTER SECTION	0.1131E 04	0.2920E 04	0.4040E 01	0.1205E 01	0.3750E 01	0.5110E 04
	AFT TANKWALL	0.344CE 03	0.1541E 04	0.3400E C1	0.1446E 01	0.3720E 01	0.1851E 04
	AFT SKIRT	0.5110E 03	0.2604E 04	0.3910E C1	0.1281E 01	0.3640E 01	0.2382E 04

NOTE-UNIT WT FOR SHELLS-TOTAL WT FOR BULKHEADS

ALTERNATE DESIGN COMPONENT COST

STAGE	COMPONENT	WEIGHT PER UNIT	FABRICATION COST PER UNIT	MATERIAL COST PER UNIT	TOTAL COST PER UNIT
1					
	INTERSTAGE	3285.	34947.	3088.	38035.
	FWD SKIRT	0.	0.	0.	0.
	FWD TANKWALL	4183.	26164.	3932.	30095.
	CENTER SECTION	5110.	36187.	4804.	40991.
	AFT TANKWALL	1851.	11118.	1740.	12858.
	AFT SKIRT	2382.	16817.	2239.	19056.

ALTERNATE DESIGN COMPONENT MERIT FUNCTIONS

STAGE	COMPONENT	WEIGHT PER UNIT	DELTA DOLLARS PER UNIT	DELTA WEIGHT PER UNIT	DELTA PAYLOAD PER UNIT	COST RATIO
1						
	INTERSTAGE	3285.	-26539.	-259.	40.	-658.
	FWD SKIRT	0.	0.	0.	-0.	-0.
	FWD TANKWALL	4183.	-27801.	202.	-31.	984.
	CENTER SECTION	5110.	-35964.	-395.	61.	-650.
	AFT TANKWALL	1851.	-11561.	159.	-25.	467.
	AFT SKIRT	2382.	-19164.	-177.	27.	-698.

For the insulated design concepts, the additional weight of the thermal protection system has been included, but the cost associated with its fabrication has not been fully considered. It is extremely difficult to determine the cost of such an undeveloped thermal protection system, which is at best ill-defined with regard to its structural elements; only a simplified weight and insulation thickness description has been assessed in the synthesis evaluation. Therefore, all the aluminum designs are under-evaluated and will produce favorable cost ratios.

The effects of structural refurbishment on the shell weight and fabrication costs have not been considered in this preliminary evaluation. Also the cost ratios quoted are for the total structural cost being amortized over only one flight payload's worth; this would be true for an expendable vehicle system. The first stages here are supposed to be fully recoverable, and their costs should include the refurbishment costs. These should be considered for the payload improvement throughout the life of the vehicle. Therefore, the cost ratio should be redefined for recoverable vehicles as follows:

$$CR = \frac{\$_{Advance} - \$_{Base\ point}}{Payload_{Advance} - Payload_{Base\ point}}$$

where

$$\$ = \$_{Production} + n \times \$_{Refurbishment}$$

$$Payload = W_{Payload} \times n$$

n = total number of flights per vehicle.

Tables 22 through 33 show the three types of merit functions for the five structural components of the recoverable stages. The merit functions were developed for both the "hot structure" and the aluminum concept with an outer insulation. Component weights quoted include two types of non-optimum design factors added to the basic shell unit weight. The first factor is dependent on the type of construction to account for closeouts, end fit, etc., and the second factor is dependent on the shell component. Insulated structures were assumed to have a 1.5-lb/ft^2 weight penalty for the total thermal protection system.

The best design in terms of weight is the aluminum honeycomb sandwich. Next are the top-hat stringer and waffle construction which are equal in weight to the integral stiffener base point and, finally, the Z-section stiffeners, which is slightly heavier. Relative weight efficiencies of the

TABLE 22. - MERIT FUNCTIONS FOR 1.3×10^6-POUND VEHICLE - ALUMINUM PLUS INSULATION

Component	Base Point ⊥	Construction			
		⎍⎍	Z	H	W
Weight (Pounds)					
Crew compartment	3544	3285	3596	2523	3521
Forward tank wall	3980	4183	4087	3270	3956
Center section	5505	5110	5587	3907	5468
Aft tank wall	1691	1851	1771	1503	1641
Aft skirt	2559	2382	2604	1802	2532
Equivalent Payload Gained (Pounds)					
Crew compartment	—	40	-8	159	4
Forward tank wall	—	-31	-17	111	4
Center section	—	61	-13	249	6
Aft tank wall	—	-25	-12	29	8
Aft skirt	—	27	-7	118	4
Effective Cost Ratio (Dollars per Pound)					
Crew compartment	—	-658	3254	73	-491
Forward tank wall	—	884	1685	96	-66
Center section	—	-650	3108	53	-325
Aft tank wall	—	467	940	163	-74
Aft skirt	—	-698	2661	47	-345

TABLE 23.- MERIT FUNCTIONS FOR 1.3×10^6-POUND VEHICLE - RENÉ 41

Component	Base Point	Weight (Pounds)																
		No Temperature Restriction (Minimum Weight)					Maximum Allowable Entry Temperature											
							1000°R					1100°R				1200°R		
		⊓	Z	⊥	H	W	⊓	Z	H	⊥	W	⊓	Z	⊥	H	⊓	H	H
Crew compartment	3544	3 803	4499	4282	1332	3 818	6 884	6 383	9 949	6147	5422	5115	4499	4282	6200	3803	4211	3 002
Forward tank wall	3980	4 259	4996	4786	1815	4 082	8 215	7 652	12 248	7338	6521	5408	4996	4746	7633	4509	5184	3 664
Center section	5505	5 967	6980	6637	2016	5 891	10 824	10 006	15 683	9578	8519	8049	6980	6637	9774	5967	6637	4 733
Aft tank wall	1691	1 202	1981	2219	828	1 527	3 678	3 445	5 725	3430	3064	2351	1981	2219	3568	1966	2423	1 728
Aft skirt	2559	2 752	3205	3053	881	2 666	5 131	4 778	7 530	4572	4070	3858	3205	3053	4686	2752	3187	2 266
		Equivalent Payload Gained (Pounds)																
Crew compartment	-	-40	-148	-115	344	-43	-519	-441	-996	-405	-292	-244	-148	-115	-413	-40	-104	84
Forward tank wall	-	-43	-158	-119	337	-16	-659	-571	-1 286	-522	-395	-222	-158	-119	-568	-82	-187	49
Center section	-	-72	-229	-176	543	-60	-827	-700	-1 583	-633	-469	-396	-229	-176	-664	-72	-176	120
Aft tank wall	-	-2	-45	-82	134	26	-309	-273	-627	-270	-213	-103	-45	-82	-292	-43	-114	-6
Aft skirt	-	-30	-101	-77	261	-17	-400	-345	-773	-313	-235	-202	-101	-77	-331	-30	-98	46
		Effective Cost Ratio (Dollars per Pound)																
Crew compartment	-	-1 844	-561	-2716	382	-5 256	-220	-244	-244	-728	-708	-374	-561	-2716	-471	-1844	-1630	1 816
Forward tank wall	-	-2 053	-624	-3242	455	-15 567	-213	-233	-225	-720	-782	-468	-624	-3242	-403	-1124	-1053	3 596
Center section	-	-1 717	-595	-2752	377	-5 163	-225	-251	-242	-703	-681	-380	-595	-2752	-480	-1717	-1504	1 997
Aft tank wall	-	-21 865	-894	-2068	492	3 687	-202	-217	-207	-857	-805	-439	-894	-2068	-348	-939	-763	-17 751
Aft skirt	-	-1 875	-620	-2927	359	-9 467	-218	-240	-233	-678	-646	-350	-620	-2927	-433	-1875	-1266	2 456

TABLE 24. - MERIT FUNCTIONS FOR 1.3 x 10^6-POUND VEHICLE - TITANIUM

Component	Base Point	No Temperature Restriction (Minimum Weight)					Maximum Allowable Entry Temperature										
							1000°R					1100°R				1200°R	
		⎍⎍	Z	⊥	H	W	⎍⎍	Z	⊥	H	W	⎍⎍	Z	⊥	H	⎍⎍	H
Weight (Pounds)																	
Crew compartment	3544	2738	3213	3056	1075	2931	4543	4199	3935	6200	3 531	3 574	3284	3056	4299	2738	3153
Forward tank wall	3980	2883	3392	3215	1378	2946	5278	4866	4604	7633	4 104	4 075	3750	3499	5282	2883	3828
Center section	5505	4233	4982	4733	1638	4507	7105	6592	6189	9774	5 538	5 607	5149	4733	6763	4233	4957
Aft tank wall	1691	1150	1343	1268	613	1104	2341	2173	2075	3568	1 857	1 793	1652	1549	2469	1454	1789
Aft skirt	2559	1952	2292	2172	726	2049	3352	3092	2911	4693	2 605	2 612	2446	2172	3248	1952	2380
Equivalent Payload Gained (Pounds)																	
Crew compartment		125	51	76	384	95	-155	-102	-61	-413	2	-5	41	76	-117	125	61
Forward tank wall		171	91	119	405	161	-202	-138	-97	-568	-19	-15	36	75	-202	171	24
Center section		198	81	120	601	155	-249	-169	-106	-668	-5	-16	56	120	-196	198	85
Aft tank wall		84	54	66	168	91	-101	-75	-60	-292	-26	-16	6	22	-121	37	-15
Aft skirt		94	41	60	285	79	-123	-83	-55	-332	-7	-8	8	60	-107	94	28
Effective Cost Ratio (Dollars per Pound)																	
Crew compartment		554	1500	5327	343	3855	-638	-917	-7352	-521	189 807	-17 928	1934	5327	-1520	554	2723
Forward tank wall		473	974	4039	376	2348	-594	-822	-5700	-448	-22 954	-6 808	2650	6873	-1067	473	8081
Center section		580	1562	5230	341	3670	-650	-908	-6840	-509	-122 630	-8 741	2339	5230	-1477	580	3041
Aft tank wall		395	671	3351	389	1650	-522	-667	-4202	-389	-7 332	-2 762	6687	9146	-791	1036	-5563
Aft skirt		557	1403	4861	330	3233	-611	-858	-6485	-476	-39 941	-7 596	3449	4861	-1263	557	4370

TABLE 25. - MERIT FUNCTIONS FOR 1.3×10^6-POUND VEHICLE - INCONEL

Component	Base Point	No Temperature Restriction (Minimum Weight)					Maximum Allowable Entry Temperature: 1000°R					1100°R				1200°R		
		⊓	Z	⊥	H	W	⊓	Z	⊥	H	W	⊓	Z	⊥	H	⊓	H	H
Weight (Pounds)																		
Crew compartment	3544	3 865	4534	4317	1563	3 863	6154	5705	5419	8 661	4777	4 411	4534	4317	4974		3 455	
Forward tank wall	3980	4 194	4888	4659	1925	4 005	7197	6676	6376	10 663	5660	4 194	4888	4659	6124		4 298	
Center section	5505	6 009	7022	6679	2366	5 948	9575	8868	8514	13 652	7502	6 953	7022	6679	7841		5 447	
Aft tank wall	1691	1 672	1945	1845	864	1 501	3207	2994	2878	4 984	2584	1 672	1945	1845	2863		1 983	
Aft skirt	2559	2 752	3225	3073	1027	2 693	4538	4211	4001	4 001	3548	3 312	3225	3073	3765		2 609	
Equivalent Payload Gained (Pounds)																		
Crew compartment		-50	-154	-120	308	-49	-406	-336	-291	-796	-192	-135	-154	-120	-222		14	
Forward tank wall		-33	-141	-105	320	-4	-506	-419	-372	-1 039	-261	-33	-141	-105	-333		-49	
Center section		-78	-236	-183	488	-69	-633	-523	-468	-1 267	-310	-225	-236	-183	-363		9	
Aft tank wall		3	-39	-24	129	30	-236	-203	-185	-512	-139	3	-39	-24	-182		-45	
Aft skirt		-30	-104	-80	238	-21	-308	-257	-224	-224	-154	-117	-104	-80	-188		-8	
Effective Cost Ratio (Dollars per Pound)																		
Crew compartment		-4 301	-1393	-2591	991	-4 685	-528	-638	-1011	-384	-1385	-1 591	-1393	-2591	-1373		22 061	
Forward tank wall		-7 111	-1676	-3661	1046	-64 239	-473	-564	-1064	-322	-1182	-7 111	-1676	-3661	-1003		-6 775	
Center section		-4 234	-1406	-2725	958	-5 219	-524	-634	-1035	-368	-1369	-1 473	-1406	-2725	-1285		51 298	
Aft tank wall		29 620	-2288	-7081	1024	3 188	-383	-446	-1022	-257	-1029	29 610	-2288	-7081	-724		-2 904	
Aft skirt		-5 038	-1463	-2969	902	-7 861	-493	-590	-1031	-956	-1276	-1 294	-1463	-2969	-1143		-27 448	

TABLE 26. - MERIT FUNCTIONS FOR 1.9 X 10^6-POUND VEHICLE—ALUMINUM PLUS INSULATION

Component	Weight (Pounds)				
	Base Point +	Construction			W
		⎍	Z	H	
Crew compartment	4084	3768	3750	2613	4158
Forward tank wall	5434	5678	5204	4163	5713
Center section	8310	7676	7639	5341	8462
Aft tank wall	2096	2205	2044	1735	2181
Aft skirt	3864	3584	3584	2480	3934
Equivalent Payload Gained (Pounds)					
Crew compartment		49	52.	227	-12
Forward tank wall		-38	36	198	-44
Center section		99	105	464	-24
Aft tank wall		-17	8	56	-13
Aft skirt		44	44	216	-11
Effective Cost Ratio (Dollars per Pound)					
Crew compartment		-601	-569	62	-77
Forward tank wall		979	-1049	75	-19
Center section		-605	-572	43	-74
Aft tank wall		857	-1828	100	43
Aft skirt		-635	-635	43	-123

TABLE 27. - MERIT FUNCTIONS FOR 1.9 X 10^6 - POUND VEHICLE - RENÉ

Component	Base Point	No Temperature Restriction (Minimum Weight)					Maximum Allowable Entry Temperature											
							1000°R					1100°R				1200°R		
		⊓	Z	H	⊥	W	⊓	Z	H	⊥	W	⊓	Z	⊥	H	⊓	H	H
Weight (pounds)																		
Crew compartment	4084	4489	5 260	1732	5 030	4813	7 564	6 977	10 374	6 688	5 925	5 425	-	-	6 475	-	4418	3159
Forward tank wall	5434	5989	7 024	2673	6 684	6181	10 999	10 171	15 595	9 664	8 514	8 059	-	-	9 733	-	6586	4693
Center section	8310	9126	10 682	3446	10 223	9735	15 596	14 363	21 442	13 631	12 130	11 194	-	-	13 382	-	9132	6528
Aft tankwall	2096	2152	2 520	1106	2 389	2095	4 432	4 116	6 608	3 947	3 524	3 380	-	-	4 124	-	2779	1971
Aft skirt	3864	4210	4 943	1518	4 719	4435	7 420	6 897	10 364	6 422	5 770	5 402	-	-	6 468	-	4405	3146
Equivalent Payload Gained (pounds)																		
Crew compartment	-	-63	-184	367	-148	-114	-544	-452	-983	-407	-288	-210	-	-	-373	-	-52	144
Forward tank wall	-	-87	-248	431	-195	-117	-869	-740	-1 587	-661	-481	-410	-	-	-672	-	-180	116
Center section	-	-128	-371	760	-299	-223	-1 138	-946	-2 051	-831	-597	-451	-	-	-792	-	-128	278
Aft tank wall	-	-9	-66	155	-46	0	-365	-316	-705	-289	-223	-201	-	-	-317	-	-107	20
Aft skirt	-	-54	-169	366	-134	-89	-555	-474	-1 015	-400	-298	-240	-	-	-407	-	-85	112
Effective Cost Ratio (Dollars per pound)																		
Crew compartment	-	-1387	-533	422	-2 283	-2468	-235	-266	-272	-1 000	-1 129	-477	-	-	-580	-	-3631	1200
Forward tank wall	-	-1436	-555	493	-2 540	-3180	-218	-242	-240	-810	-936	-369	-	-	-453	-	-1463	2060
Center section	-	-1475	-562	414	-2 361	-2566	-239	-271	-267	-914	-1 109	-477	-	-	-560	-	-3025	1274
Aft tank wall	-	-5229	-762	533	-4 530		-207	-226	-219	-795	-819	-308	-	-	-385	-	-978	4801
Aft skirt	-	-1613	-573	396	-2 542	-2883	-232	-258	-256	-894	-1 069	-427	-	-	-515	-	-2162	1486

TABLE 28. - MERIT FUNCTIONS FOR 1.9×10^6 - POUND VEHICLE - TITANIUM

Component	Base Point	No Temperature Restriction (Minimum Weight)					Maximum Allowable Entry Temperature											
							1000°R					1100°R				1200°R		
		⊓	Z	H	⊥	W	⊓	Z	H	⊥	W	⊓	Z	⊥	H	⊓	H	H
Crew compartment	4084	3250	3764	1389	3612	3691	5 031	4654	6 465	4 344	3 990	4 002	--	--	4502	3 316	--	2492
Forward tank wall	5434	4099	4789	2033	4567	4468	7 066	6514	9 719	6 113	5 465	5 506	--	--	6698	4 901	--	3718
Center section	8310	6603	7646	2776	7352	7456	10 398	9468	13 363	9 553	8 132	8 197	--	--	9304	6 854	--	5131
Aft tank wall	2096	1491	1713	830	1622	1512	2 830	2614	4 118	2 484	2 173	2 175	--	--	2838	2 065	--	1575
Aft skirt	3864	3045	3540	1240	3387	3398	4 907	4512	6 459	4 210	3 837	3 879	--	--	4488	3 304	--	2471
Equivalent Payload Gained (Pounds)																		
Crew compartment	--	130	50	421	74	61	-148	-89.	-372	-41	15	13	--	--	-65	120	--	249
Forward tank wall	--	209	101	531	135	151	-255	-169.	-669	-106	-5	-11	--	--	-197	83	--	268
Center section	--	267	104	864	150	133	-326	-181.	-789	-194	28	18	--	--	-155	227	--	497
Aft tank wall	--	94	60	199	74	91	-115	-81.	-316	-61	-12	-12	--	--	-116	5	--	81
Aft skirt	--	128	51	410	74	73	-163	-101.	-405	-54	4	-2	--	--	-98	87	--	218
Effective Cost Ratio (Dollars per Pound)																		
Crew compartment	--	634	1821	368	6384	7411	-755	-1184.	-640	-11 543	32 723	7 487	--	--	-3154	1 556	--	696
Forward tank wall	--	545	1239	397	4986	3762	-636	-908.	-503	-6 986	-135 089	-12 130	--	--	-1455	3 097	--	889
Center section	--	665	1876	365	6544	6926	-734	-1239.	-618	-5 507	35 693	11 506	--	--	-2715	1 678	--	712
Aft tank wall	--	446	766	410	3557	2152	-558	-747.	-429	-4 682	-20 420	-4 299	--	--	-989	21 194	--	1156
Aft skirt	--	643	1787	356	6049	5977	-691	-1048.	-570	-9 114	113 831	-38 672	--	--	-2039	2 053	--	763

TABLE 29. - MERIT FUNCTIONS FOR 1.9 X 10^6 - POUND VEHICLE - INCONEL

Component	Base-Point	No Temperature Restriction (Minimum Weight)					Maximum Allowable Entry Temperature											
							1000°R					1100°R				1200°R		
		⎍	Z	⊥	H	W	⎍	Z	H	⊥	W	⎍	Z	⊥	H	⎍	H	H
Weight (Pounds)																		
Crew compartment	4084	4 526	5 297	5 085	2047	4 860	6 784	6 251	9 031	5 909	5 299	4 838			5 206		3 631	
Forward tank wall	5434	5 879	6 900	6 572	2841	6 055	9 674	8 956	13 576	8 438	7 460	5 879			7 826		5 458	
Center section	8316	9 164	10 758	10 319	4059	9 852	13 965	12 864	18 666	12 099	10 836	10 018			10 759		7 505	
Aft tank wall	2096	2 117	2 468	2 348	1150	2 048	3 853	3 578	5 752	3 416	3 030	2 117			3 316		2 295	
Aft skirt	3864	4 237	4 971	4 756	1777	4 481	6 658	6 163	9 022	5 784	5 116	4 668			5 191		3 618	
Equivalent Payload Gained (Pounds)																		
Crew compartment		-69	-190	-156	318	-121	-422	-339	-773	-285	-190	-118			-175		71	
Forward tank wall		-69	-229	-178	405	-97	-662	-550	-1 272	-469	-316	-69			-374		-4	
Center section		-133	-382	-314	664	-238	-883	-711	-1 618	-592	-395	-267			-383		126	
Aft tank wall		-3	-58	-39	148	8	-275	-232	-571	-206	-146	-3			-191		-31	
Aft skirt		-58	-173	-139	326	-97	-437	-359	-806	-300	-196	-126			-207		38	
Effective Cost Ratio (Dollars per Pound)																		
Crew compartment		-1 279	-519	-2 212	500	-2 319	-279	-327	-323	-1, 457	-1 665	-784			-1 141		2 540	
Forward tank wall		-1 772	-596	-2 788	530	-3 692	-260	-296	-278	-1, 056	-1 215	-1 772			-748		-65 644	
Center section		-1 413	-547	-2 249	486	-2 403	-284	-333	-317	-1, 283	-1 631	-748			-1 071		2 921	
Aft tank wall		-13 862	-858	-4 851	564	16 915	-247	-278	-250	-1, 061	-1 100	-13 862			-584		-3 152	
Aft skirt		-1 500	-561	-2 436	456	-2 756	-273	-313	-301	-1, 191	-1 538	-741			-931		4 504	

TABLE 30. - MERIT FUNCTION FOR 2.5 x 10^6-POUND VEHICLE - ALUMINUM PLUS INSULATION

Component	Base Point ⊥	Construction			
		⎍⎍	Z	H	W
		Weight (Pounds)			
Crew compartment	4 534	4188	4 480	3265	4 636
Forward tank wall	7 485	7950	7 589	5959	7 798
Center section	10 287	9487	10 181	7392	10 518
Aft tank wall	3 164	3442	3 267	2696	3 117
Aft skirt	4 791	4422	4 771	3426	4 931
		Equivalent Payload Gained (Pounds)			
Crew compartment	–	54	9	200	-16
Forward tank wall	–	-73	-16	240	-49
Center section	–	126	17	456	-36
Aft tank wall	–	-44	-16	74	7
Aft skirt	–	58	3	215	-22
		Effective Cost Ratio (Dollars per Pound)			
Crew compartment	–	-630	-3 958	73	3
Forward tank wall	–	711	3 219	83	-102
Center section	–	-618	-4 660	48	6
Aft tank wall	–	497	1 347	119	65
Aft skirt	–	-604	-10 771	52	-58

TABLE 31 .- MERIT FUNCTIONS FOR 2.5×10^6-POUND VEHICLE - RENÉ 41

Component	Base Point	Weight (Pounds)																
		No Temperature Restriction (Minimum Weight)					Maximum Allowable Entry Temperature											
							1000°R					1100°R				1200°R		
		⊓	Z	⊥	H	W	⊓	Z	H	⊥	W	⊓	Z	⊥	H	⊓	H	H
Crew Compartment	4 534	4 988	5 832	5 623	2124	5 529	7 993	7 371	10 479	6 942	6 203	5 684			6 558		4 481	3228
Forward tank wall	7 485	8 378	9 813	9 371	3660	8 964	14 527	13 405	19 803	12 660	11 086	10 409			12 342		8 399	5994
Center section	10 287	11 354	13 239	12 753	4712	12 493	18 316	16 966	24 209	15 952	14 179	13 067			15 152		10 354	7436
Aft tank wall	3 164	3 246	3 829	3 635	1642	3 316	6 355	5 877	9 149	5 595	4 909	4 720			5 702		3 856	2745
Aft skirt	4 791	5 276	6 174	5 924	2087	5 756	8 765	8 139	11 807	7 716	6 757	6 227			7 379		5 039	4143
Equivalent Payload Gained (Pounds)																		
Crew Compartment		-73	-204	-171	379	-157	-544	-447	-936	-379	-263	-181			-319		8	206
Forward tank wall		-140	-366	-297	602	-233	-1 108	-932	-1 939	-814	-567	-460			-764		-144	235
Center section		-160	-465	-388	877	-347	-1 264	-1 051	-2 191	-892	-613	-438			-766		-11	449
Aft tank wall		-13	-105	-74	240	-24	-502	-427	-942	-383	-275	-245			-399		-109	66
Aft skirt		-76	-216	-178	426	-152	-626	-527	-1, 104	-460	-309	-226			-407		-39	102
Effective Cost Ratio (Dollars per Pound)																		
Crew Compartment		-1 320	-524	-2 154	456	-2 021	-248	-285	-301	-1 159	-1 338	-581			-724		24 449	912
Forward tank wall		-1 230	-522	-2 249	484	-2 228	-228	-255	-259	-942	-1 090	-432			-529		-2 457	1371
Center section		-1 369	-548	-2 222	446	-2 075	-254	-288	-294	-1 035	-1 308	-576			-688		-44 098	951
Aft tank wall		-5 340	-733	-3 814	520	-8 281	-218	-242	-236	-899	-918	-361			-444		-1 409	2105
Aft skirt		-1 416	-550	-2 297	428	-2 179	-245	-276	-279	-997	-1 229	-533			-616		-5 651	2046

TABLE 32. - MERIT FUNCTIONS FOR 2.5×10^6-POUND VEHICLE - TITANIUM

Component	Base Point	No Temperature Restriction (Minimum Weight)					Maximum Allowable Entry Temperature											
							1000°R					1100°R				1200°R		1300°R
		⊓	Z	⊥	H	W	⊓	Z	H	⊥	W	⊓	Z	⊥	H	⊓	H	H
Weight (Pounds)																		
Crew compartment	4 534	3653	4182	4051	1637	4 285	5 304	4 896	6 549	4 584	4 361	4 275			4 566		3387	2554
Forward tank wall	7 485	4924	6676	6418	2811	6 529	8 814	8 674	12 342	8 080	7 278	6 834			8 522		6259	4668
Center section	10 287	8269	9490	9186	3675	9 661	12 189	11 268	15 131	10 418	9 923	9 768			10 548		7803	5879
Aft tank wall	3 164	2275	2607	2483	1225	2 415	4 072	3 748	5 702	3 529	3 099	3 157			3 937		2867	2124
Aft skirt	4 791	3845	4430	4269	1676	4 446	5, 861	5 443	7 369	5 018	4 658	4 670			5 734		3795	2846
Equivalent Payload Gained (Pounds)																		
Crew compartment		139	55	76	456	39	-121	-57	-317	-8	27	41			-5		181	312
Forward tank wall		403	127	168	736	151	-209	-187	-764	-94	33	102			-163		193	443
Center section		318	125	173	1041	98	-299	-154	-762	-21	57	82			-41		391	694
Aft tank wall		140	88	107	305	118	-143	-92	-399	-57	10	1			-122		47	164
Aft skirt		149	57	82	409	54	-168	-103	-406	-36	21	19			-54		157	306
Effective Cost Ratio (Dollars per Pound)																		
Crew compartment		656	1795	6553	378	13 176	-974	-1 957	-796	-63 408	18 914	2 473			-44 770		1112	601
Forward tank wall		357	1356	5134	394	5 385	-992	-1 097	-583	-11 428	27 454	1 710			-2 348		1794	722
Center section		685	1893	6561	375	11 949	-940	-1 725	-757	-60 892	20 989	2 966			-12 210		1171	615
Aft tank wall		459	794	3692	404	2 657	-654	-960	-492	-7 560	36 204	74 417			-1 377		3213	843
Aft skirt		687	1966	6585	372	10 079	-803	-1 251	-679	-17 933	27 444	6 076			-4 427		1384	658

TABLE 33. - MERIT FUNCTIONS FOR 2.5×10^6 - POUND VEHICLE - INCONEL

Component	Base-Point	Weight (Pounds)																
		Maximum Allowable Entry Temperature																
		No Temperature Restriction (Minimum Weight)				1000°R						1100°R				1200°R		
		⊓	Z	H	⊥	W	⊓	Z	H	⊥	W	⊓	Z	⊥	H	⊓	H	H
Crew compartment	4 534	5 044	5 879	2517	5 688	5 635	7 158	6 704	9 131	6 259	5 201	5 100			5 277		3 696	
Forward tank wall	7 485	8 201	9 603	3908	9 194	8 848	12 792	11 933	17 239	11 157	9 829	8 201			9 990		7 002	
Center section	10 287	11 439	13 325	5577	12 883	12 736	16 452	15 402	21 096	14 374	13 019	11 654			12 191		8 538	
Aft tank wall	3 164	3 198	3 748	1715	3 578	3 264	5 562	5 141	7 964	4 868	4 253	3 198			4 591		3 194	
Aft skirt	4 791	5 318	6 216	2456	5 988	5 860	7 877	7 257	10 289	6 905	6 350	5 642			5 935		4 143	
		Equivalent Payload Gained (Pounds)																
Crew compartment		-80	-212	318	-182	-173	-413	-341	-724	-271	-184	-89			-117		132	
Forward tank wall		-113	-333	563	-269	-215	-835	-700	-1 535	-578	-369	-113			-394		76	
Center section		-181	-428	741	-409	-386	-970	-805	-1 701	-643	-430	-215			-300		275	
Aft tank wall		-5	-92	228	-65	-16	-377	-311	-756	-268	-171	-5			-225		-5	
Aft skirt		-83	-224	368	-188	-168	-486	-387	-865	-333	-245	-134			-180		102	
		Effective Cost Ratio (Dollars per Pound)																
Crew compartment		-1 207	-509	561	-2 032	-1 855	-301	-347	-365	-1 456	-1 846	-1 097			-1 833		1 466	
Forward tank wall		-1 511	-565	523	-2 420	-2 455	-275	-312	-305	-1 212	-1 654	-154			-948		4 401	
Center section		-1 273	-534	543	-2 111	-1 899	-305	-351	-355	-1 403	-1 844	-1 087			-1 630		1 603	
Aft tank wall		-12 902	-823	551	-4 459	-12 876	-263	-302	-274	-1 311	-1 449	-12 902			-726		-30 761	
Aft skirt		-1 310	-536	508	-2 176	-1 997	-292	-345	-334	-1 499	-1 532	-343			-1 289		2 046	

aluminum designs change depending upon the load intensity, geometry, etc. It can be seen that the top-hat design is lighter than the base-point design for the unpressurized components but becomes heavier for the tank wall. Also waffle construction is better than the base-point design for the small vehicle but is worse for largest vehicle. This crossover is due to the increase of the compressive load intensity and the larger diameter. To fully understand the fundamental significance of the relative cost ratios and deduce a meaningful interpretation of the results, one must know the basic assumptions that are inherent in the cost model. If only the cost changes involved with the fabrication of the structural component are considered, and these costs are translated into dollars per pound of payload in orbit, the resulting magnitude of the cost ratios could be misleading. This is due to several significant factors that have not been considered, such as costs of research, development, testing, flight vehicles, etc. The true value of these ratios can be derived by comparing the cost ratios and obtaining a relative ordering of significance. Even with an ordering of cost ratios, a misunderstanding is present if a cost ratio associated with a small vehicle system is compared in magnitude to that obtained from a large vehicle system. A series of cost ratios unique to a specific vehicle system can be compared to define the relative significance of the various structures and materials improvements when applied to that vehicle system.

It should be remembered that the base-point design cost ratios do not include the cost of the thermal protection system, and when costs are assigned the ratios can be modified as follows

$$CR^* = CR_{\text{No thermal}} - \frac{\$_{\text{Thermal protection}}}{\Delta_{\text{Payload}}}$$

It is seen that the cost ratios for Rene´ and Inconel constructions other than honeycomb with no temperature limitations are still unfavorable. In fact, these constructions have a reduced payload compared to the base-point designs: honeycomb construction without temperature limitations, although quoted in the merit function tables, is not possible because of the high induced thermal stresses during reentry which would cause load-failure of the component. When only temperature restriction is imposed (1000 to 1200°R), the resulting weight increases, payload drops, and cost ratio worsens. It appears that from an effectiveness standpoint the Rene´ and Inconel designs are inefficient for the recoverable stages of this type of vehicle. The heating profile when the vehicle is staged at 6500 ft/sec and 150,000 feet is sufficiently small so that the temperature during reentry does not impose severe design criteria and does not warrant the use of superalloys such as Rene´ and Inconel for the "hot-structure" concept.

Titanium structures with no temperature limitations are lighter than the insulated aluminum concepts. The boost design conditions result in skin thickness for minimum weight designs that act as a good heat sink and restrain the maximum entry temperature to less than 1200°R. Although the titanium component is lighter than the base point, it cost more with the cost ratios ranging from 1500 to 6000 for milled construction (integral skin stringer and waffle) to 300 to 1500 for the other construction types. This indicates that the latter types of construction fabricated from titanium are the most efficient. These cost ratios of 300 to 1500 will be reduced when the additional cost of the thermal protection system of the base point is included, and the effects of reusability and total number of flights throughout the lifetime of the vehicle are assessed.

COMPUTER PROGRAM TURNOVER

The computer program turnover to NASA OART for Phase III of this contract deals with the vehicle synthesis and structural design synthesis programs for expendable vehicle systems. In Phase I, the North American Rockwell Corporation Space Division Launch Vehicle Synthesis programs were modified and used to synthesize families of vertically launched, tandem-staged launch vehicles. Wherever possible, these programs were written for a generalized vehicle and structural system and as such will synthesize most boost vehicles with up to four stages for a very large range of payload sizes, engine/propellant systems and structural design concepts fabricated with conventional and advanced materials.

There are two separage program decks which perform the synthesis operation: the main overall program for both vehicle and structural design synthesis and a secondary deck which breaks out the structural design synthesis from the main program as a separate package. A detailed description of the synthesis evaluation, program listing, input data sheets, and computer output format is given in Volume II of this report.

The computer programs were written in FORTRAN IV and have been checked out in NAASYS, the North American Rockwell adaption of the IBM 7090/7094/IBSYS/IBJOB system and the NASA system at the Electronic Research Center, Boston, Massachusetts.

The large program contains the vehicle synthesis, structural design synthesis and cost assessment subroutines. Output from this series of subroutines includes:

1. Parametric stage size sensitivities
2. Efficient stage velocity apportionment
3. Stage mass fraction weight/performance definition
4. Generalized payload exchange ratios
5. Structural component description for various materials/ construction concepts with structural element details

6. Structural cost of component design, equivalent payload change and a merit function of a cost/payload ratio

A secondary program for the structural design synthesis only has been supplied separately to allow users the ability to perform structural synthesis of cylindrical shells irrespective of vehicle systems. This separate second program will be useful for the preliminary design of the structural elements after the conceptual design studies have been conducted and the overall system design frozen.

The vehicle synthesis programs have the ability to define the performance and weight breakdown for multistage (up to four stages) expendable bipropellant launch vehicles. The programs are sufficiently general to be able to handle a large spectrum of vehicle sizes, shapes, and configurations, but there are a few limitations currently built into the subroutines. These limitations could easily be removed to suit the individual users requirements with fairly minor modifications. With the vehicle system defined in terms of size, weight, performance, and loading environment, the individual cylindrical shell components can be synthesized for the minimum weight detailed design to meet the design criteria, stability, and strength. These designs are practical configurations, which are subject to the users' imposed manufacturing restrictions, such as minimum gauge, minimum stiffener pitch, maximum sandwich height, etc.

The method of structural evaluation involves a component-by-component substitution in the base-point vehicle systems. Estimated manufacturing complexity factors, material costs with year, and man-hour requirements are included in the cost assessment. Cost assessment is accomplished by isolating each structural component and performing a comparative evaluation of the new component to the base point component. Final assessment is made in terms of component weight reduction, equivalent payload gained from this reduction, and cost ratio for the new component, which is identified as additional dollars cost per pound of payload gained. The three merit functions are then organized in arrays to order their importance.

The synthesis program (fig. 65) is composed of an executive control program (MAIN) and 25 individual subroutines; six are called from MAIN, two from MAIN1, five from mass fraction routine (TRANUB), six from STRESS, two from both MAXPL, and MINTO, and the last two called from CNALF or WEIGHT.

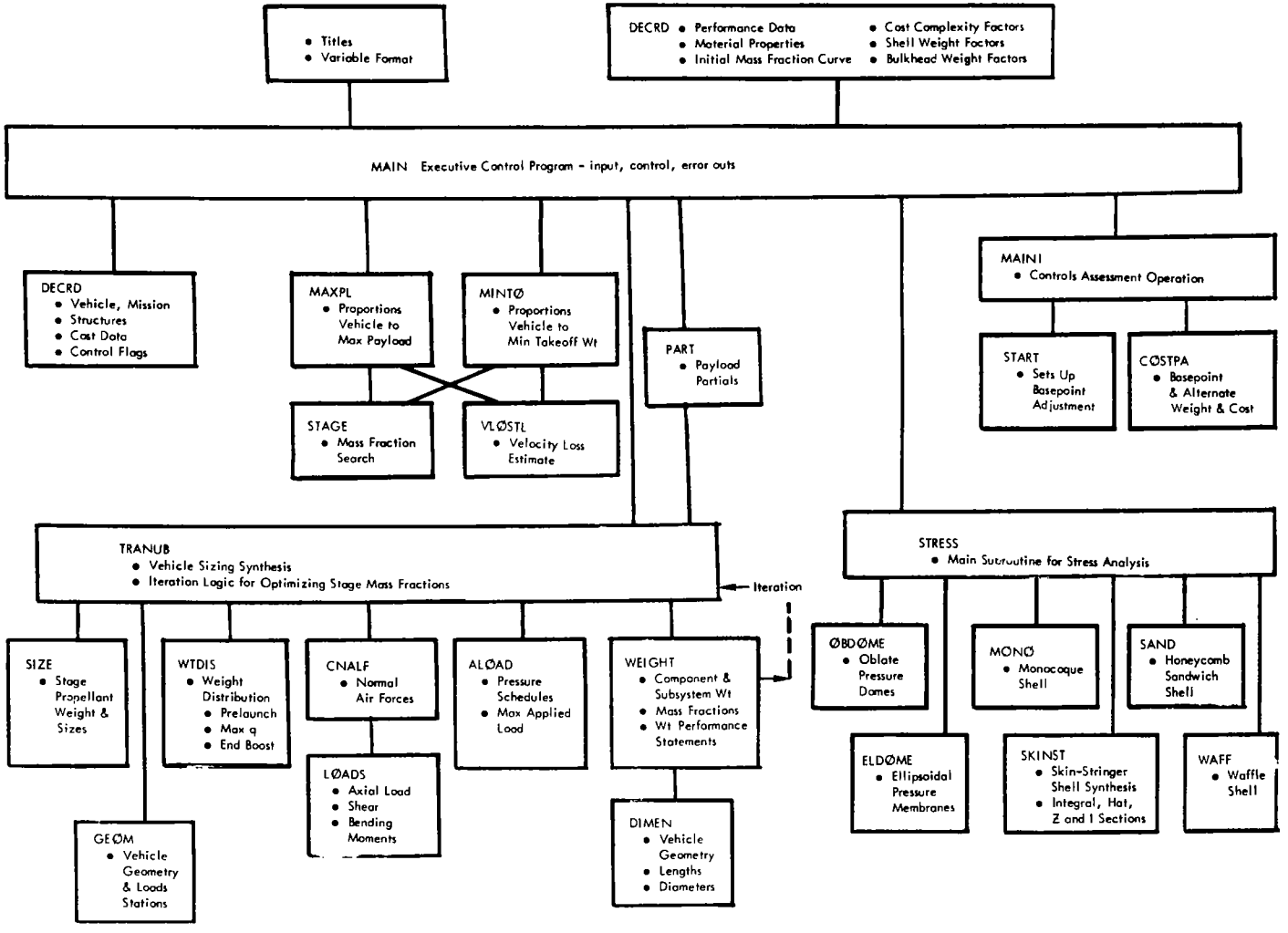

Figure 65. - Synthesis Program

The name of each subroutine and a description of its use follows:

Subroutine Name	Subroutine Description
MAIN	The master executive control for the synthesis routing, calling sequence, input and "error out" messages.
DECRD	Allows a simple input format to be used for data transmittal to main programs. With multirun jobs input data remains identical to previous run unless physically altered.
MAXPL	Dynamic programming technique to maximize the payload for a given launch liftoff weight. For a multistage vehicle will define optimum staging velocity for maximum performance vehicle, test stage empty and propellant weights.
MINTO	Dynamic programming technique to minimize the launch weight of a "multistage vehicle" for a prescribed payload requirement. Defines optimum staging velocity and stage weights.
STAGE	Search for prescribed stage mass fraction from stored input data of mass fraction size relationships.
VLOSTL	Defines the velocity losses associated with the individual stages of the vehicle system.
TRANUB	A second-level subroutine control and iteration loop routine for the stage mass fraction evaluation. Performs the monitoring job of ensuring that the evaluated mass fraction and weight-size breakdown are consistent with performance and constraint requirements.
SIZE	Determines the weight and volumes associated with a particular stage for a given mass fraction and performance requirement.
GEOM	Describes the physical size and dimensions for the overall stages and sets up body station positions for future load points.

Subroutine Name	Subroutine Description
WTDIS	Distributes the stage weights—inert and propellants—along the vehicle length for various flight regimes—prelaunch, maximum dynamic pressure, and end boost. Evaluates the centers of gravity at these three flight times.
CNALF	Dummy subroutine to determine the aerodynamic force coefficients and forces on the payload and major elements of the stage.
LOADS	Determines the inertias (axial and pitching) for three flight times (prelaunch, maximum dynamic pressure, end boost) due to wind forces and flight motion. Develops axial load, shear, and bending moment along the vehicle length.
ALOAD	Evaluates the tank pressures (ullage, hydrostatic head, etc.) along flight path. Resolves the load and pressures into shell load intensities (tension and compression) and defines a maximum design load envelope.
WEIGHT	Generates the weight description of the structural systems to meet load requirements and defines other subsystem empirical weights.
DIMEN	Develops the vehicle geometry-station map to define the component length and diameters.
PART	Computes the generalized payload exchange ratios for the individual synthesized stages.
STRESS	A secondary control program for a sequencing of required stress synthesis subroutines.
ELDOME	Synthesizes ellipsoidal membrane bulkheads to meet internal pressure requirements.
OBDOME	Synthesizes oblate spheroid bulkheads to meet internal pressure requirements.
MONO	Develops the required shell thickness for a monocoque construction to meet design load intensity, checks for strength and stability.

Subroutine Name	Subroutine Description
SKINST	Structural synthesis of a skin-stringer-ring type of construction. Stiffener sections can be integral, Z, I, and top hat. Evaluates for strength and stiffness, (Local and general instability) of individual stiffener elements, skin, and overall shell. Defines thickness, sizes, and pitch of stiffener elements for pressurized and unpressurized, buckled and unbuckled designs.
SAND	Generates honeycomb sandwich structural design to fulfill design load and temperature environments. Defines facing sheet thickness, core height, and density requirements to preclude instability failure, using current buckling "knock down" factors.
WAFF	Synthesis of a 45 degree oriented waffle type construction for pressurized and unpressurized design requirements. Design output will be a minimum weight design consistent with imposed design and manufacturing restrictions.
MAIN1	Secondary control program for the structural cost assessment operation.
START	Program for evaluating nonoptimum design factors dependent on type of structural component.
COSTPA	Evaluates the fabrication and material costs associated with the structural components of the basepoint designs and all the requested alternate materials and/or constructions. Defines the component weight and cost, the alternate designs weight reduction, cost change, equivalent payload improvement, and its effective cost ratio.

The program has 11 choices of paths through the subroutines, as indicated in table 34. These are in addition to using the alternate stress subroutines to synthesize a structural shell.

TABLE 34. - OPTIONS ON PROGRAM ROUTING

Synthesis Subroutines	Selection Paths										
	1	2	3	4	5	6	7	8	9	10	11
Maximum payload stage proportioning	X			X			X			X	
Minimum liftoff stage proportioning		X			X			X			X
Stage mass fraction determination			X	X	X	X	X	X	X	X	X
Derivation of payload exchange ratios						X	X	X	X	X	X
Base-point structural designs									X	X	X
Base-point structural costs									X	X	X
Alternative structural designs									X	X	X
Alternative structural costs									X	X	X

CONCLUSIONS AND RECOMMENDATIONS

This study has demonstrated the applicability of the Recoverable First-Stage Synthesis subroutines to the identification of favorable structural materials, constructions, and thermal protection systems. The results of any such study are strongly dependent on the specific mission requirements, payload configuration, ascent trajectory, staging velocity and altitude, and structural design criteria. The specific conclusions and recommendations discussed below are applicable only to the vehicles and missions described on pages 9 to 70; however, the synthesis program, with minor modification, can be run to analyze alternate configurations such as the first stage of a two-stage recoverable vehicle, or a horizontally launched first stage. Therefore, it is suggested that this program be utilized in the future to identify the effects of structures and materials research on the capability of other future recoverable first stages.

Construction Concepts

The insulated concept with an aluminum load-carrying structure offers distinct weight advantages over the hot structural concept. This is true only if the thermal protection system used can be fabricated for about 1.5 lb/ft^2, if it does not require extensive refurbishment after each flight, and if its cost is not exorbitant. For the aluminum concepts, the conventional constructions (skin stringer, waffle, and honeycomb sandwich) are best because of the fuselage's small diameter and fairly small compressive load intensities. The use of advanced constructions with multiwall and double-wall concepts discussed in Phase II is not beneficial with the low design loading intensities. Honeycomb sandwich construction was the lightest design considered. Although honeycomb sandwich could be 50-percent lighter than the base-paint integral skin-stringer design when the additional weight for the thermal protection system is added, the weight reduction is now only 25 percent.

The most attractive weight-to-cost design is an aluminum skin-stiffened concept using Z-section or top-hat stringers. Although other designs exist which are lighter, their structural costs are appreciably higher. A relative payload "worth index" must be assigned to the vehicle system before the best choice is defined. If a structural worth index of $300 per pound of payload is assigned, it is best to use the skin-stiffened concept for the first stages.

Hot structural concepts using titanium, Rene'or Inconel did not appear to be the lightest designs for these recoverable stages. This is because the ascent trajectory environment is the predominant design condition for the maximum compressive loading intensity. This intensity was less than 6000 lb/in. and does not allow the resulting designs to take advantage of the material's high strength and thermal properties. The compressive intensity due to external loads during entry when the stage is unloaded was found to be extremely small, and the thermal stresses for the single-sheet design should not present additional design requirements for the basic shell panels.

With a minimum weight design based upon the boost environment, the resulting structural configurations have sufficiently thick skins, which will act as an effective heat sink during entry, so that the maximum surface temperatures will be less than 1300°R for Rene'41 and 1200°R for titanium and Inconel. For the thin-skin honeycomb sandwich at high temperatures, a severe thermal gradient, which could produce excessive thermal stresses, was found. For the single-skin designs the thermal stresses will not be so severe as to result in additional design requirements. Titanium designs of the three materials considered for the "hot structure" was found to produce the lightest weight designs.

If thermal limits are imposed upon the structural design for material reusability, internal temperature control, etc., then severe weight penalties will result due to the increased skin thicknesses necessary for the heat sink. This weight penalty is severe for honeycomb sandwich concepts with the temperature restricted to 1000°R.

Structural Costs

The basic structural costs assumed for this study were only those associated with production fabrication and materials. With the recoverable stages, an important cost factor is the refurbishment cost. The cost ratio used here was only production and material costs per pound of payload for one flight and does not have much significance in comparing radically different design concepts. Refurbishment cost and the total effective payload charge for all flights throughout the vehicle's life should be included in the cost ratio. The implication of this new cost ratio would be selection of the lightest weight design, i.e., the greatest payload improvement. The initial fabrication cost of construction would not be too significant when amortized over many flight missions. The only other criteria for the selection of the lightest design would be not to have excessive refurbishment requirements.

For the superalloy designs when the basic material costs are appreciably higher than aluminum, it was found that waffle and integral skin stringer designs were uneconomical. Their relative weight differences from built-up sections did not justify the additional cost of the material parent stock, of which 90 percent could be machined away. The material costs for waffle and integral designs exceeded the fabrication construction costs.

Manufacturing Development

The above discussions consistently allude to the fact that research would be highly beneficial when devoted to increasing know-how in manufacturing of new and advanced structural concepts and in the development of the manufacturing technology to fabricate structures from highly advanced materials or from new materials with radically different properties. Such efforts would undoubtedly lead to reduced structures and materials costs and make the advanced structural concepts much more competitive than presently. From the study results, it appears that research in improvement of the strength properties of current material does not offer significant advantages. Improvement of the material properties that influence the fabrication process, while not analyzed in detail in this study, will effectively reduce construction costs and save weight of the secondary structure, such as weld lands, attachment points, etc.

The lightest designs considered were the insulated aluminum construction. These concepts require an effeciently designed thermal protection system, which is non-load carrying and can easily be refurbished. The system investigated had a thin superalloy heat shield, standoff support, and a minimum of insulation. This lightweight concept will require manufacturing development to control the weight for the thermal protection system. The large thermal expansion of the heat shield relative to the load-carrying structure, its repair, and replacement will result in major manufacturing problems.

Material Strength Improvement

Application of improved-strength material should be to aluminum sandwich construction concepts. Improvement in the material's compressive yield and ultimate tensile stress is beneficial and should be applied to constructions having very thin facing sheets which are highly loaded. An ordering of constructions which most benefit by material improvements is as follows: honeycomb sandwich, multiwall corrugated, and skin stiffened.

Percentage increases in the material properties do not correspond to identical percentage weight reductions. At best, the effect of a 10-percent compressive-yield increase results in an 8-percent weight reduction of the load-carrying structure if the designs considered are both optimum concepts (minimum weight). When this 8-percent weight reduction is combined with the unchanged thermal protection system weight, it will be reduced to perhaps a 4-percent weight improvement. For the other three materials, Rene', titanium, and Inconel, the temperature restrictions will influence the construction skin thickness for its heat sink capability. These thicker skins will result in an off-optimum design, working at a low-stress level which cannot benefit from material strength improvements.

REFERENCES

1. Reusable Orbital Transport Second Stage, Research and Technology Implications. GD/C Rept. DCB 65-018, vol. V, 1965.

2. Boddy, Jack A.; Mitchell, James C.: Influence of Structure and Material Research on Advanced Launch Systems' Weight, Performance, and Cost, Summary Report, NASA CR-974, December 1967.

3. Local Normal Force Coefficients Distribution on Saturn IB and Saturn V Spacecraft. NASA Memo from B. W. Hunley, George C. Marshall Space Center, Huntsville, Ala., May 1965.

4. USAF Stability and Control Datcom. USAF Contract AF 33(616)6460, AF Flight Dynamics Laboratory, Wright-Patterson AFB, Octover 1960.

5. Dusinberre, G. M.: Numerical Analysis of Heat Flow. McGraw-Hill Book Co., Inc., 1949.

6. Thermo-Structural Analysis Manual. Republic Aviation Rept. RAC-679-1(R8), September 1960.

7. Titanium Tankage Program, Phase 1, Advanced Tankage Configuration Study. NAA S&ID Final Rept. SSD-TOR-63-1, February 1963.

8. Koelle, H. H.: Handbook of Astronautical Engineering. McGraw-Hill Book Co., Inc., 1961, pp. 3-2 to 11-26.

9. Launch Vehicle Components Cost Study. Lockheed Missiles and Space Co. Rept. LMSC 895424, June 1965.

NATIONAL AERONAUTICS AND SPACE ADMINISTRATION
WASHINGTON, D.C. 20546
OFFICIAL BUSINESS

FIRST CLASS MAIL

POSTAGE AND FEES PAID
NATIONAL AERONAUTICS AN
SPACE ADMINISTRATION

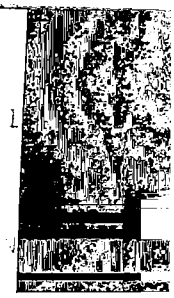

"The aeronautical and space activities of the United States shall be conducted so as to contribute . . . to the expansion of human knowledge of phenomena in the atmosphere and space. The Administration shall provide for the widest practicable and appropriate dissemination of information concerning its activities and the results thereof."

—NATIONAL AERONAUTICS AND SPACE ACT OF 1958

NASA SCIENTIFIC AND TECHNICAL PUBLICATIONS

TECHNICAL REPORTS: Scientific and technical information considered important, complete, and a lasting contribution to existing knowledge.

TECHNICAL NOTES: Information less broad in scope but nevertheless of importance as a contribution to existing knowledge.

TECHNICAL MEMORANDUMS: Information receiving limited distribution because of preliminary data, security classification, or other reasons.

CONTRACTOR REPORTS: Scientific and technical information generated under a NASA contract or grant and considered an important contribution to existing knowledge.

TECHNICAL TRANSLATIONS: Information published in a foreign language considered to merit NASA distribution in English.

SPECIAL PUBLICATIONS: Information derived from or of value to NASA activities. Publications include conference proceedings, monographs, data compilations, handbooks, sourcebooks, and special bibliographies.

TECHNOLOGY UTILIZATION PUBLICATIONS: Information on technology used by NASA that may be of particular interest in commercial and other non-aerospace applications. Publications include Tech Briefs, Technology Utilization Reports and Notes, and Technology Surveys.

Details on the availability of these publications may be obtained from:

SCIENTIFIC AND TECHNICAL INFORMATION DIVISION

NATIONAL AERONAUTICS AND SPACE ADMINISTRATION

Washington, D.C. 20546